Investigation into the Regulation and Transfer of Conjugative Transposons of the Tn*916*-like Family

Thesis submitted by

Azmiza Syawani Binti Jasni

For the degree of

DOCTOR OF PHILOSOPHY

in the

Faculty of Medical Sciences

University College London

Division of Microbial Diseases

UCL Eastman Dental Institute

256 Gray's Inn Road

London WC1X 8LD

UK

2012

Declaration

I hereby certify that the work embodied in this thesis is the result of my own investigation, except where otherwise stated. Investigation into the effect of biocides on the regulation of Tn*916* was carried out in collaboration with Maria A. Seier-Petersen, Technical University of Denmark.

Abstract

The Tn*916*-like family of conjugative transposons are broad host range mobile genetic elements and are clinically important as they are one of the major vectors responsible for the spread of antibiotic resistance among bacterial pathogens. This study was designed to investigate the behaviour of the conjugative transposons Tn*916* and Tn*5397*, focusing on the transcriptional regulation and transfer. The proposed regulatory system of Tn*916* involves transcriptional attenuation upstream of *tet*(M) and is regulated by tetracycline. The translation of *orf12* is central to this regulatory mechanism as it is the translating ribosome upon *orf12* RNA that is hypothesised to destroy, or prevent the formation of the transcriptional terminators. This hypothesis was tested using a *Bacillus subtilis* construct, with a 2 bp mutation disrupting the start codon of *orf12*. This construct is expected to result in the transcriptional terminators being permanently formed as the ribosome will no longer translate the *orf12* and destroy them. Results indicate a lower transcription of *tet*(M) and downstream genes which was supported by the slower growth rate of the *B. subtilis* mutant compared to the wild type upon challenged with tetracycline. When tetracycline is present, a reduced fitness of this mutant was observed compared to the wild type. However, the transfer frequency of the *B. subtilis* mutant was similar to that of the wild type.

The transcription of Tn*916* and Tn*5397* was investigated by quantifying the expression level using reporter assays, where the P*tet*(M) promoter and the open

reading frames upstream of *tet*(M) were cloned upstream of a β-glucuronidase gene. In the presence of tetracycline, Tn*916* wild type construct was upregulated whereas the Tn*5397* wild type construct showed a constant expression level. Disruption of the start codon of *orf12* (Tn*916*) and *orf26* (Tn*5397*) has also led to a constant expression level of β-glucuronidase.

The termination efficiency of the Tn*916* terminators was estimated using promoter assays and a published algorithm. Results suggest that the large terminator is more efficient [47% (± 18)] than the small terminator [23% (± 15)], which was supported by the algorithm analysis for Tn*916*.

Finally, reciprocal gene transfer of Tn*5397* between *Clostridium difficile* and *Enterococcus faecalis* was demonstrated. The transfer frequency [± standard deviation (SD)] detected was 8.85×10^{-8} ($\pm 2.14 \times 10^{-7}$) per recipient. Tn*5397* integrates into the genome of *E. faecalis* at a single site that is within an orf encoding the phosphotransferase (PTS) IIA component. Comparative growth curves showed that the acquisition of Tn*5397* has a very small effect on the growth of *E. faecalis*.

This work has extended the current knowledge of the regulation and transfer of conjugative transposons of the Tn*916*-like family. It has provided a better understanding about the mechanism of transcriptional regulation of these elements.

Acknowledgements

I would like to extent my heartfelt gratitude to my supervisor Dr. Adam Roberts, whose help, brilliant ideas and enthusiasm have guided my studies from its conception to its completion. His continual support and great mentorship were truly inspiring.

Special thanks to Prof. Peter Mullany for his excellent advice and constant encouragement. My thanks also go to all my colleagues in the Eastman Dental Institute, especially Dr. Philip Warburton, Dr. Haitham Hussain and Ms. Hashimatul Hashim for the countless help and friendship.

I am immensely grateful to the Malaysian Government for their funding, expert feedbacks and continued responsiveness to my needs. I would also like to acknowledge the academic and technical support of the Universiti Putra Malaysia and its staff. It is my greatest pleasure to be part of the team!

Lastly, I would like to thank my family for the unceasing love and encouragement. Greatest thanks to my parents, whose infinite patience and faithful support have contributed immeasurably to the success of this undertaking.

Thank you.

Table of Contents

List of Figures

Chapter 1

Chapter 2

Chapter 3

List of Tables

Chapter 1

Chapter 2

Chapter 3

List of Equations

Chapter 2

Chapter 5

Abbreviations

BHI	Brain heart infusion
bp	Base pair
^{o}C	Degrees Celsius
DNA	Deoxyribonucleic acid
dNTP	Deoxynucleotide triphosphate
EDTA	Ethylenediaminetetraacetic acid
g	Gravitational force
h	Hour
kb	Kilobase
λ	Bacteriophage lambda
LB	Luria-Bertani
µg	Microgram
µl	Microlitre
µm	Micrometre
ml	Millimetre
µM	Micromolar
mM	Millimolar
min	Minute
nm	Nanometre
OD	Optical density
orf	Open reading frame

oriT	Origin of transfer
PCR	Polymerase chain reaction
RBS	Ribosome binding site
RNA	Ribonucleic acid
rpm	Revolutions per minute
sec	Second
UV	Ultra violet
v/v	Volume for volume
w/v	Weight for volume

Chapter 1.0

General Introduction

1 General introduction

1.1 Antibiotic resistance

Antibiotics are chemical substances that work to either inhibit bacterial growth (bacteriostatic agents) or kill them (bactericidal agents) (Russell and Chopra, 1996). Since the first discovery and clinical application of antibiotics, there has been a major improvement of the treatment of infectious diseases, which has resulted in a reduction in the morbidity and mortality associated with these illnesses (Alanis, 2005). However, continuous exposure to antibiotics has accelerated the emergence of antibiotic resistance (Heinemann *et al*., 2000), predominantly among pathogens causing nosocomial infections (Emori and Gaynes, 1993; Hsueh *et al*., 2002). The increased prevalence of antibiotic resistance in bacterial pathogens has become a formidable public health concern and this phenomenon has led to collaborative efforts from various sectors to combat the rising antibiotic resistance. To date, a number of strategies have been implemented and these include the most recent antibiotic re-engineering approach (Xie *et al*., 2011), surveillance of antibiotics use and resistance as well as educating the health practitioners on the proper use of antibiotics during treatment (Hadley, 2004).

1.2 Nosocomial infections

Nosocomial infections, also called hospital-acquired or health-care associated infections are those acquired in, or associated with, hospitals or because of healthcare interventions (Jamieson, 2008; Breathnach, 2009). Infections are considered nosocomial if they appear 48-72 h after hospitalisation or within 30 days after discharge. The frequency of nosocomial infections amongst patients in British and Irish hospitals has been estimated to be 5-10% (Smyth *et al*., 2008), with the highest in surgical wards and intensive care units (ICU) (Majumdar and Padiglione, 2012). Nosocomial infections include surgical, wound, catheter-associated urinary tract, respiratory tract and gastrointestinal infections. These infections can be caused by any pathogen found in hospitals or healthcare units via direct contact with patients as well as the contaminated environmental surfaces (Eckstein *et al*., 2006). In recent years, nosocomial infections and antibiotic-resistance have become the subjects of considerable media, public and political interests (Breathnach, 2009). Antibiotic-resistant nosocomial infections have been linked to a substantial increase in morbidity, mortality and the financial burden associated with patient management and implementation of infection control measures (Jamieson, 2008; Woodford and Livermore, 2009). Among the predominant antibiotic-resistant bacteria causing nosocomial infections are the Gram-positive *Clostridium difficile* and vancomycin-resistant enterococci (VRE) (Pituch, 2009; Cartman *et al*., 2010; Majumdar and Padiglione, 2012).

1.2.1 *Clostridium difficile*

C. difficile is an anaerobic, spore-forming and toxin-producing bacillus and the leading cause of antibiotic-associated disease which can range from mild, self-limiting diarrhoea to severe pseudomembranous colitis (Huang *et al*., 2009). *C. difficile* strains have been classified and grouped using various molecular typing methods. One such method is ribotyping which is a typing method based on the sequence of the 16S – 23S region of the genome. In the UK up to 2003, it was reported that ribotype 001 contributed approximately 60% of *C. difficile*-associated diarrhoea (CDAD) cases. Molecular surveillance in 2006 however showed that 40% of isolated *C. difficile* was PCR-ribotype 027 which is a highly transmissible and virulent strain (Barbut *et al*., 2007; Sundram *et al*., 2009). The genome sequence of the virulent and multidrug-resistant *C. difficile* 630 reveals the presence of numerous mobile genetic elements, particularly conjugative transposon (CTn); CTn*1*, CTn*2*, CTn*4-7* (Brouwer *et al*., 2011). Some of this CTns are related to the vancomycin resistance transposons of *Enterococcus* sp. e.g CTn*2*, CTn*4* and CTn*5* which share homology to Tn*1549* (Sebaihia *et al*., 2006). Resistance to antimicrobials among *C. difficile* varies widely, however, all isolates remain susceptible to metronidazole and vancomycin, which is the treatment of choice for *C. difficile* infection (CDI). However, recently fidaxomicin, which has been shown to be as effective as vancomycin, has been approved in the USA (since May 2011) and Europe (since December 2011) as an alternative medication for CDI patients (Cornely *et al*., 2012).

1.2.2 *Enterococcus faecalis*

Enterococcus spp. are commensal bacteria which usually reside in the gastrointestinal tract and are occasionally associated with urinary tract infections (Rice, 2006; Amyes, 2007). However, in the late 1980s, *Enterococcus* spp. has emerged as one of the most important nosocomial pathogens due to the outbreaks of VRE (Bensoussan *et al*., 1998). The emergence of VRE is associated with the distribution of the mobile elements Tn*1546,* which contains *vanA,* and Tn*1549* and Tn*5382,* which contain *vanB* (Bonten *et al*., 2001; Launay *et al*., 2006). The emergence of VRE has been linked to the higher use of vancomycin (Kirst *et al*., 1998) which, as mentioned above, remains as the conventional antimicrobial treatment, along with metronidazole, of CDI in the UK (Pepin, 2008; Baines *et al*., 2009; Leffler and Lamont, 2009).

1.3 Horizontal gene transfer

One of the mechanisms for the spread of antibiotic resistance genes among bacteria is the acquisition of mobile genetic elements, transferred via horizontal gene transfer (HGT). During HGT the genetic material can be transferred without the requisite reproduction associated with vertical inheritance (Poole, 2009). The three fundamentally distinct mechanisms involved are transformation, transduction and conjugation.

1.3.1 Transformation

Transformation was the first mechanism of HGT to be discovered and is a process of DNA uptake by bacteria from the environment (Frost *et al*., 2005). Transformation was first observed when avirulent strains of *Streptococcus pneumoniae* acquired virulence by incubation with an extract from killed virulent cells (Griffith, 1928). Transformation occurs when the bacterial cells enter a competence state, commonly in late logarithmic phase (Dale and Park, 2010). Competence of bacteria can be either natural or artificially induced (Mandel and Higa, 1970). In some bacteria, transformation is selective, where a short species-specific sequence is required for efficient uptake of extracellular DNA. For example, the transformation of the piliated *Neisseria meningitidis* is mediated by the presence of a specific 10 bp sequence (GCCGTCTGAA) known as the uptake signal sequence (USS), that appears nearly 2000 times in its genome (Elkins *et al*., 1991). In contrast, *Bacillus subtilis* and *S. pneumoniae* have been shown to take up virtually any DNA molecule. Transformation is one of the main mechanisms mediating transfers of genetic material encoding antibiotic resistance determinants amongst clinically important bacteria (Woegerbauer *et al*., 2002; Kim *et al*., 2006; Domingues *et al*., 2012). Hannan *et al*. (2010) have demonstrated the transfer of conjugative transposon Tn*916* which encodes for tetracycline resistance from *Veillonella dispar* to *Streptococcus* spp. in biofilms via transformation. Additionally, development of tetracycline and kanamycin resistance in *Campylobacter jejuni* has also been demonstrated by the same mechanism (Jeon *et al*., 2008).

1.3.2 Transduction

Transduction is the process by which DNA is acquired following a phage infection. Transduction has often been classified into two categories; generalised and specialised (or restricted) transduction (Ozeki and Ikeda, 1968). In generalised transduction, any region of the bacterial chromosome has an equal chance of being transduced whereas in specialised transduction, the DNA transferred is limited to a very small region of the host chromosome (Dale and Park, 2010) as it is packaged with the bacteriophage genome. Generalised transduction was first identified by Zinder and Lederberg (1952) where the phage P22 was shown to transfer chromosomal DNA from one strain of *Salmonella* to another. Phages that mediate generalised transduction generally breakdown host DNA into a suitable sized fragments thus allowing it to be incorporated into the phage head. In some cases, the bacterial plasmid or host chromosomal DNA is taken up into the phage head in place of the phage DNA. The transducing particles then have the ability to infect susceptible hosts and the DNA becomes incorporated into the recipient genome by homologous recombination (Fineran *et al*., 2009).

Whereas in typical generalised transduction, the bacterial DNA is packaged without the phage DNA, specialised transduction can packaged the host DNA along with some, or all of the phage DNA (Fineran *et al*., 2009). The mechanism of specialised transduction was first observed using *E. coli* and phage lambda (λ) (Morse *et al*.,

1956). Specialised transduction relies on temperate phages (e.g. phage λ and phage Mu) that are able to form prophage during lysogenic cycle (Fineran *et al*., 2009). In specialised transduction, the excision of phage DNA from the host genome is imprecise, which leads to the formation of the hybrid circular DNA containing phage and bacterial DNA. Once the transducing particles have been packaged, they are then capable of infecting a new host. Upon injection, the transducing phage lysogenises the host, resulting in the stable integration of the genes into the new host genome as part of the prophage (Hendrix, 2002). If this lysogeny breaks down, and the phage enters the lytic cycle, all of the progeny will then harbour the bacterial DNA.

1.3.3 Conjugation

Conjugation is a process of DNA transfer via a proteinaceous cell-to-cell junctions or a bridge-like tunnel between bacterial cells, although the nature of some of these structures remains unclear. In general, the mechanism of conjugation involves three main steps: mating formation, signaling event for transfer to occur and transfer of DNA (Frost *et al*., 2005). In most cases, this involves self-transmissible conjugative elements, which include plasmids and integrative conjugative elements (ICEs) (e.g. conjugative transposons). The two mechanisms of conjugation show differences between these two types of element and are detailed below.

1.3.3.1 Conjugative plasmids

Conjugative plasmids are self-replicating, double-stranded closed circular units of DNA that are capable of horizontal transmission. For many years, the conjugative plasmids have been associated with the dissemination of antibiotic resistance amongst bacterial pathogens (Palmer *et al*., 2010). The conjugative mechanisms of plasmids are different between those of Gram-negative and Gram-positive bacteria. The Gram-negative bacteria use a type IV secretion system (T4SS), also known as the mating pair formation (Mpf) apparatus to form a pilus (Lawley *et al*., 2003; Thomas and Nielsen, 2005). Conjugation is initiated by contact between pili and a suitable recipient resulting in a pore or channel formation (Lawley *et al*., 2003). Once contact is established, a mating signal is generated and a protein called relaxase nicks the plasmid DNA at a specific site known as the origin of transfer (*oriT*) to give a single-stranded substrate that is suitable for transfer (Grohmann *et al*., 2003). In the recipient cell, DNA synthesis converts the single-strand DNA into a double-stranded molecule (Dale and Park, 2010).

Some Gram-positive bacteria can stimulate mating by producing a pheromone-like peptide as observed in many enterococcal strains (Hirt *et al*., 2002; Chandler and Dunny, 2004). This peptide which is a chemical signal for interbacterial communications is transmitted from the recipient cells to the donor cells (Chandler and Dunny, 2004). Activation of this signal leads to the production of two proteins; aggregation substance (AS) and binding substance (BS) that appear on the surface

of both the donor and the recipient cells (Clewell and Weaver, 1989). Synthesis of these proteins is responsible for the cell-to-cell contact and thus initiates the transfer of the plasmid (Waters and Dunny, 2001). Plasmid DNA is transferred to the recipient cells through the same mechanisms as observed in Gram negative bacteria.

1.3.3.2 Conjugative transposons

Conjugative transposons, or integrative conjugative elements (ICEs) are genetic elements that encode enzymes which can catalyse their own integration, excision, transposition and conjugation (Franke and Clewell, 1981). Conjugative transposons were first identified in the early 1980s (Buu-Hoi and Horodniceanu, 1980) where the transfers of chromosome-borne multiple antibiotic resistance markers were observed in beta-hemolytic groups streptococci (Horodniceanu *et al*., 1981). There are many distinct families of conjugative transposons as illustrated in Table 1.1. The two most extensively studied conjugative transposons are Tn*916* and Tn*1545*, which have a broad host range and are clinically important, as they are one of the major vectors responsible for the spread of antibiotic resistance among bacterial pathogens (Clewell *et al*., 1995; Scott and Churchward, 1995). Conjugative transposons are capable of being transferred via conjugative transposition from genomes of donor cells to those of recipients, sometimes across large phylogenetic distances (Roberts *et al*., 2001a). The steps involve in the transposition and transfer of conjugative transposons was proposed by Salyers *et al*. (1995) and is illustrated

in Figure 1.1. The mechanism of integration and excision of conjugative transposons is mediated by either tyrosine recombinases (Landy, 1989), serine recombinases (Stark *et al*., 1992) or DDE transposase (Brochet *et al*., 2009), which were classified based on their evolutionary and mechanistic relatedness (Smith and Thorpe, 2002).

Table 1.1 Conjugative transposons family

Conjugative transposons	Original host	Size (kb)	Characteristics	Reference
Tn*916* family				
Tn*916*	*Enterococcus faecalis*	18.3	Confers tetracycline resistance	Franke and Clewell, 1981
Tn*925*	*Bacillus firmus*	18.0	Confers tetracycline resistance	Christie *et al*. 1987
Tn*1545*	*Streptococcus pneumoniae*	25.3	Confers tetracycline, kanamycin and chloramphenicol resistance	Courvalin and Carlier, 1986
Tn*2009*	*Streptococcus pneumoniae*	23.5	Confers tetracycline, erythromycin and macrolide resistance	Del Grosso *et al*. 2004
Tn*2010*	*Streptococcus pneumoniae*	26.3	Confers tetracycline, erythromycin and macrolide resistance	Del Grosso *et al*. 2006
Tn*2017*	*Streptococcus pneumoniae*	28.5	Confers tetracycline, erythromycin and macrolide resistance	Del Grosso *et al*. 2009
Tn*3872*	*Streptococcus pneumoniae*	23.3	Confers tetracycline and erythromycin resistance	McDougal *et al*. 1998
Tn*5386*	*Enterococcus faecium*	29.5	Confers immunity to subtilisin	Rice *et al*. 2007
Tn*5251*	*Streptococcus pneumoniae*	18.0	Confers tetracycline resistance	Ayoubi *et al*. 1991
Tn*5397*	*Clostridium difficile*	20.6	Confers tetracycline resistance	Mullany *et al*. 1990
Tn*6000*	*Enterococcus casseliflavus*	33.2	Confers tetracycline resistance	Brouwer *et al*. 2010

Conjugative transposons	Original host	Size (kb)	Characteristics	Reference
Tn*916* family				
Tn*6003*	*Streptococcus pneumoniae*	25.1	Confers tetracycline, erythromycin, kanamycin and MLS (macrolide, lincosamide and streptogramin B) resistance	Cochetti *et al*. 2008
Tn*6009*	*Klebsiella pneumoniae*	17.8	Confers tetracycline and mercury resistance	Soge *et al*. 2008
Tn*6087*	*Streptococcus oralis*	21.2	Confers tetracycline and CTAB (cetyltrimethylammonium bromide) resistance	Ciric *et al*. 2011
Composite conjugative transposon				
Tn*3701*	*Streptococcus pyogenes*	>50.0	Confers tetracycline and erythromycin resistance	Le Bouguènec *et al*. 1988
Tn*5252*	*Streptococcus pneumoniae*	47.5	Confers chloramphenicol resistance	Ayoubi *et al*. 1991
Tn*5253*	*Streptococcus pneumoniae*	65.5	Tn*5251* inserted into Tn*5252*	Ayoubi *et al*. 1991
Tn*5385*	*Enterococcus faecalis*	65.0	Confers tetracycline, erythromycin, gentamicin, mercuric chloride, streptomycin and penicillin resistance. Conjugation of this element may be due to a smaller conjugative element, Tn*5381* located within this element	Rice and Carias, 1998
Tn*5276*	*Lactococcus lactis*	70.0	Confers production and immunity to nisin and a sucrose metabolic pathway	Rauch and De Vos, 1992

Conjugative transposons	Original host	Size (kb)	Characteristics	Reference
Conjugative transposons from *Bacteroides*				
XBU4422	*Bacteroides*	65.0	Cryptic element	Bedzyk *et al*. 1992
Tc^r Em^r 7853	*Bacteroides*	70.0-80.0	A distinct class of *Bacteroides* conjugative transposons. Confers resistance to tetracycline and erythromycin	Nikolich *et al*. 1994
Tc^r Em^r DOT	*Bacteroides*	70.0-80.0	A distinct class of *Bacteroides* conjugative transposons. Confers resistance to tetracycline and erythromycin	Shoemaker *et al*. 1989
Other conjugative transposon				
Tn*4371*	*Ralstonia eutropha*	55.0	Confers biphenyl catabolism. Conjugative transfers has not been demonstrated although conjugative genes are present	Merlin *et al*. 1999
Tn*5301*	*Lactococcus lactis*	70.0	A distinct class of conjugative transposons. Confers nisin production and sucrose metabolism	Horn *et al*. 1991
CTn*scr94*	*Salmonella seftenberg*	100.0	Encodes a sucrose fermentation pathway	Hochhut *et al*. 1997
R391	*Proteus rettgeri*	93.9	Confers resistance to kanamycin and mercury	Murphy and Pembroke, 1995
SXT	*Vibrio cholerae*	62.0	Confers resistance to sulfamethoxazole, trimethoprim and streptomycin	Waldor *et al*. 1996

A. Intracellular transposition

B. Intercellular transposition

Figure 1.1 Intracellular and intercellular transposition of a conjugative transposon. (A) The integrated form of the conjugative transposon excises from the chromosome to form a covalently closed double-stranded and non-replicative DNA circular which is the

transposition intermediate. Filled boxes indicate the two ends of the conjugative transposon. Integration can occur into a chromosome or a plasmid. (B) The integrated form excises to form the transposition intermediate circle. The circular form is nicked at an *oriT* (filled circle) and a single strand is transferred by a similar process to plasmid transfer. The double-stranded form (dashed arrows) of the circular intermediate is regenerated in both donor and recipient cells, followed by integration. (Copied from Salyers *et al*., 1995)

1.4 Genetic organisation of Tn*916*

Tn*916* is an 18 kb conjugative transposon that was originally discovered in the chromosome of the hemolytic multidrug-resistant *Enterococcus faecalis* DS16 (Franke and Clewell, 1981; Flannagan *et al*., 1994). This element is the paradigm of a large family of conjugative elements, which are found in an extremely broad range of bacteria. Tn*916* has 24 open reading frames (*orf*s), which encode putative proteins ranging from 2.9 to 93.7 kDa in molecular mass (Clewell *et al*., 1995). Almost all known conjugative transposons from Tn*916* family confer tetracycline resistance via *tet*(M), either alone or associated with other resistance genes as reported in Tn*1545* (Courvalin and Carlier, 1986). However, an exception to this was observed for Tn*5386* from *E. faecium* which contains a series of ORFs with homology to lantibiotic immunity genes inserted into the same location where *tet*(M) is found in Tn*916* (Rice *et al*., 2007). Similarly, CTn*1* from *C. difficile* contains an ABC transporter inserted into the same location. Genes on Tn*916*-like elements are organized in modules, involved in the recombination, conjugation, regulation and accessory functions (Figure 1.2).

Figure 1.2 A schematic representation of Tn*916* showing the four functional modules: conjugation (blue); recombination (red); regulation (green) and the accessory gene *tet*(M) (grey). Arrow boxes represent the open reading frames (*orf*s) and the orientation of the genes. Filled triangle represents the position of the *ori*T (origin of transfer), which is the conjugation-nicked-site. (Adapted from Roberts and Mullany, 2009)

1.4.1 Recombination of Tn*916*

The first step in the conjugative transposition of Tn*916* involves the staggered endonucleolytic cleavages at each ends of the transposon. These cleavages generate a 6 bp protruding 5'-hydroxyl ends termed coupling sequences (Rudy and Scott, 1994; Manganelli *et al*., 1996; Marra and Scott, 1999). The non-complementary sequences are then joined, resulting in a circular intermediate molecule with a heteroduplex at the circle joint (Caparon and Scott, 1989). The double stranded circular intermediate is nicked at the origin of transfer (*oriT*) site (represented by black triangle in Figure 1.2) (Jaworski and Clewell, 1995) and a single strand of the circularised transposon is transferred to the recipient, where the complementary strand is synthesised. Scott *et al*. (1994) has postulated that this transfer process is somewhat similar to the process that occurs during transfer of plasmids. Integration of Tn*916* into a target site can be visualised as a reversal of the excision process with an AT rich region becoming the preferred target site (Clewell *et al*., 1995; Lu and Churchward, 1995).

Studies by Scott *et al*. (1994) and Nelson *et al*. (1997) have postulated that a conserved sequence of Tn*916* target sites in multiple mutants examined is TTTTTnnnnnnAAAAA, with the 6 "N's" can be any of the four bases. Further to this, study by Cookson *et al*. (2011) has shown that the consensus sequence TTTTT*TATATA*AAAAA (the italicised hexanucleotides is variable and forms the

coupling sequence) is used by Tn*916* for integration in 123 insertion sites in *Butyrivibrio proteoclasticus* strain B316^{T}. More recently, Mullany *et al*. (2012) indicates that Tn*916* has preferentially inserted the genome of *C. difficile* strains 630 and R20291 at an intergenic regions, with a consensus sequence of 5'-TTTTTA[AT][AT][AT][AT]AAAAA. Integration of Tn*916* into the target site involves a formation of heteroduplex regions on either side of the conjugative transposon. These mismatched bases are either resolved during replication or corrected by DNA repair (Manganelli *et al*., 1997).

Ultimately, the ability of Tn*916* to transpose inter- and intracellularly is mediated by two transposon-encoded proteins; integrase (Int) and excisionase (Xis) (Jaworski *et al*., 1996; Rudy *et al*., 1997). In Tn*916*, the genes that encode for these proteins are located at one end of the element (Figure 1.2). Int and Xis are required for excision and integration, whereas only Int is required for integration (Storrs *et al*., 1991). Int is a member of tyrosine recombinases family and belongs to a distinct subgroup of heterobivalent recombinases which perform highly directional recombination reactions (Abani *et al*., 2005). Xis is a small and highly basic (p*I*=9) protein of 67 amino acids (Rudy *et al*., 1997) and modulates the recombination by either facilitating or preventing the binding of Int to sites required for recombination (Abbani *et al*., 2005).

1.4.2 Conjugation of Tn*916*

Conjugation of Tn*916*/Tn*916*-like elements contributes to the dissemination of antibiotic resistant genes among various Gram-positive and Gram-negative bacteria. Despite the fact that the specific mechanism of conjugation of these elements is somewhat limited, a study by Senghas and co-workers (1988) using Tn*5* (a non-conjugative transposon) mutagenesis has suggested that *orf24* to *orf13* are involved in this process (Figure 1.2). This study however, did not complement the Tn*5* insertions to exclude the polar effects. The *orf*s spanning the conjugation region of Tn*916* has been studied widely, and thus the specific functions of these proteins or homologs of these proteins are shown in Table 1.2.

The initial step in conjugation of Tn*916* requires Orf20 to nick a sequence known as *oriT*. Orf20 is the Tn*916* relaxase protein and the gene is situated downstream of its cognate *oriT* (Rocco and Churchward, 2006). The *oriT* sequence of Tn*916* is a 466 bp in length, containing 6 sets of inverted repeats and lies within the intercistronic space that separates *orf21* and *orf20* (Jaworski and Clewell, 1995). Interaction between the *oriT* and the Tn*916* tyrosine recombinase has also been demonstrated,. This interaction has been postulated to prevent premature transfer of the element (Rocco and Churchward, 2006).

Table 1.2 Known (experimentally proven) functions of *orfs* within Tn*916* conjugation module (Adapted from Ciric *et al*. 2011)

Coding region	Closest Homolog	Accession number	Function	Reference
orf21	*Streptococcus agalactiae* 2603V/R Tn*916*, FtsK/SpoIIIE family protein	NP_687949	FtsK/SpoIIIE family protein required for DNA segregation during cell division	Wu and Errington, 1994
orf20	*Streptococcus pneumoniae* putative conjugative transposon initiation factor	CBW39427	Endonuclease which cleaves Tn*916* at *ori*T	Rocco and Churchward, 2006
orf18	*Ureaplasma urealyticum* serovar 9 str. ATCC 33175 conjugative transposon protein	ZP_03079519	Anti-restriction protein responsible for DNA restriction immunity (Ard)	Serfiotis-Mitsa *et al*. 2008

1.4.3 Regulation of Tn*916*

Knowledge about the regulation of Tn*916*/Tn*916*-like elements is almost completely limited to Tn*916*. The regulatory model of Tn*916* has never been experimentally proven, although it is fundamentally important. The proposed regulatory region of Tn*916* consists of *orf12*, *orf9*, *orf7* and *orf8* (Figure 1.2). The regulatory region of Tn*916* is conserved in nearly all Tn*916*-like elements, suggestive of the important of this region in the transcriptional regulation of these elements (Roberts and Mullany, 2009; Ciric *et al*., 2011).

The *orf12* located upstream of *tet*(M) is an 86 bp open reading frame corresponding to a 28 kDa protein. It encodes rare amino acids and several inverted repeat sequences that would form hairpins in mRNA followed by uridine residues. The run of uridines has been proposed to be a rho factor-independent transcriptional terminator (Su *et al*., 1992). Regulation of Tn*916* involves an interaction between the ribosomes with tetracycline, which results in the destruction of the transcriptional terminator. This regulatory mechanism is known as transcriptional attenuation (described in Section 1.8.1.2.3) (Su *et al*., 1992).

In the presence of tetracycline, most ribosomes are inactivated by the reversible binding of tetracycline. This event retards the protein synthesis, thus results in the build-up of charged tRNA molecules. At this stage, a few ribosomes remain active

Figure 1.3 Structure of various members of the Tn*916*/Tn*916*-like elements. Functional modules are represented as shown in the key. The organisms from which the elements were isolated are shown at the left end. Mobility of the elements is denoted by a capital M on the right. (Taken from Roberts and Mullany, 2009).

due to the protection by the low and basal level of Tet(M). The increased availability of the charged tRNA molecules enables a more rapid translation of *orf12* by these protected ribosomes. Additionally, this event increases the rate of protein translation, which is normally slow due to the presence of rare codons in *orf12*. The ribosomes are predicted to catch up the RNA polymerase (RNAP) and prevent the formation of or destroy the terminator structures (designated 5S:6S and 7:8 in Figure 1.4. Transcription therefore proceeds from the promoter upstream of *orf12* and extends into, and through, *tet*(M) and into the downstream genes.

However, under normal growth conditions, where the tetracycline is absent, the ribosomes pauses on the leader sequences of *orf12*. This is due to the shortage of tRNA molecules for the rare codons within *orf12* (Figure 3.1). As a result, the ribosome lags behind the extending RNAP allowing the formation of the predicted strong 5S:6S terminator and/or the weaker 7:8 terminator. At this stage, the majority of transcripts are terminated. This event results in a limited expression of Tet(M), due to a basal level of read-through transcription of the termination site. These terminators are not likely to be 100% efficient as in some instances, the RNAP escapes the termination site (Du and Babitzke, 1998) and leads to the transcriptional read-through into *tet*(M). As it has been postulated that the synthesis of Tet(M) could still occur without the translation of the leader peptide (since free ribosomes are able to bind to *tet*(M) Shine-Dalgarno site) (Su *et al*., 1992), therefore this event might be of important particularly in maintaining the basal level of Tet(M) under drug-free conditions.

Figure 1.4 The alternative secondary structures that are predicted to form in mRNA of Tn*916*. The stem-loops 1:2, 3:4 and 5S:6S are mutually exclusive of structure 5L:6L. The free-energy values of each structure are shown in kcal mol^{-1}. The red-shaded area represents the *orf12*. The Shine-Dalgarno sequences are underlined and labeled. The start codon of *tet*(M) is shaded yellow. The structures which include the terminators are labeled (T). (Copied from Roberts and Mullany, 2009)

Transcriptional analysis by Celli and Trieu-Cout (1998) revealed that other than Ptet(M), Tn*916* also contains another three promoters, namely Porf7, Porf9 and Pxis. In the absence of tetracycline, transcription through *orf9* is proposed to produce an antisense RNA, which results in the downregulation of Porf7. This will have an effect of reducing the transcription of *orf7*, *orf8* and downstream genes. However, when tetracycline is present, *orf9* is transcribed at a lower level as antisense *orf9* RNA is produced from the transcription initiating at the promoter upstream of *tet*(M) leading to an upregulation of Porf7. This led to an increased transcription of *orf7*, *orf8* and downstream genes as Orf7 is predicted to upregulate its own promoter. (Figure 1.5).

The translation rate will return to the previous level once the majority of the ribosomes are protected by Tet(M). At this stage, the level of charged tRNAs is smaller as most of them are being used by the protected ribosomes, which in turn leads to a slower translation rate. The ribosomes translating the *orf12* will once again lag behind the transcribing RNAP, enabling the formation of the terminator structures, thus reducing the transcription of *tet*(M). This regulatory system allows the cell to sense the presence or absence of tetracycline, and react either by downregulating or upregulating the transcription and translation of Tn*916* (Su *et al*., 1992; Celli and Trieu-Cout (1998).

Figure 1.5 Regulation of expression of the transfer genes within Tn*916*. ORFs are represented by block arrows, pointing towards the probable direction of transcription. The transcription level was presented by the thick and thin arrows, which denoted the higher and lower transcription, respectively. In the absence of tetracycline (-Tc), most of the transcripts initiated at Ptet terminate at Pal*orf12*. P*orf9* transcribes the *orf9* gene efficiently, while P*orf7* directs a low level of transcription through *orf7* and *orf8*. In these conditions, P*orf7* and P*xis* direct a low level of transcription through the transposition and downstream genes. In the presence of tetracycline (+Tc), the transcripts initiated at the Ptet read-through the Pal*orf12*, Pal*orf10*, Pal*orf7*and Pal*orf8*. This condition decreased the transcription of *orf9* genes from the P*orf9* and increased transcription of *orf7* and *orf8* from the P*orf7*. The resulting overexpression of ORF7 and ORF8 stimulated the activity of P*orf7*, thus leads to an increased transcription of downstream genes. Orf9 could repress the activity of P*orf7*. (Copied from Celli and Trieu-Cuot, 1998)

Regulation of Tn*916* is not necessarily dependent on the presence or absence of tetracycline but the key event to this mechanism is the change in the translation rate, which is associated with the level of charged tRNA (Roberts and Mullany, 2009). An increased amount of charged tRNA is likely to result in the upregulation of the majority of Tn*916* genes. Based on this fact, any malfunction in the cell's translational apparatus will lead to a drop in the translational rate, and thus increase the tRNA concentration. This event is expected to be deleterious to the cell. Upon sensing this cellular distress, Tn*916* will then activate its own transcription and movement.

1.4.4 Accessory genes of Tn*916*

Accessory genes that include antibiotic resistance determinants have been demonstrated to confer evolutionary advantages on the host cells. In Tn*916*, an antibiotic resistance gene, *tet*(M) which encodes for tetracycline resistance determinant is present (Flannagan *et al*., 1994). This gene is replaced by a variety of other accessory genes in other elements as shown in Figure 1.3. The *tet*(M) gene was identified as a coding sequence corresponding to a 72 kDa protein (Su *et al*., 1992). Other accessory genes such as *erm*(B) (encodes for erythromycin resistance), *mef*(E) (encodes for macrolide efflux pump protein) and ABC transporters are also present in Tn*916*-like elements, sometimes replacing *tet*(M) (Figure 1.3).

1.5 Genetic organisation of Tn*5397*

Tn*5397* is a 21 kb conjugative transposon originally identified in the Gram-positive pathogen *C. difficile* 630 (Mullany *et al*., 1996). Tn*5397* which was first named Tc-CD confers tetracycline resistance via *tet*(M) (Mullany *et al*., 1990). This element is closely related to Tn*916* in the central regions that are involved in conjugation, however the regions required for transposition are completely different. In Tn*5397*, the excision and integration mechanism are dependent on a large resolvase subgroup of site-specific recombinases, termed TndX which was encoded by *tndX* located at one end of this element (Figure 1.6). Another characteristic that distinguishes Tn*5397* from Tn*916* is the presence of a group II intron, inserted within *orf14* of Tn*916* (Mullany *et al*., 1996).

1.5.1 Recombination of Tn*5397*

Sequence analysis of the ends of Tn*5397* has shown that this element contains a gene, *tndX* that encodes for a large serine recombinase TndX, which is a member of the resolvase family of site-specific recombinases (Wang *et al*., 2000). TndX is a 61.5 kDa protein and is closely related to TnpX resolvase from Tn*4451* of *C. perfringens* (Bannam *et al*., 1995) with 37% identity and 61% similarity (Wang *et al*., 2000). TndX mediates recombination via a concerted cleavage and rejoining mechanism, as described for the resolvase/invertases (Stark *et al*., 1992).

Figure 1.6 A schematic representation of Tn*5397* showing the four functional modules: conjugation (blue); recombination (red); regulation (green) and the accessory gene *tet*(M) (grey). Arrow boxes represent the open reading frames (*orf*s) and the orientation of the genes. Filled triangle represents the position of the *ori*T (origin of transfer), which is the conjugation-nicked-site. A group II intron is inserted into *orf14*. (Adapted from Roberts and Mullany, 2009)

TndX promotes the excision of Tn*5397* by introducing 2 bp staggered cuts at the 3' ends of the directly repeated GA dinucleotides at each end of the transposon. Excision of the transposon as a circular intermediate and regeneration of the original target site occurs during strand exchange. A circular intermediate of the transposon is formed by ligation of the two ends. A single strand of the circular intermediate can then be transferred to a new host by conjugation. Integration of Tn*5397* into the new genome occurs when TndX promotes a site-specific recombination with the joint of the circular intermediate. This event extended upon recognition of a suitable target site that contains a central GA dinucleotide at the crossover site within the target genome (Wang *et al*., 2000; Wang *et al*., 2006). Strand exchange and ligation result in the site-specific integration of Tn*5397* to the target genome flanked by directly repeated GA dinucleotides.

1.5.2 Conjugation of Tn*5397*

As previously described, Tn*5397* and Tn*916* are closely related despite several insertions and deletions in Tn*5397*. The left end of Tn*5397* showed an absence of the first 201 bp of Tn*916* sequence and was replaced by 180 bp of unrelated DNA sequence. This has result in the deletion of *orf24*. Since no studies have been carried out confirming the functional role of this open reading frame, the specific effect of this deletion to the transfer of Tn*5397* is undetermined. The other major difference between Tn*916* and Tn*5397* is the presence of a group II intron in the reading frame analogous to *orf14* of Tn*916* (Figure 1.6) (Roberts *et al*., 2001b).

Group II introns are a class of genetic element, categorised by their secondary structure which is essential for splicing via RNA-catalysed pathways (Michel and Ferat, 1995). Group II introns are also capable of moving from an intron-containing allele to an intronless allele (a process called homing) at high frequency and to ectopic sites at a much lower frequency (Belfort and Perlman, 1995; Michel and Ferat, 1995). The intron within Tn*5397* has been postulated to encode a multifunctional protein; maturase, reverse transcriptase and endonuclease which are required for splicing, homing and transposition activities (Mullany *et al*., 1996).

1.5.3 Regulation of Tn*5397*

The regulatory region of Tn*5397* has an 84 bp deletion effectively removing the leader peptide *orf12* (Roberts *et al*., 2001b). This deletion disrupts one of the predicted terminators (5S:6S) (Figure 1.4) that is predicted to be crucial for regulation of *tet*(M) in Tn*916* (Su *et al*., 1992). This deletion also results in the formation of two alternatives orfs; *orf25* and *orf26* (Roberts *et al*., 2001b). Although knowledge about the regulatory mechanism of Tn*5397* is somewhat limited, studies have shown that despite the differences between the regulatory region of Tn*5397* and Tn*916*, the expression of tetracycline resistance determinant, Tet(M) is still inducible, as determined by comparative growth curve analysis and reverse transcriptase PCR (Roberts, 2001).

1.6 Ribosomal protection proteins

Ribosomal protection-mediated tetracycline resistance was first discovered in streptococci (Burdett, 1986). There are 11 ribosomal protection proteins (RPPs) identified to date with Tet(O) and Tet(M) being the best studied of these determinants (Connell *et al*., 2003). RPPs confer resistance to tetracycline through interactions with the ribosome, thus prevent the antibiotic from binding to the ribosome (Burdett, 1990). These proteins are hypothesised to interact with the base of h34 protein within the ribosome and initiate an allosteric disruption of the primary tetracycline binding sites, thereby freeing the ribosomes from the inhibitory effects of tetracycline (Connell *et al*., 2003). Protein synthesis resumes as the ribosomes return to its normal conformation. However, it is unknown whether the ribosomal proteins actively prevent reattachment of the tetracycline after they have been released.

A new class of tetracycline resistant determinant primarily encodes for RPPs has been discovered. These genes arise by recombination between the wild type resistant determinants, predominantly the *tet*(M), *tet*(W) and *tet*(O) genes. Although these hybrid genes demonstrated different mosaicism, the final size of the genes remains the same. The best example is *tet*(O/32/O), which has *tet*(32) sequence in the central region and flanked by *tet*(O) sequence. Some mosaic genes confer higher resistant level than the wild type as seen in *tet*(O/W/O), with

resistance level of 128 to >256 μg ml^{-1} as compared to 64 μg ml^{-1} conferred by *tet*(O) or *tet*(W) genes (Stanton *et al*., 2004). Recently, two mosaics *tet*(S/M) were identified in *Streptococcus bovis* and *S. intermedius* (Barile *et al*., 2012; Novais *et al*., 2012). In *S. bovis*, this hybrid was mainly composed of Tet(M) whereas Tet(S) dominated the sequence in *S. intermedius* (Novais *et al*., 2012). Although the role of mosaic genes remains unclear, they have been shown to be widespread and abundant (Patterson *et al*., 2007) which suggested that their presence in the environment are prevalent and significant, thus should be considered in future surveillance programs (Thaker *et al*., 2010).

1.7 Bacterial gene expression

Gene expression involves two consecutive steps; transcription and translation in which the information is converted from one form to another. Transcription produces a complementary RNA copy of one strand of a DNA duplex, which is catalysed by RNA polymerase (RNAP). RNAP is the key enzyme of gene expression and regulation not only in bacteria, but also in eukaryotes and archaea (Borukhov and Nudler, 2008). The complete RNAP or holoenzyme consists of six subunits ($\alpha_2\beta\beta'\sigma\omega$) and can be separated into two components, the core enzyme ($\alpha_2\beta\beta'\omega$) and the sigma factor (the σ polypeptide), which is devoted to direct the core RNAP to specific initiation sites called promoters (Wigneshweraraj *et al*., 2008; Krebs *et al*., 2010). The transcription reaction is divided into three stages; initiation, elongation and termination as illustrated in Figure 1.7. Initiation of transcription

Figure 1.7 Main features of bacterial transcription. Transcription involves three stages; the RNA polymerase binds to the promoter and unwound the DNA to form an open complex, moves along the DNA template during elongation and dissociates at terminator site. (Adapted from Dale and Park, 2010)

involves the binding of an RNAP to the double-stranded DNA at promoters. The start point of transcription is assigned as +1 and the value increases as they go downstream. The elongation step occurs in a 5’ to 3’ direction as the RNAP covalently adds ribonucleotides to the 3’-end of the growing single-stranded RNA chain. As the enzyme moves, it unwinds the duplex DNA, separating the DNA strands thus exposing the template strand for ribonucleotide base pairing. The DNA duplex is reformed behind the RNAP. The termination of transcription involves recognition of a specific DNA sequence known as terminator. At this point, no further bases should be added to the RNA chain, thus the enzyme and the synthesised RNA dissociate from the DNA template strand allowing reformation of DNA duplex. The synthesised RNA is called a transcription unit, and encodes either protein coding RNA (mRNA) or non-coding RNAs (rRNA and tRNA).

In translation, the messenger RNA (mRNA) which carries the information for a specific amino acid sequence in the form of genetic code is decoded by the ribosome. The mRNA is read in a group of 3 nucleotides (Crick *et al*., 1961) or codons, deriving a specific amino acid chain or polypeptide that will later fold into an active protein. The protein translation involves four stages; initiation, elongation, translocation and termination. In the initiation step, the 30S subunit of the ribosome binds to a specific sequence on the mRNA, known as the ribosome binding site (RBS) followed by association of the charged-initiation tRNA with the start codon (AUG, GUG or CUG). The 50S subunit then attaches to this complex and initiates the translation. The initiation step is modulated by the activation of non-

ribosomal proteins known as initiation factors that regulate the binding of mRNA to the ribosomal complex. The assembled ribosome has two tRNA-binding sites called A- and P-sites. The aminoacylated tRNA normally binds to the A-site, while their anticodon region pairs with the mRNA. The tRNA moves to the P-site once the peptide bond is formed. Movements of tRNA from A-site to P-site are called translocation. The ribosomes move along the mRNA, translating it into amino acids until one of the three termination codons (UAA, UAG or UGA) appears in the A-site. At this point, the polypeptide chain is released and the ribosome dissociates from the mRNA, with the aid of the protein factors called release factors.

1.8 Regulation of gene expression

Regulation of gene expression in bacteria is essential to control the way that the information in genes is turned into gene products in response to environmental changes. Bacterial cells have evolved many different complex mechanisms to regulate the transcription and translation of genes (Gollnick and Babitzke, 2002). A number of studies have shown that the principal in the regulatory event in most organisms is at the level of transcription initiation (Gollnick and Babitzke, 2002; Henkin and Yanofsky, 2002; Naville and Gautheret, 2009) although there are numerous essential regulatory factors that are also involved such as gene copy number, stability of the mRNA and post-translational modification (Dale and Park, 2010).

1.8.1 Transcriptional control

Transcriptional regulation is one of the major mechanisms used by bacteria to control the gene expression. The regulation of gene expression has been identified for all three stages of transcription; initiation, elongation and termination. At the transcription initiation level, the efficiency of genes being transcribed is determined by the affinity of RNAP for the promoter (Busby and Savery, 2007). This regulatory mechanism involves a number of regulatory factors, of which promoters are particularly important. Once transcription is initiated the nascent transcripts may fold into specific secondary structures that signal the transcribing RNAP to pause or terminate transcription. This post-initiation regulatory mechanism is categorised as transcription termination.

1.8.1.1 Transcription initiation

1.8.1.1.1 Promoter activity

Earlier work on gene regulation focused interest on promoters involves in the transcription initiation (Cheng *et al*., 1991), which is the primary stage in the regulation of gene expression in bacteria. Bacterial promoters have a conserved sequence that constitutes a recognisable signal for RNAP to bind and form an open complex. There are four conserved features in bacterial promoters that specify the initial binding of RNAP; the -35 and -10 hexamers, the distance between -35 and -10

hexamers, and the AT rich region located upstream of the -35 hexamer (UP element) (Hawley and McClure, 1983; Ross *et al*., 1993; Krebs *et al*., 2010). The -35 and -10 hexamers are named for their locations that are centred at 35 and 10 bp upstream of the +1 transcription start site (TSS) (Harley and Reynolds, 1987). The consensus sequences of -10 and -35 are TTGACA and TATAAT, with a few exceptions. It has been postulated that the strong promoters tend to have a sequence close to this consensus, and function more efficiently (Browning and Busby, 2004). The distance separating the -35 and -10 hexamers is crucial as it holds the two motifs at the appropriate separation for an efficient contact with the RNAP. The optimal distance is between 16-18 bp, and spacing outside this range leads to the inefficient contact between the RNAP and the promoters as the contact points would not lie on the same side of the DNA helix (Figure 1.8) (Harley and Reynolds, 1987). UP element interacts with the α subunit of RNAP and facilitate the initial binding of RNAP to the promoter (Rao *et al*., 1994; Strainic *et al*., 1998). In fact, the presence of UP element in some promoters (e.g. *rrnB* P1 of *E. coli*) has been shown to increase the frequency of transcription 30-90 fold (Estrem *et al*., 1998; Dale and Park, 2010).

Figure 1.8 Importance of the distance separating the -35 and -10 regions of a promoter. A. An optimal distance (16-18 bp) between -35 and -10 is crucial for an efficient contact with the RNAP. B. An increase in the spacing leads to inefficient contact between the RNAP and the promoter. (Adapted from Dale and Park, 2010)

1.8.1.1.2 Alternative promoters and σ factors

During transcription initiation, the σ factor binds to the core RNAP to form a holoenzyme, which recognises the hexameric promoter elements by the consensus sequences, thus determines the specificity of RNAP (Dombroski *et al*., 1992). The promoter consensus described above is recognised by the primary σ factor, σ^{70} helps the RNA polymerase transcribe most genes required in exponentially growing cells (Saitoh and Ishihama, 1977). However, most bacterial species possess several different σ factors, which in turn results in recognition of distinct promoter sequences by the RNAP (Table 1.3). These alternative σ factors control the expression of genes in bacteria as a response to the environmental conditions and stresses.

The initial binding of the holoenzyme to the promoter leads to the formation of the closed binary complex in which the promoter DNA remains duplex. The closed complex is converted into an open complex via isomerisation process, which separate the DNA duplex from position -11 to +4, overlapping the -10 hexamer (Paget and Helmann, 2003). After a nascent RNA of 8-10 nucleotides has been synthesised, the σ factor is no longer necessary, thus released to allow elongation to proceed and RNAP to escape the promoter (Paget and Helmann, 2003). In some cases, however, the σ factor remains associated with the RNAP throughout the elongation process, which suggested that this factor does not need to be released

Table 1.3 Alternative promoters and σ factor sequences.

-35 region	Spacer (bp)	-10 region	Sigma factor	Regulated genes	Reference
TTGACA	16-18	TATAAT	σ^{70}	General housekeeping genes	Gruber and Gross, 2003
CTTGAAA	13-15	CCCATNT*	σ^{32}	Heat-shock genes	Arsene *et al*. 2000
CTGGNA	6	TTGCA	σ^{54}	Nitrogen-assimilation genes	Studholme and Buck, 2000
		CTACACT	σ^{38}	Stationary-phase/general stress genes	Tanaka *et al*. 1995
GTTTAA	12-14	GGGTAT	σ^{B}	General stress genes*	Hecker and Volker, 2001
TAAA	15	GCCGATAA	σ^{28}	Flagellum genes	Liu and Matsumura, 1995

*Present in *B. subtilis*. All others are in *E. coli*

*N=A, T, C or G

from the core RNAP upon the transition from initiation to elongation process (Mukhopadhyay *et al*., 2001).

1.8.1.2 Transcription termination

Bacteria use two different strategies to regulate the gene expression at the level of transcription termination; rho-independent or intrinsic termination and rho-dependent termination (Henkin and Yanofsky, 2002).

1.8.1.2.1 Rho-independent termination

Intrinsic terminators, which are hypothesized to play a major role in the transcriptional attenuation mechanism described above, are encoded in the genome of most prokaryotes and are used to signal transcription termination at the end of a gene and as control elements in the attenuators that are found just downstream of the promoters (Greenblatt, 2008). These terminators consist of a GC rich hairpin in the secondary structure followed by a series of uridine residues (d' Aubenton Carafa *et al*., 1990). In intrinsic termination, the RNA transcribed from the inverted palindrome DNA template folds into a stable hairpin, thus favouring the RNA-RNA interaction over the RNA-DNA interaction that normally occurs during transcription elongation (Figure 1.9). The hairpin is thought to interact with the transcribing RNAP, causing it to pause at the terminator site. The elongation factor,

Figure 1.9 Intrinsic or rho-independent termination. Dashed arrows show inverted repeat sequences, that when transcribed into RNA, fold into a stable hairpin structure with a stem and a loop. This structure is normally followed by a series of uridine (U) residues. Interaction between the hairpin structure and the transcribing RNAP leads to pausing of the RNAP. The U residues downstream of the structure destabilises the RNA-DNA hybrid during the pausing time, allowing the transcription complex to disassemble and terminates the transcription.

NusA that bound to the RNAP stabilises this interaction, thus increases the pausing time and creates an opportunity for termination to occur. The downstream uridine residues destabilise the RNA-DNA hybrid when RNAP pauses at the hairpin. The rU-dA interactions are extremely unstable and less energy is required for dissociation of this RNA-DNA hybrid. When the RNAP pauses at the hairpin structure, the weak rU-dA terminal region unwind hence terminates the transcription completely (Krebs *et al*., 2010).

1.8.1.2.2 Rho-dependent termination

In rho-dependent termination, a protein called rho factor is required to terminate the RNA synthesis at the termination sites. Rho factor is a hexameric ATP-dependent helicase (Platt and Richardson, 1992) that binds to the specific recognition sequences in RNA called rho utilization (*rut*) site and tracks along the RNA in a 3' direction until it catches up the RNAP. The *rut* site is identified as a cytosine-rich sequence, approximately 70-80 bp in length and has no secondary structure (Guérin *et al*., 1998). Once the RNAP reaches the termination site, it pauses and allows time for the rho protein to translocate to the RNA-DNA hybrid region and starts to unwind the hybrid at the active site of RNAP, causing dissociation of the RNA transcript. Figure 1.10 illustrates the mechanism of rho-dependent termination.

Figure 1.10 Mechanisms of rho-dependent termination. Rho factor binds to the rho-utilization site (*rut*) on mRNA and moved along the transcript in a 3' direction. At the terminator stem loop structure, the Rho factor is able to catch up the paused RNAP. Rho then unwinds the RNA-DNA hybrid in the transcription bubble which results in the disassociation of all components hence terminate the transcription.

1.8.1.2.3 Transcription attenuation

Other mechanism used by bacteria to control the gene expression is attenuation. Attenuation causes premature termination of RNA transcription at the beginning of a transcription unit (Naville and Gautheret, 2009). This mechanism which is controlled by external events are responsible in regulating the formation of the hairpin needed for transcription termination. At present, a number of attenuation mechanisms have been identified and these include the attenuation-based RNA thermometers, riboswitches, T-boxes, amino acid operon leaders and by RNA-protein interactions (Figure 1.11) (Naville and Gautheret, 2009).

In the attenuation-based RNA thermometers system, bacteria regulate gene expression using RNA sequences that change their conformation in response to temperature. The three major temperature-responsive genes classes that have been identified are virulence genes, heat shock genes and cold shock genes (Naville and Gautheret, 2009; Kortmann and Narberhaus, 2012). At low temperature, the RNA thermometers fold into a structure that entirely or partially includes the 5' untranslated region (5' UTR) of an mRNA, thus control the accessibility of ribosomes for the Shine-Dalgarno sequence. As the temperature gradually shifts, the terminator structure melts, and permits ribosome access thereby increasing the efficiency of translation initiation.

Figure 1.11 Mechanisms of transcription attenuation in bacteria. (A) Riboswitch. Small ligands bind directly to the RNA aptamer. The concentration of ligand decides whether the riboswitch should fold into a terminator (red) or and antiterminator structure (dashed arrow). (B) T-box. The specific uncharged tRNA interacts with the T-box and leads to the formation of antiterminator structure (dashed arrow). The charged tRNA is unable to bind to the T-box, thus the terminator (red) forms. (C) Amino acid operon leaders. The alternative folding into a terminator (red) or an antiterminator (dashed arrow) is determined by the translation rate of the ORF (short arrow) which in turn depends on the concentration of the corresponding charged tRNAs available. (D) RNA-protein interactions. The alternative terminator/antiterminator folding is controlled by interaction with and RNA-binding protein. (Adapted from Naville and Gautheret, 2009)

Riboswitches are complex folded RNA domains that undergo allosteric structural changes in response to particular metabolites, leading to premature transcription termination. Riboswitches can detect a variety of metabolites which include amino acids and derivatives, nucleotides and derivatives (Sudarsan *et al*., 2008), sugars, vitamin cofactors (Regulski *et al*., 2008) and metal ions (Dann *et al*., 2007). These regulatory elements comprise of a receptor (aptamer) which is the metabolite-binding domain and an expression platform that undergo conformational switch in response to the changes in the aptamer (Narberhaus *et al*., 2005). Most riboswitches have an inhibitory effect in the bound state, although in certain instances, metabolites binding leads to the formation of a structure that interferes with the terminator (Mandal and Breaker, 2004).

T-boxes regulate gene expression using uncharged tRNA as the signal molecule for structural shift. T-boxes are normally found in the 5' UTR of genes concerned with aminoacyl-tRNA synthetases, or related amino acid metabolism in Gram-positive bacteria, especially *Firmicutes* (Vitreschak *et al*., 2008). These elements can fold into two alternative hairpin structures, an intrinsic transcription terminator that results in a premature termination or an antiterminator that allows continued transcription into the downstream genes. The specific pairing of T-box and an uncharged tRNA stabilises the alternate antiterminator structure, thereby preventing transcription termination (Gutiérrez-Preciado *et al*., 2009). Antitermination forms when there is high level of uncharged tRNA, which leads to an increase in the concentrations of charged tRNA for protein synthesis.

Transcription attenuation by the amino acid operon leaders involves the leader peptide as the sensor element which can fold to form two alternative hairpin structures, a terminator or an antiterminator (Henkin and Yanofsky, 2005). This leader peptide contains codons for a specific amino acid and is located between the TSS and the start of the first structural gene. The terminator is formed when there is excess amino acids and therefore of the charged cognate tRNAs in the cell. This leads to ribosomal read-through and an efficient translation of the leader peptide, which prevent the formation of antitermination. Alternatively, a shortage of charged tRNA in the cell causes ribosome to pause on the leader peptide, thus lagging behind the transcribing RNAP. This leads to the formation of a terminator and subsequent transcription termination (Naville and Gautheret, 2009). As this system exploits the ribosome as a mediator to sense the charged tRNA, it is therefore known as ribosome-mediated transcription attenuation (Lyubetskaya *et al*., 2003; Merino and Yanofsky, 2005) and examples of resistance genes that are regulated by this mechanism are the chloramphenicol (*cat*) (Lovett, 1990; Moffat *et al*., 1994) and erythromycin (*erm*) (Gryczan *et al*., 1980; Min *et al*., 2008) genes.

The transcription attenuation mediated by the RNA-protein interactions is differ from the previous attenuation mechanism in such a way that the decision to terminate transcription or to read-through into the structural genes is determined by the sequence specific RNA-binding proteins. An excess of amino acid activates the RNA-binding protein, leading to its binding to the 5’ antiterminator hairpin. The free 3’ segment concurrently paired with the adjacent RNA segment and form a

terminator and so the transcription halts in the leader region. Instead, under conditions of limiting amino acid, the RNA-binding protein does not bind to the nascent RNA transcript, therefore an antiterminator is formed, allowing transcription of the downstream structural genes (Gollnick and Babitzke, 2002).

1.8.1.2.4 Tryptophan (*trp*) operon

The tryptophan (*trp*) operon, was first described by Yanofksy (1981) is a group of structural genes that regulate the biosynthesis of tryptophan in the cell. This operon contains a 162 bp leader sequence that lies between the transcription start site (TSS) and the start of the structural gene, *trpE* (Figure 1.12 A). The leader sequence is able to form several alternative base-paired conformations under different conditions as illustrated in Figure 1.12 B. In between the leader peptide, they are two tryptophan codons that require the presence of tryptophan within the cell to be incorporated into the peptide.

When tryptophan is absent or limited, the ribosomes stall at the *trp* codons which is part of region 1. The presence of ribosomes at this point sequesteres region 1, thus preventing it from base-pairing with region 2. This means that region 2 is able to form a stem-loop structure by base-pairing with region 3. As this structure is not a terminator, the transcription is continues to express the *trp* operon.

In the presence of sufficient tryptophan, ribosomes are able to proceed through the leader peptide until they reach the stop codon, which lies between regions 1 and 2. As the ribosomes occupy this position, region 2 is therefore prevented from forming a stem-loop structure with region 3. This allows regions 3 and 4 to form a termination stem-loop and leads to transcriptional termination. The presence of tryptophan therefore prevents the expression of the *trp* operon.

Figure 1.12 Transcriptional attenuation in the *trp* operon. A. Organisation of the *trp* operon of *E. coli*. The *trp* operon consists of structural genes preceded by a control region including

attenuator. The leader peptide of *trp* operon consists of 14 amino acids, with two successive codons for tryptophan (single letter codes: M: methionine; K: lysine; A: alanine; I: isoleucine; P: proline; V: valine; L: leucine; G: glycine; W: tryptophan; R: arginine; T: threonine and S: serine. B. Attenuation of *trp* operon. The four regions can base pair. Region 1 complementary to region 2, which is complementary to region 3, which is complementary to region 4. (I) In the absence of protein synthesis, conformations 1:2 and 3:4 are able to form, thus lead to transcriptional termination. (II) When tryptophan is limited, ribosome stalls at the *Trp* codons, and thus region 1 cannot base pair with region 2. This allows region 2 and region 3 to base pair, preventing the terminator hairpin from forming, allowing RNA polymerase to read through the attenuator and continues the transcription. (III) When tryptophan is abundant, ribosomes are able to synthesise the leader peptide, and proceed to the UGA codon within region 1 and region 2, thus preventing it from base pairing with region 3. The terminator hairpin forms via base pairing between the free-region 3 and region 4. Under this condition, the RNA polymerase terminated at the attenuator. (Copied from Dale and Park, 2010)

1.9 Aims of the study

The aim of this study was to investigate the behaviour of the conjugative transposons Tn*916* and Tn*5397*, focusing on the transcriptional regulation and transfer. Specific aims are to:

1. investigate the role of *orf12* in the regulation of Tn*916*
2. investigate the activity of the promoter P*tet*(M) in Tn*916* and Tn*5397*
3. determine the termination efficiency of terminators in Tn*916*
4. investigate the transfer of Tn*5397* between *Clostridium difficile* and *Enterococcus faecalis*

Chapter 2.0

Materials and Methods

2 Materials and Methods

This chapter outlined the materials and methods that are used throughout the project. The specific materials and methods are outlined at the beginning of the relevant chapter.

2.1 Sources of media, enzymes and reagents

Luria-Bertani (LB) agar and broth were obtained from Difco (Oxford, UK). Brain heart infusion (BHI) agar and broth and the *Clostridium difficile* selective supplement (CDSS) (D-cycloserine and cefoxitin) were obtained from Oxoid Ltd (Basingstoke, UK). All antibiotics were obtained from Sigma-Aldrich (Poole, UK) and were used at a concentration of 5 μg ml^{-1} (fusidic acid, Fa), 10 μg ml^{-1} (tetracycline, Tc; chloramphenicol, Cm; and erythromycin, Em), 25 μg ml^{-1} (rifampicin, Rif) and 100 μg ml^{-1} (ampicillin, Amp), unless stated otherwise. All restriction enzymes were obtained from New England Biolabs (NEB) Ltd (Hertfordshire, UK). Defibrinated horse blood was obtained from E & O Laboratories (Scotland, UK).

2.2 Bacterial strains, plasmids and transposons

All bacterial strains, plasmids and transposons used in this study are listed in Table 2.1 and Table 2.2. Bacterial strains, plasmids and transposons were obtained from UCL Eastman Dental Institute.

Table 2.1 Bacterial strains used in this study

Bacterial strains	Characteristics	Resistance marker	Reference/source
C. difficile 630	Contains Tn*5397* and Tn*5398*, donor strain	Em^r, Tc^r	Hachler *et al*. 1987
C. difficile R20291	Ribotype 027, recipient strain	Em^r	Anaerobe Reference Laboratory, Cardiff, UK
C. difficile CD37	Recipient strain	Rif^r	Wust and Hardegger, 1983
E. faecalis JH2-2	Recipient strain	Fa^r, Rif^r	Jacob and Hobbs, 1974
E. faecalis EF20A	Transconjugant (CD 630 x EF JH2-2)	Tc^r, Fa^r, Rif^r	This study
E. coli (α-select bronze efficiency)	Competent cells	Amp^r	Bioline (London, UK)
B. subtilis BS34A	Contains Tn*916*	Tc^r	Roberts *et al*. 2003
B. subtilis BS59A	Contains Tn*916*Δ*E*	Em^r	Hussain *et al*. 2005
B. subtilis BS79A	Contains Tn*916*Δ*orf12*	Tc^r	This study
B. subtilis BS80A	Contains Tn*916* and pHCMCO5/Tn*916* P*tet*(M) WT	Tc^r, Cm^r	This study
B. subtilis BS81A	Contains Tn*916* and pHCMCO5/Tn*916* P*tet*(M) PO	Tc^r, Cm^r	This study
B. subtilis BS82A	Contains Tn*916* and pHCMCO5/Tn*916* P*tet*(M) ST	Tc^r, Cm^r	This study
B. subtilis BS83A	Contains Tn*916* and pHCMCO5/(-)P*tet*(M)	Tc^r, Cm^r	This study
B. subtilis BS84A	Contains Tn*916* and pHCMCO5/Tn*5397* P*tet*(M) WT	Tc^r, Cm^r	This study

Bacterial strains	Characteristics	Resistance marker	Reference/source
B. subtilis BS85A	Contains Tn*916* and pHCMCO5/Tn*5397* P*tet*(M) PO	Tc^r, Cm^r	This study
B. subtilis BS86A	Contains Tn*916* and pHCMCO5/Tn*5397* P*tet*(M) ST	Tc^r, Cm^r	This study
B. subtilis BS87A	Contains Tn*916* and pHCMCO5/ P*tet*(M) ST I	Tc^r, Cm^r	This study
B. subtilis BS88A	Contains Tn*916* and pHCMCO5/ P*tet*(M) LT I	Tc^r, Cm^r	This study
B. subtilis BS89A	Contains Tn*916* and pHCMCO5/ P*tet*(M) ST II	Tc^r, Cm^r	This study
B. subtilis BS90A	Contains Tn*916* and pHCMCO5/ P*tet*(M) LT II	Tc^r, Cm^r	This study
B. subtilis BS91A	Contains Tn*916* and pHCMCO5/ P*tet*(M) LTST II	Tc^r, Cm^r	This study
B. subtilis BS92A	BS34AΔ*amyE*, contains Tn*916*	Tc^r, Cm^r	This study

Abbreviations: Em^r, Erythromycin-resistant; Tc^r, tetracycline-resistant; Rif^r, rifampicin-resistant; Fa^r, fusidic acid-resistant; Amp^r, ampicillin-resistant, Cm^r, chloramphenicol-resistant; P*tet*(M) WT, wild type promoter construct; P*tet*(M) ST, start codon promoter construct; P*tet*(M) PO, promoter only construct; (-) P*tet*(M), promoter-less construct; P*tet*(M) LT, large terminator construct; P*tet*(M) ST, small terminator construct; P*tet*(M) LTST, large and small terminators construct.

Table 2.2 Plasmids and conjugative transposons used in this study

Plasmids/transposons	Characteristics	Resistance marker	Reference/source
pUC19	Cloning vector	Amp^r	Yanisch-Perron *et al*. 1985
pGEM-T Easy	Cloning vector	Amp^r	Promega (Southampton, UK)
pAPR108	pGEM-T Easy/Tn*916* fragment	Amp^r, Tc^r	This study
pAPR109	pGEM-T Easy/ Tn*916*Δ*orf12* fragment	Amp^r, Tc^r	This study
pHCMCO5	Shuttle vector	Amp^r,Cm^r	*Bacillus* Genetic Stock Center, Ohio, USA
pHCMCO5-lacO/Pspac	Shuttle vector	Amp^r,Cm^r	This study
pHCMCO5-P*tet*(M)	Shuttle vector	Amp^r,Cm^r	This study
pHCMCO5/Tn*916* P*tet*(M) WT	Expression vector	Amp^r,Cm^r	This study
pHCMCO5/Tn*916* P*tet*(M) PO	Expression vector	Amp^r,Cm^r	This study
pHCMCO5/Tn*916* P*tet*(M) ST	Expression vector	Amp^r,Cm^r	This study
pHCMCO5/(-)P*tet*(M)	Expression vector	Amp^r,Cm^r	This study
pHCMCO5/Tn*5397* P*tet*(M) WT	Expression vector	Amp^r,Cm^r	This study
pHCMCO5/Tn*5397* P*tet*(M) PO	Expression vector	Amp^r,Cm^r	This study
pHCMCO5/Tn*5397* P*tet*(M) ST	Expression vector	Amp^r,Cm^r	This study

Plasmids/transposons	Characteristics	Resistance marker	Reference/source
pHCMCO5/ P*tet*(M) ST I	Expression vector	Amp^r,Cm^r	This study
pHCMCO5/ P*tet*(M) LT I	Expression vector	Amp^r,Cm^r	This study
pHCMCO5/ P*tet*(M) ST II	Expression vector	Amp^r,Cm^r	This study
pHCMCO5/ P*tet*(M) LT II	Expression vector	Amp^r,Cm^r	This study
pHCMCO5/ P*tet*(M) LTST II	Expression vector	Amp^r,Cm^r	This study
pDL	Integration vector	Amp^r,Cm^r	*Bacillus* Genetic Stock Center, Ohio, USA
pDLΔ*bgaB*	Integration vector	Amp^r, Cm^r	This study
pUC19-Pcwp2-GusA	Cloning vector	Amp^r	Emerson *et al*. 2009
pUC19-GusA	Cloning vector	Amp^r	This study
pUC19-P*tet*(M)-GusA	Cloning vector	Amp^r	This study
Tn*916*	Conjugative transposon	Tc^r	Franke and Clewell, 1981
Tn*916*Δ*E*	Conjugative transposon, Tn*916* containing *erm*B gene	Em^r	Rubens and Heggen, 1988
Tn*5397*	Conjugative transposon	Tc^r	Mullany *et al*. 1990; Mullany *et al*. 1996

2.3 Growth conditions

All bacteria were grown at 37^{o}C unless stated otherwise. *Escherichia coli* was grown on LB agar or in LB broth. *Bacillus subtilis* strains and *Enterococcus faecalis* were grown on BHI agar or in BHI broth. All bacterial cultures were incubated under shaking condition (200 rpm). *C. difficile* was grown on BHI agar supplemented with 5% (v/v) defibrinated horse blood and in pre-reduced BHI broth. *C. difficile* was incubated in an anaerobic chamber (Don Whitley Scientific Ltd, Shipley, UK) with an atmosphere of 80% nitrogen, 10% hydrogen and 10% carbon dioxide. All media were supplemented with appropriate antibiotics unless stated otherwise. Media components are listed in Appendix B.

2.4 Storage of bacterial strains

All bacterial stocks were maintained in 1 ml aliquots of 10% (v/v) sterilised glycerol at -80^{o}C (Sambrook *et al*., 1989).

2.5 Molecular biology techniques

2.5.1 Plasmid DNA purification

Plasmid DNA purification was carried out using QIAprep Spin Miniprep Kit (Qiagen, Crawley, UK). This protocol was designed for purification of up to 20 µg of high copy

plasmid DNA from 1-5 ml overnight cultures of *E. coli* in LB medium. All centrifugation steps were carried out at 17,900 x *g* (13,000 rpm) in a table-top microcentrifuge. The bacterial cells were pelleted and the supernatant discarded. The pelleted cells were resuspended in 250 µl of Buffer P1 and transferred to a microcentrifuge tube. Buffer P2 (250 µl) was then added and the tube was inverted gently for 4-6 times. 350 µl of Buffer N3 was added to the mixture, and again the tube was immediately inverted 4-6 times. The tube was centrifuged for 10 min and the supernatants were applied to the QIAprep spin column by decanting or pipetting. The spin column was centrifuged for 1 min and the flow-through discarded. The spin column was washed by adding 750 µl of Buffer PE and centrifuging for 1 min. The flow-through was discarded and the spin column was centrifuged for an additional minute to remove residual wash buffer. The QIAprep spin column was then placed in a clean 1.5 ml microcentrifuge tube. The DNA was eluted by adding 30-50 µl of Buffer EB (10 mM Tris-Cl, pH 8.5) or distilled water to the centre of the spin column membrane, left to stand for 1 min at room temperature (25^{o}C) and centrifuged for 1 min. The plasmid DNA was ready for further applications.

2.5.2 Genomic DNA purification

Genomic DNA purification was carried out using the PUREGENE® DNA Purification Kit (Gentra Systems, Minneapolis, USA) with slight modifications. This protocol was designed for DNA purification of 0.5 ml bacterial culture, with an expected yield of

3-30 µg DNA. All centrifugation steps were carried out at 17,900 x *g* (13,000 rpm) in a table-top microcentrifuge. The overnight culture was briefly placed on ice prior centrifugation for 1 min. The supernatant was removed as much as possible using pipet. The pelleted cell was resuspended in 300 µl of Cell Suspension Solution. 1.5 µl of Lytic Enzyme Solution was added and the tubes were inverted 25 times. The tubes were incubated at 37^{o}C for 30 min to digest the cell walls. Samples were inverted occasionally during the incubation. The cells were centrifuged for 1 min and the supernatant discarded. The cell pellet was resuspended in 300 µl of Cell Lysis Solution and heated at 80^{o}C for 5 min to complete cell lysis. This was followed by RNase treatment, where 1.5 µl of RNase A Solution was added to the cell lysate. Sample was mixed by inverting the tube 25 times and incubating at 37^{o}C for 15-60 min. Subsequently, sample was cooled to room temperature (approximately 10-15 min) prior to addition of 100 µl of Protein Precipitation Solution. Sample was vortexed vigorously at high speed for 20 sec to ensure even mixing and centrifuged for 3 min. After this step, the precipitated proteins should be visible as a tight white pellet. The supernatant containing the DNA was poured into a clean 1.5 ml microcentrifuge tube containing 300 µl 100% isopropanol. Sample was mixed by inverting the tube 50 times and centrifuged for 1 min. The DNA should be visible as a small white pellet after centrifugation. Supernatant was poured off and the tube was briefly drained on a clean absorbent paper. 300 µl of 70% ethanol was added and the tube was inverted several times to wash the DNA pellet. The tube was centrifuged for 1 min and supernatant discarded. The DNA pellet was air dried for

10-15 min and re-dissolved overnight at room temperature (25^{o}C) in 100 µl of DNA Hydration Solution or sterile distilled water.

2.5.3 DNA extraction from agarose gel

DNA extraction from agarose gel was carried out using QIAquick Gel Extraction Kit from Qiagen, Crawley, UK. This protocol was designed for DNA extraction of up to 10 µg. All centrifugation steps were carried out at 17,900 x *g* (13,000 rpm) in a table-top microcentrifuge. The DNA fragment was excised from the agarose gel with a clean and sharp scalpel. The gel slice was weighed in a colourless tube. 3 volumes of Buffer QG was added to 1 volume gel (100 mg ~ 100 µl) and incubated at 50^{o}C until the gel slice completely dissolved. Mixture was vortexed occasionally during this incubation to help dissolve the gel slice. 1 volume of isopropanol was then added and mixed by inverting the tube several times. A QIAquick spin column was placed into a provided 2 ml collection tube. Sample was applied to the spin column and centrifuged for 1 min to bind the DNA. The flow-through was discarded and the spin column was placed back into the same tube. 0.75 ml of Buffer PE was added to the spin column and centrifuged for 1 min to wash the DNA. The flow-through was discarded and once more, the spin column was placed back into the 2 ml collection tube and centrifuged for an additional 1 min to remove the residual wash buffer. The spin column was placed into a clean 1.5 ml microcentrifuge tube. The DNA was eluted by adding 30 µl of Buffer EB (10 mM Tris-Cl, pH 8.5) or sterile distilled water to the centre of the QIAquick membrane, left to stand for 1 min at

room temperature (25^{o}C) and centrifuged for 1 min. The DNA was ready for further applications.

2.5.4 PCR purification

PCR purification was carried out using QIAquick PCR Purification Kit (Qiagen, Crawley, UK). This protocol was designed to purify single or double stranded DNA fragments from PCR and other enzymatic reactions. All centrifugation steps were carried out at 17,900 x *g* (13,000 rpm) in a table-top microcentrifuge. 5 volumes of Buffer PB was added to 1 volume of the PCR sample and mixed. The QIAquick spin column was placed into a provided 2 ml collection tube. Sample was applied to the spin column and centrifuged for 1 min to bind the DNA. The flow-through was discarded and the spin column was placed back into the same collection tube. 0.75 ml of Buffer PE was added and centrifuged for 1 min. The flow-through was discarded and once more, the spin column was placed back into the 2 ml collection tube and centrifuged for an additional 1 min to remove the residual wash buffer. The spin column was placed into a clean 1.5 ml microcentrifuge tube. The DNA was eluted by adding 30 µl of Buffer EB (10 mM Tris-Cl, pH 8.5) or sterile distilled water to the centre of the QIAquick membrane, left to stand for 1 min at room temperature (25^{o}C) and centrifuged for 1 min. The DNA was ready for further applications.

2.5.5 Agarose gel electrophoresis

DNA fragments were mixed with 0.1 volume of loading buffer (Appendix A) and were separated on 1-2% (w/v) agarose (Bioline, London, UK) gel electrophoresis. Gels were prepared to the relevant percentage in 1X TAE (tris-acetate-EDTA) buffer. The electrophoresis was run for 30-45 min at 50-100 V. The HyperLadder I (Bioline, London, UK) and 1 kb marker (NEB,UK) were used as a size reference. Nucleic acid was stained either with GelRed™ (Biotium Inc, Cambridge, UK) or ethidium bromide (Promega, Southampton, UK), both at a concentration of 0.5 μg ml^{-1}. The nucleic acid was visualised using a UV transilluminator (320 nm). Gel images were produced using AlphaImager equipment and computer software (Innotech Corporation, UK).

2.5.6 Restriction endonuclease reactions

DNA was digested using restriction enzymes (NEB, Hertfordshire, UK) according to the manufacturer's instructions. All restriction endonuclease reactions were carried out at 37^{o}C unless stated otherwise.

2.5.7 DNA ligation reactions

Ligation of DNA was carried out using either T4 DNA ligase or Quick T4 DNA ligase (NEB, Hertfordshire, UK) according to the manufacturer's instructions. Ligation was carried out using a molar ratio of 1:3 vector to insert. The ligation mixture was incubated overnight at 4^{o}C with regular T4 DNA ligase or incubated for 10 min at room temperature (25^{o}C) with Quick T4 DNA ligase, dependent on the requirement of the experiment.

2.5.8 Dephosphorylation reactions

Dephosphorylation was carried out to remove the 5'-phosphate groups from each end of the linearised vector to minimize the self-ligation of the vector during cloning. The linearised vector (1 µg) was incubated with 0.01 U pmol^{-1} of Calf Intestinal Alkaline Phosphatase (CIAP) and 5 µl of CIAP 10X Reaction Buffer for 30 min at 37^{o}C. Dephosphorylation mixture was set up in 50 µl reaction. After 30 min incubation, an equivalent amount of CIAP previously used was added to the reaction mixture and incubation continued for an additional 30 min. Dephosphorylation was stopped with the addition of 0.5 mM ethylenediaminetetraacetic acid (EDTA) and incubated at 75^{o}C for 10 min. Subsequently, the dephosphorylated vector was purified using QIAquick PCR Purification Kit (Qiagen, Crawley, UK) and ready for further applications.

2.5.9 Preparation of *B. subtilis* competent cells

The *B. subtilis* competent cells were prepared according to the protocol described by Hardy (1985). A single colony from a fresh overnight plate was inoculated into 10 ml SPI broth (Appendix A) in a 200 ml conical flask. The culture was incubated overnight with shaking (200 rpm) at 30^{o}C. A 10 ml of the overnight culture was then transferred to the 100 ml fresh pre-warmed SPI medium in a 1 L flask and grown at 37^{o}C with shaking (200 rpm) until the rate of increase in the OD_{600} decreased. At the end of the logarithmic growth, a 10 ml of this culture was transferred to the 90 ml SPII broth (Appendix A) and the culture was incubated for 1.5 h at 37^{o}C under shaking condition (200 rpm). Cells were harvested by centrifugation at 3,000 x *g* (5,000 rpm) for 10 min at 20^{o}C. The cells were resuspended in 10 ml supernatant, to which sterile glycerol had been added to 10% (v/v). Aliquots of 500 µl were dispensed on ice and the cells frozen and stored at -80^{o}C until required.

2.5.10 Transformation of *B. subtilis*

The aliquots of *B. subtilis* competent cells were quickly thawed at 37^{o}C and were added to a 50 ml conical tube containing 0.5 µg DNA. The tube was incubated at 37^{o}C for 1 h under gentle agitation (50 rpm). 5 ml of LB broth was then added followed by a further 1.5 h incubation at 37^{o}C with shaking (200 rpm). Aliquots of 100 µl was spread onto BHI agar supplemented with appropriate antibiotics. The remaining cells were spun down at 3,000 x *g* (5,000 rpm) for 10 min and

supernatant discarded. The pelleted cells were resuspended in 100 µl of fresh LB medium and spread onto BHI agar supplemented with appropriate antibiotics. All plates were incubated overnight at 37^{o}C for 24-48 h.

2.5.11 Transformation of *E. coli*

E. coli transformation was carried out using competent cells "α-select bronze efficiency" (Bioline, London, UK). 100-1000 pg of DNA was added to a 100 µl aliquot of cells and mixed gently by tapping the tube. The cells were incubated on ice for 30 min prior heat shock treatment by placing them in a 42^{o}C water bath for 45 sec. The cells were placed back on ice for 2 min. 900 µl of SOC medium (Appendix A) was added to the cells and incubated at 37^{o}C for 1 h with shaking condition (200 rpm). Aliquots of 100 µl was spread onto LB agar supplemented with appropriate antibiotics. The remaining cells were spun down at 3,000 x *g* (5,000 rpm) in a table-top microcentrifuge for 10 min and supernatant discarded. The pelleted cells were resuspended in 100 µl of fresh LB medium and spread onto LB agar supplemented with appropriate antibiotics. All plates were incubated overnight at 37^{o}C.

2.5.12 Blue/white colour screening

Ligated DNA was transformed into *E. coli* α-select bronze efficiency. Transformants containing recombinant plasmids were selected for on LB agar containing 100 μg ml^{-1} ampicillin, 40 μg ml^{-1} chromogenic substrate 5-bromo-4-chloro-indolyl-β-D-galactopyranoside (X-Gal) and 0.1 M non-metabolisable *lac*Z inducer isopropyl-β-D-thiogalactoside (IPTG). Plates were incubated overnight at 37^{o}C. White colonies, which indicate the presence of recombinant plasmids were selected for further investigation.

2.5.13 Oligonucleotides synthesis

All oligonucleotides were synthesised by Sigma-Aldrich (Poole, UK). Sequences of all primers used throughout this study were listed in Table 2.3.

Table 2.3 Primers used throughout this study

Primers	Sequence (5'→ 3')	Amplicon
AJ1	CTGGCAACAGCATTTAGTGG	4.1 kb Tn*916* fragment
AJ4	TTTTTATTGGCGTTTAGTAGTG	4.1 kb Tn*916* fragment
AJ15	GAATATCTGTGCGCTTTGTATGCC	4.0 kb Tn*916* fragment (Δ*orf12*)
AJ16	TCCGGATACTTTAGAATCACATGAT	4.0 kb Tn*916* fragment (Δ*orf12*)
CTn9824F	GAAAACTTTAGTGATTGGTGG	*orf14* junction in Tn*916*
CTn13562	GGGATACGCTATGGTTGTG	*orf9* junction in Tn*916*
O10R	CCCGTCATTCACATAGTAGG	*orf14* junction in Tn*916*
O14R	GATGTACTTCATGGCCGACG	*orf9* junction in Tn*916*
catF	GAGTTTTATGATTTATACCTTTCTG	*cat* : *amyE* junction
catR	AGGTATAAATCATAAAACTCTTTGA	*cat* : amyE junction
ycgB	TTCTTCTTTTTATCGTCTGCGGCGG	*cat* : *amyE* junction
ldh	CCGTAAGATGTTTTGACCGGTTGTG	*cat* : *amyE* junction
tetM F	GCTCAATGTTGATGCAGGAA	tet(M) fragment
tetM R	TATATATGCAAGACGCTGTCT	tet(M) fragment
Ptet(M) For	GGCGGCGGGTACCCAAAGCAACGCAGGTATCTC	Ptet(M) Tn*916* fragment
Ptet(M) Rev	GGCGGCGGAATTCGTGATTTTCCTCCAT	Ptet(M) Tn*916* fragment
Ptet(M) For5397	GGCGGCGGGTACCCAAAGCAACGCAAGTATCTC	Ptet(M) Tn*5397* fragment
Ptet(M) Rev5397	GGCGGCGGAATTCTCAGGTGATTTTCCTCCAT	Ptet(M) Tn*5397* fragment
For916 ST	GAATATCTGTGCGCTTTGTATGCC	Tn*916* start codon promoter construct
Rev916 ST	TCCGGATACTTTAGAATCACATGAT	Tn*916* start codon promoter construct
For916 PO	ATGGAGGAAAATCACGAATTCCTGC	Tn*916* promoter only construct
Rev916 PO	ACAGATATTCTCCGGATACTTTAGA	Tn*916* promoter only construct
For5397 ST	GGTTAGTTTTGGCGTACCCAGTGAT	Tn*5397* start codon promoter construct
Rev5397 ST	CCTCCTAAAAAGGGACATCTAATT	Tn*5397* start codon promoter construct

Primers	Sequence (5'→ 3')	Amplicon
For5397 PO	ATGGAGGAAAATCACGAATTCCTGC	Tn*5397* promoter only construct
Rev5397 PO	GGCGGCGGAATTCTAATTATTTGTTCCCACTATC	Tn*5397* promoter only construct
LT For	ATCCCAGTGATAAGAGTATTTATCACTGGGATTTT TATGGAGGAAAATC	Tn*916* large terminator construct (set I)
LT Rev	AAAAATCCCAGTGATAAATACTCTTATCACTGGG ATACAGATATTCTCCG	Tn*916* large terminator construct (set I)
LT II For	TTATCACTGGGACGGTCATGCCCTTTTGGG	Tn*916* large terminator construct (set II)
LT II Rev	ATACTCTTATCACTGGGATTTTTATGCATA	Tn*916* large terminator construct (set II)
ST For	GCCCTTTTGGGCTTTTATGGAGGAAAATCA	Tn*916* small terminator construct (set I)
ST Rev	AAAAGCCCAAAAGGGCACAGATATTCTCCG	Tn*916* small terminator construct (set I)
ST II For	TGCCCTTTTGGGCCGGCGAATGGAGGAAAA	Tn*916* small terminator construct (set II)
ST II Rev	TAAAAATCCCAGTGATAAATACTCTTATCA	Tn*916* small terminator construct (set II)
LTST Rev	TGACCGTCCCAGTGATAAATACTCTTATCA	Tn*916* small and large terminator construct (set II)
LEO	CCACTTGATATGAAAAATCAAATGGCTC	sspPCR, CI*, left end transposon:genome junction
REO	ACGTGTATCAAGCAGAGGGAATCGGTAAA	sspPCR, CI*, right end transposon:genome junction
TndX (F300)	CTTTAGGGAAAATAACTGAT	1.6 kb fragment of *tndX*
TndX (F30)	CTTACAATGTTAAAACAGCAAGC	1.6 kb fragment of *tndX*
PTS (For)	GTGTCAATGACCGCAGAAGA	Chromosomal target site, left end transposon:genome junction

*Circular intermediate

Primers	**Sequence (5'→ 3')**	**Amplicon**
PTS (Rev)	TCGCTAGAATGACCTGTAGAAGAA	Chromosomal target site, left end transposon:genome junction
M13 For	GTAAAACGACGGCCAGT	SSPPCR
M13 Rev	CAGGAAACAGCTATGAC	SSPPCR
RT1	TTCAAGCTCTATCCTACAGCGACAGC	Tn*916* fragment
RT2	ATATACGAGTTTGTGCTTGT	Tn*916* fragment

2.5.14 Standard PCR protocol

PCR amplification was carried out using GeneAmp 2400 PCR system (Perkin-Elmer Cetus, USA) with the following standard conditions: initial denaturation step at 94^{o}C for 4 min, 30-35 PCR cycles [94^{o}C, 1 min; 53-60^{o}C, 1 min (dependent on primer annealing temperature); 72^{o}C, 1-4 min (dependent on expected amplicon size, usually 1 min for each 1 kb is allowed]; 1 cycle of 4 min at 72^{o}C and preservation at 4^{o}C until the sample were analysed. All of the temperature and times are variable. The melting temperatures (Tm) of the primers were calculated by the following equation;

Equation 2.1 Tm = 67.5 + [0.34 x % (G+C)] - (395/n), where n is the length of the primers

The annealing temperature was derived as 5^{o}C below the Tm of the primer with the lowest Tm. The PCR reaction mixture contains 5 µl of 10X *Taq* polymerase buffer (NEB, Hertfordshire, UK), 1 µl of 10 pmol µl^{-1} of each forward and reverse primers (Sigma-Aldrich, Poole, UK), 1 µl of 10 mM dNTP mix (NEB, Hertfordshire, UK), 0.5 U µl^{-1} of *Taq* polymerase (NEB, Hertfordshire, UK) and 1 µl of DNA template (approximately 0.2 ng µl^{-1}). The total volume of PCR mixture was made up to 50 µl using distilled water. All PCR products were purified using QIAquick PCR Purification Kit (Qiagen, Crawley, UK) as described previously.

2.5.15 Site-directed mutagenesis

Site-directed mutagenesis reaction was carried out using the Phusion® Site-Directed Mutagenesis Kit from NEB (Hertfordshire, UK). The entire plasmid (pGEM-T Easy) was amplified using phosphorylated primers that introduce the desired mutations. The amplified, linear PCR product containing the mutations is then circularised in a 10 min ligation reaction with Quick T4 DNA Ligase. The resulting plasmid was then transformed into *E. coli* α-select bronze efficiency using a standard transformation protocol. The site-directed mutagenesis protocol was illustrated in Figure 2.1.

2.5.15.1 5'-Phosphorylation of oligonucleotides

The following components were added to a microcentrifuge tube; 300 pmol oligonucleotides, 5 µl 10X T4 Polynucleotide Kinase Reaction Buffer, 1 µl T4 Polynucleotide Kinase 10 U μl^{-1}, 5 µl 10 mM ATP and distilled water to a final volume of 50 µl. The reaction mixture was incubated at 37^{o}C for 30 min. The T4 Polynucleotide Kinase was inactivated at 65^{o}C for 20 min. The reaction products were stored at -20^{o}C until required.

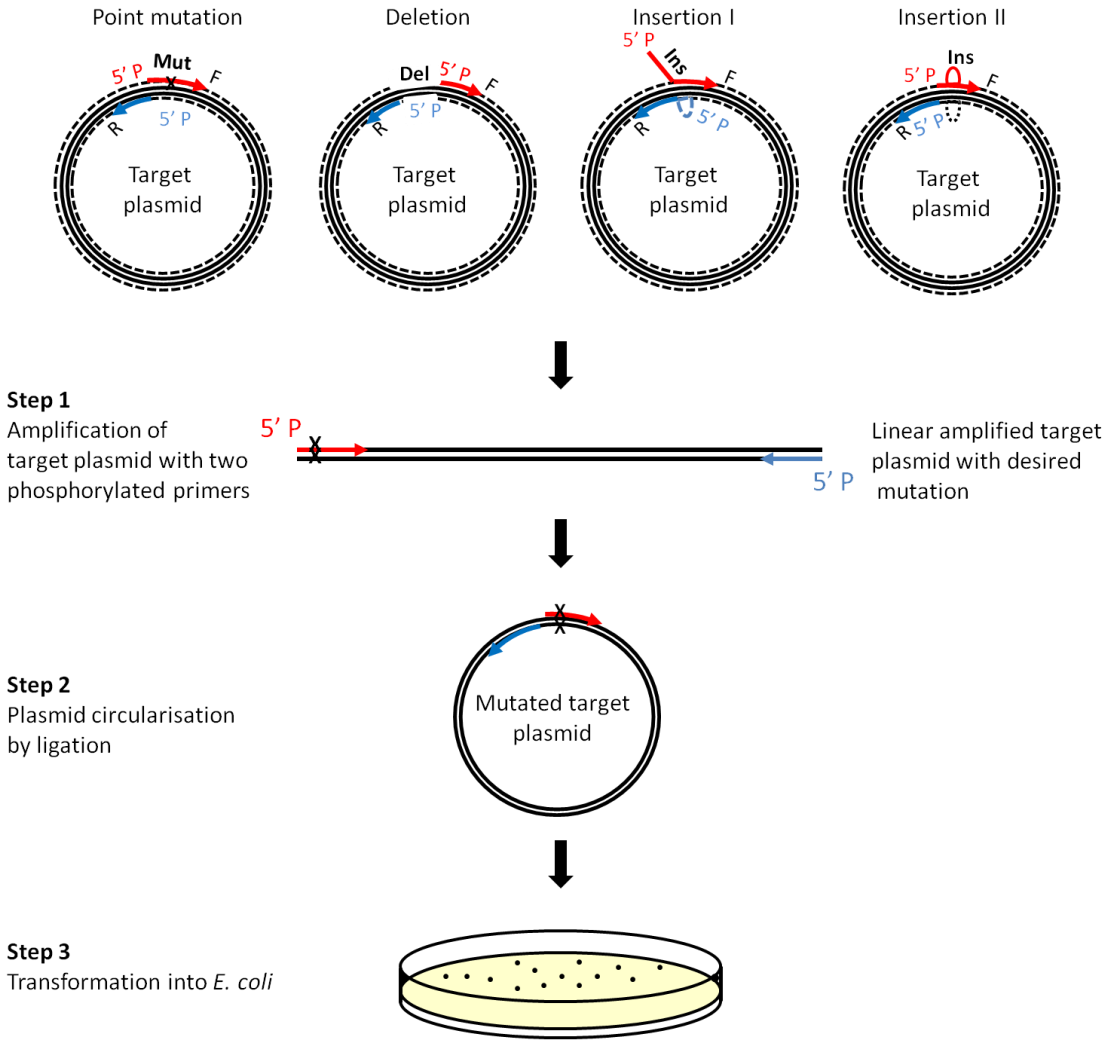

Figure 2.1 Schematic diagram of the site-directed mutagenesis protocol. There are four types of mutations that can be introduced using this protocol; point mutation, deletion, and 2 types of insertion which involves 3 main steps. Phosphorylated primers are used for the PCR amplification.

2.5.15.2 PCR amplification

All tubes were carefully mixed and centrifuged before opening to improve recovery. PCR reaction mixture was prepared as follows: distilled water to a final volume of 50 µl, 10 µl of 5X Phusion® HF Buffer, 1 µl 10 mM dNTPs, 1 µl of phosphorylated forward and reverse primers, 1 µl of DNA template (approximately 0.2 ng μl^{-1}), 0.5 µl Phusion® Hot Start II DNA Polymerase (0.02 U μl^{-1}). The PCR amplification was carried out using the following conditions: initial denaturation step at 98°C for 30 sec; 25 PCR cycles (98°C, 5-10 sec; 65-72°C, 10-30 sec; 72°C, 15-30 sec kbp^{-1}); final extension at 72°C, 5-10 min and preservation at 4°C until the sample were analysed.

2.5.15.3 Ligation

The volume of 25 ng PCR product was adjusted (usually equivalent to 1-5 µl of PCR reaction) to 5 µl with distilled water. 5 µl of 2X Quick Ligation Reaction Buffer was added and mixed. 0.5 µl of Quick T4 DNA Ligase was then added and mixed followed by a brief centrifugation. The ligation mixture was incubated at room temperature (25°C) for 10 min and chilled on ice prior to *E. coli* transformation.

2.5.15.4 *E. coli* transformation

Transformation of the ligated products was carried out using a standard *E. coli* transformation protocols as described previously. 1-10 µl of the reaction mixture was transformed into 50 µl chemically competent *E. coli* cells.

2.5.15.5 Analysis of transformants

Successful transformants harbouring the recombinant plasmid were screened through blue/white selection using standard protocol as described in Section 2.5.12. The mutants were analysed by DNA sequencing.

2.5.16 DNA sequencing reactions

Sequencing reactions were carried out at the Department of Biochemistry, University of Cambridge and the Wolfson Institute for Biomedical Research, University College London. The concentrations used for DNA sequencing were 100 ng μl^{-1} for plasmids and 1 ng μl^{-1} per 100 bp for PCR products and was determined either by agarose gel electrophoresis or the NanoDrop™ 1000 Spectrophotometer (Thermo Scientific, Surrey, UK).

2.5.17 DNA sequence analysis

Analysis of DNA sequence was carried out using a web-based tool Biology Workbench (http://workbench.sdsc.edu/) and the Basic Local Alignment Search Tool (BLAST) (http://blast.ncbi.nlm.nih.gov/).

2.6 Filter mating

The filter mating experiments were conducted as described by Roberts *et al*. (2000). The donor and recipient strains were grown overnight on BHI agar supplemented with appropriate antibiotics. The colonies were inoculated into 20 ml of antibiotic-free BHI broth (pre-reduced broth for *C. difficile*) and grown overnight at 37^{o}C in the relevant atmospheric environments. The cultures were diluted to OD_{600} ~ 0.1 and were left to grow at 37^{o}C until mid-exponential phase (OD_{600} = 0.5-0.6). The cells were harvested by centrifugation at 3,000 x *g* (5,000 rpm) for 10 min and supernatant discarded. The pelleted cells were resuspended in 1 ml pre-reduced BHI broth. Both the donor and recipient were mixed gently but thoroughly and 200 µl aliquots were spread on 0.45 µm-pore-size sterilised nitrocellulose filters (Sartorius, UK) which had previously been placed on antibiotic-free BHI agar. Plates were anaerobically incubated overnight at 37^{o}C. Filters were immersed in 1 ml pre-reduced BHI broth and vortexed for 10-20 sec prior to plating on BHI agar supplemented with appropriate antibiotics. The plates were incubated

anaerobically at 37^{o}C for 24-48 h. The transfer frequency was calculated using the following formula: number of colonies x dilution factor = number of CFUs per filter.

2.7 Southern blot and hybridisation

Southern blot hybridisation and labelling of the probe was carried out using ECL Direct Nucleic Acid Labelling and Detection Systems (Amersham, Little Chalfont, UK) according to the manufacturer's instructions.

2.7.1 Gel processing

After running the agarose gel for the appropriate length of time, the gel was placed in a suitable plastic box, covered with depurination solution (Appendix B) and agitated on an orbital shaker, ensuring that the gel moves freely. Treatment was stopped immediately once the bromophenol blue-dye has turned completely yellow (approximately 10-12 min). The depurination solution was discarded and the gel was rinsed with distilled water. The gel was then submerged with denaturation solution (Appendix B) and agitated for 25 min after the bromophenol dye has returned to its blue colour. This solution was discarded and the gel was rinsed with distilled water. The gel was subsequently covered with neutralisation solution (Appendix B) and agitated for 30 min.

2.7.2 Capillary blotting

The gel was blotted by capillary transfer using 20X SSC in the following set up (Figure 2.2). A raised platform was made in a suitable container filled with 20X SSC (Appendix A). This platform was covered with 3 sheets of 3 MM Whatman filter paper saturated with 20X SSC to act as a wick. The gel was placed onto the 3MM paper, making sure no air bubbles were present. A sheet of Hybond N+ nylon membrane (Amersham, Little Chalfont, UK) was cut to the size of the gel and placed on top of the gel without trapping air bubbles. Another 3 sheets of 3 MM paper were cut to the size of the gel and soaked with 10X SSC. These wetted papers were placed on top of the membrane, again avoiding trapping air bubbles. A 5-7 cm stack of absorbent paper towels were placed on top of the 3 MM paper. A glass plate and a 500 g weight were placed on top of the paper towels. This blotting stack was left overnight at room temperature (25^{o}C).

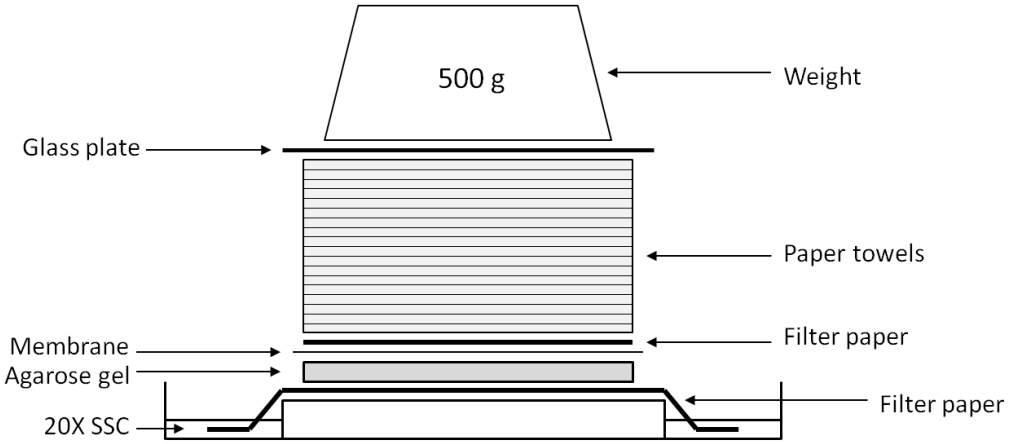

Figure 2.2 Set up of the gel blotting procedure through capillary transfer.

2.7.3 Processing the blot

The blotting stack was dismantled and the membrane and the gel were removed together. The membrane was peeled from the gel and placed side up on a clean piece of 3 MM paper. The DNA side was marked with a pencil. The membrane was placed in 6X SSC and rinsed for 1 min with gentle agitation to remove the agarose. The DNA was fixed to the membrane by UV cross-linking in a UV Stratalinker 1800 (Stratagene, Amsterdam, Netherlands) according to the manufacturer's instructions.

2.7.4 Labelling the DNA probes

Labelling of the DNA probes was carried out according to the manufacturer's instructions. The DNA to be labelled was diluted to a concentration of 10 ng μl^{-1} using sterile distilled water. The DNA (100 ng in 10 µl) was denatured by heating for 5 min in a boiling water bath and cooled immediately by incubation for 5 min on ice. The tube containing the DNA was spun briefly prior to addition of an equivalent volume (10 µl) of DNA labelling reagent. The glutaraldehyde solution (10 µl) was then added and mixed gently but thoroughly. The tube was again spun to collect the contents at the bottom of the tube. The tube was incubated for 10 min at 37^{o}C and if not used immediately was held on ice for 10-15 min.

2.7.5 Hybridisation and stringency washes

The hybridisation buffer was prepared as follows: solid sodium chloride (analytical grade) was added to 50 ml of hybridisation buffer to a final concentration of 0.5 M. The blocking agent was subsequently added [final concentration of 5% (w/v)] and immediately mixed until the blocking agent was present as a free suspension. Mixing was continued with stirring for 1 h at room temperature followed by incubation at 42^{o}C for 30 min with occasional mixing. If not used immediately, the buffer could be stored at -20^{o}C in a sterile plastic container for up to 3 months.

The pre-hybridisation procedure was performed by pre-heating the hybridisation buffer at 42^{o}C. In a suitable container, the blot was pre-wet with 5X SSC, loosely rolled up and placed in a glass hybridisation tube. The 5X SSC was poured off and the appropriate volume of hybridisation buffer (0.0625-0.125 ml cm^{-2}) was added followed by a pre-hybridisation in a rotisserie oven at 42^{o}C for at least 15 min. The labelled probe was added to the buffer, making sure not to place it directly on to the membrane. Hybridisation was carried out overnight in the rotisserie oven at 42^{o}C.

The hybridisation buffer was discarded and 50-100 ml of 5X SSC was added to the tube and replaced in the rotisserie oven for 5 min at 42^{o}C. The 5X SSC was discarded and replaced with a pre-warmed primary wash buffer (Appendix B) so that the hybridisation tube was one-third full. The tube was returned to the

rotisserie oven and the blot was washed for 20 min at 42^{o}C. The primary wash buffer was discarded and replaced with an equal volume of a fresh buffer and continued washing for 10 min. This washing step was repeated for a second time. The blot was then removed from the hybridisation tube and placed in a plastic tray soaked with an excess of secondary wash buffer (Appendix B). Incubation was done with gentle agitation on a rotary shaker for 5 min at room temperature (25^{o}C).

2.7.6 Signal generation and detection

An equal volume of detection reagent 1 and detection reagent 2 were mixed in a volume that is sufficient to cover the blot. The excess secondary wash buffer was drained, and the blot was placed onto a clean piece of Saran Wrap. The detection reagents were added directly onto the blot and incubated for 1 min at room temperature (25^{o}C). The excess detection reagents were drained and the blot was wrapped in Saran Wrap without trapping air bubbles. The blot was placed DNA side up in a film cassette and the autoradiography film was placed over the blot. The film cassette was closed and the film was exposed for 30 sec - 1 min. The film was removed under safe light conditions and developed. A second film was exposed for an appropriate length of time if required.

2.8 Statistical analysis

All data are presented as mean ± standard deviation (SD). Analysis of variance, one-way ANOVA was carried out to compare the differences between two or more means. A mean difference is considered significant when $P<0.05$. Statistical analysis was performed using Statistical Package of Social Science (SPSS) version 20.0 (SPSS Inc., Chicago, IL, USA).

Chapter 3.0

Investigation into the role of *orf12* in the regulation of Tn*916*

3 Investigation into the role of *orf12* in the regulation of Tn*916*

3.1 Introduction

Tn*916* is the paradigm of a large family of conjugative transposons commonly found in enterococci and streptococci (Franke and Clewell, 1981; Clewell and Gawron-Burke, 1986). In 1992, Su and co-workers (Su *et al*., 1992) have described a model of how transcriptional attenuation, associated with tetracycline, regulates the expression of *tet*(M) in Tn*916* (Figure 3.1). Central to this hypothesis is the transcription of the small leader peptide (*orf12*) upstream of *tet*(M). The involvement of *orf12* has never been experimentally proven in vivo, although it is fundamentally important.

In this chapter, we investigated the involvement of *orf12* using *B. subtilis*::Tn*916* with a 2 bp mutation replacing the start codon of *orf12* (ATG) with GCG which would prevent any initiation of translation of *orf12*. The translation of *orf12* is central in the proposed regulatory mechanism as it is the translating ribosome that is hypothesised to destroy, or prevent the formation of the transcriptional terminators. The mutant *B. subtilis*::Tn*916*Δ*orf12* was subjected to experiments to test for any differences in transcriptional activity, fitness cost and mobility compared to the wild type strain.

A.

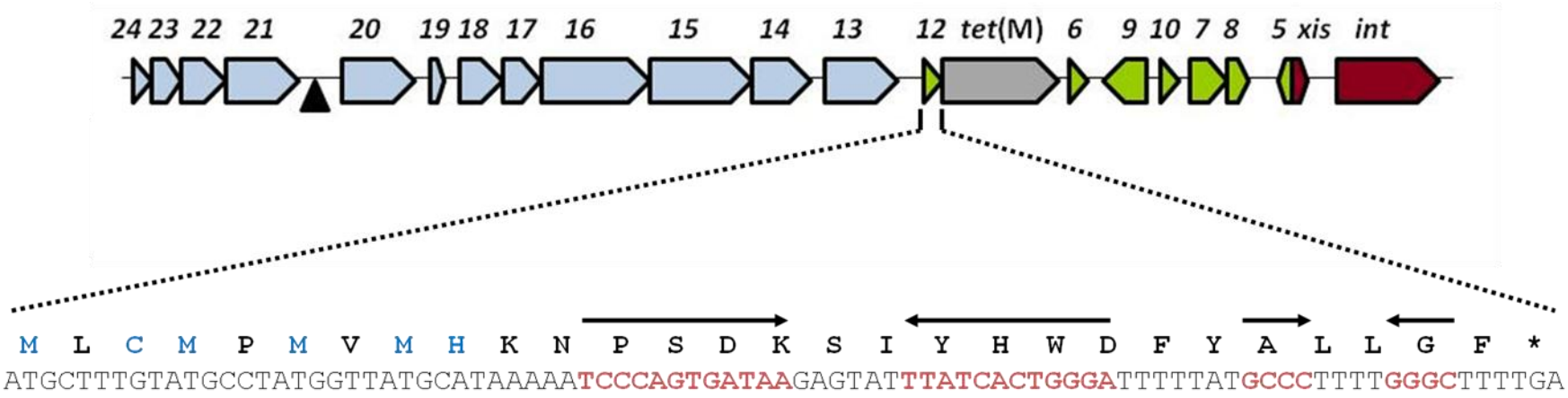
24 23 22 21 20 19 18 17 16 15 14 13 12 tet(M) 6 9 10 7 8 5 xis int
M L C M P M V M H K N P S D K S I Y H W D F Y A L L G F *
ATGCTTTGTATGCCTATGGTTATGCATAAAAATCCCAGTGATAAGAGTATTTATCACTGGGATTTTTATGCCCTTTTGGGCTTTTGA

B.

Figure 3.1 The transcriptional regulation of Tn*916*. Panel A shows the conjugative transposon Tn*916* , the inverted repeat sequences (black arrows) within the *orf12* and the amino acid sequence corresponding to the peptide product (single letter codes: M: methionine; L: leucine; C: cysteine; P: proline; V: valine; H: histidine; K: lysine; N: asparagine; S: serine; D: aspartic acid; I: isoleucine; Y: tyrosine; W: tryptophan; F: phenylalanine; A: alanine; G: glycine). The rare codons within the leader peptide are shown in blue font. Panel B shows the putative secondary structure that is predicted to form in the mRNA of Tn*916*. The red-shaded area represents *orf12*. The terminator structures are presented by the capital 'T'. The ribosome binding sites for *orf12* and *tet*(M) are underlined. The start codon of the *tet*(M) is highlighted in yellow. The free energy changes in kcal mol^{-1} for each stem loop structure are indicated as ΔG. In the absence of tetracycline, the amount of charged aminoacyl tRNA is proposed to be limited. As a result, the ribosome pauses at the codons that call for rare amino acids (cysteine, methionine and histidine), thus lags behind the extending RNA polymerase and does not interfere with the formation of the terminator structures. At this stage, most of the transcription is terminated. Conversely, in the presence of tetracycline, the reversible binding of tetracycline-ribosome leads to an increased amount of charged aminoacyl tRNA, including the rare ones (cysteine, methionine and histidine). The build up of charged aminoacyl tRNA allows the rapid translation of *orf12* by the Tet(M) protected ribosomes, the rapid translation is proposed to allow the ribosome to catch up with the RNA polymerase thus preventing the formation of, or destroying the terminator structures. These result in a long transcript that extends through the terminators into the *tet*(M) and the downstream genes (Su *et al*., 1992).

3.2 Materials and methods

3.2.1 Bacterial strains and plasmids

E. coli α-select (bronze efficiency) was used for transformation of pGEM-T Easy harbouring the Tn*916* fragment and pDL. *B. subtilis* BS59A (contains Tn*916*ΔE) was used as a host for construction of Tn*916*Δ*orf12* mutant. The *B. subtilis* mutant carrying the *cat* gene for competitive fitness assays was constructed using *B. subtilis* BS34A (contains wild typeTn*916*). *C. difficile* CD37 was used as a recipient in filter-mating experiments. All strains were grown under the conditions described in Section 2.3.

3.2.2 Bacterial transformation

B. subtilis and *E. coli* transformation was carried out according to the protocol in Section 2.5.10 and Section 2.5.11, respectively. Selection of *B. subtilis* transformants was carried out on BHI agar after 24-48 h incubation at 37^{o}C. Conversely, the *E. coli* transformants were selected on LB agar after 18-24 h incubation at 37^{o}C.

3.2.3 Construction of mutation in the regulatory region of Tn*916*

The region from the end of *orf14* to *orf9* was amplified (Figure 3.2). The PCR product (4.1 kb) was purified prior to cloning into pGEM-T Easy vector and transformed into *E. coli*. Transformants were selected on LB agar supplemented with ampicillin (100 µg ml^{-1}), tetracycline (10 µg ml^{-1}), IPTG (0.1 M) and X-gal (40 µg ml^{-1}). After 18-24 h incubation at 37^{o}C, white colonies were randomly picked and grown in LB broth supplemented with ampicillin (100 µg ml^{-1}). Plasmid extraction was then carried out. One plasmid designated pAPR108 was subjected to site directed mutagenesis (Section 2.5.15) to introduce a 2 bp mutation disrupting the start codon of *orf12*. Two phosphorylated primers were designed, with the desired mutation located in the middle of the mutagenic primer. The PCR product was ligated according to the manufacturer's instructions and designated pAPR109. This plasmid was transformed into *E. coli* and after 18-24 h incubation at 37^{o}C, the transformants were selected for plasmid purification. The purified plasmids were subsequently sequenced.

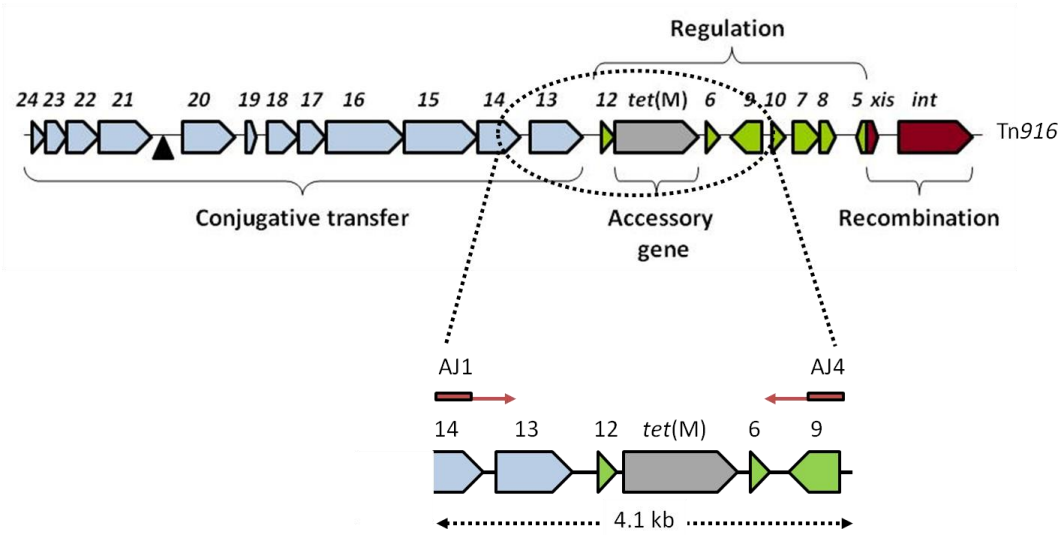

Figure 3.2 Amplification of Tn*916* regulatory fragment. Primers AJ1 and AJ4 (Table 2.3) were designed to amplify the Tn*916* from the end of *orf14* to *orf9*. The expected PCR product is 4.1 kb. The amplified PCR product was cloned into pGEM-T Easy and subsequently transformed into *E. coli*.

3.2.4 Construction of *B. subtilis* mutant

The pAPR109 vector was used as template for PCR to amplify the Tn*916*Δ*orf12* fragment, so that it can be used for transformation in *B. subtilis* BS59A (contains Tn*916*ΔE). BS59A was the result of a filter-mating with *C. difficile*::Tn*916*ΔE with *B. subtilis* CU2189 (Hussain *et al*., 2005). Primers AJ1 and AJ4 (Table 2.3) were used for the PCR amplification. A large flanking region of the Tn*916*Δ*orf12* fragment is crucial in the homologous recombination as it is expected to efficiently replace *erm*(B) in Tn*916*ΔE by allelic exchange. The allelic exchange allows selection of transformants on tetracycline. The constructed *B. subtilis* mutant was used for downstream analysis and designated BS79A (contains Tn*916*Δ*orf12*). This mutant strain is in an isogenic background to BS34A (contains wild type Tn*916*) however the exact location of the conjugative transposon in BS59A has not been determined.

3.2.5 Constructions of a *B. subtilis* mutant with a different antibiotic resistance gene

B. subtilis mutant carrying a *cat* gene marker was constructed to allow selection during competitive fitness assay. The integration vector pDL harbouring the *cat* gene, which confers resistance to chloramphenicol was used for integration within the coding sequence of the non-essential *amyE* gene of *B. subtilis* BS34A (contains wild type Tn*916*). In the first instance, the *bgaB* gene was removed from the vector

using restriction enzymes SacI and SnaBI (Figure 3.3). The *bgaB* gene was removed from the vector to avoid any background effect from this gene. The vector was re-ligated and transformed into *E. coli*. After 18-24 h incubation at 37^{o}C, plasmid extraction was carried out followed by restriction digest of the pDLΔ*bgaB* vector using PstI. The linearised fragment was subsequently transformed into *B. subtilis* BS34A. The homologous *amyE* sequence that flanked the *cat* gene is expected to integrate into the *amyE* locus in *B. subtilis* chromosome via double recombination. Transformants were selected on BHI agar supplemented with tetracycline (10 μg ml^{-1}) and chloramphenicol (5 μg ml^{-1}) after 24-48 h incubation. The constructed mutant was designated BS92A (BS34AΔ*amyE*, contains Tn*916*).

3.2.6 Validation of the integrated *cat* gene into *amyE* locus

Integration of the *cat* gene into the *amyE* locus in *B. subtilis* was confirmed using starch hydrolysis. The wild type [BS34A (contains wild type Tn*916*)] and the mutant [BS92A (BS34AΔ*amyE*, contains Tn*916*)] strains were streaked on BHI agar supplemented with starch (1%). After 24 h of incubation at 37^{o}C, the plate was flooded with Gram's iodine. A clear zone around the grown colonies indicates hydrolysis of starch. BS92A with the interrupted *amyE* gene will not be able to hydrolyse the starch, hence no clearing zone is expected.

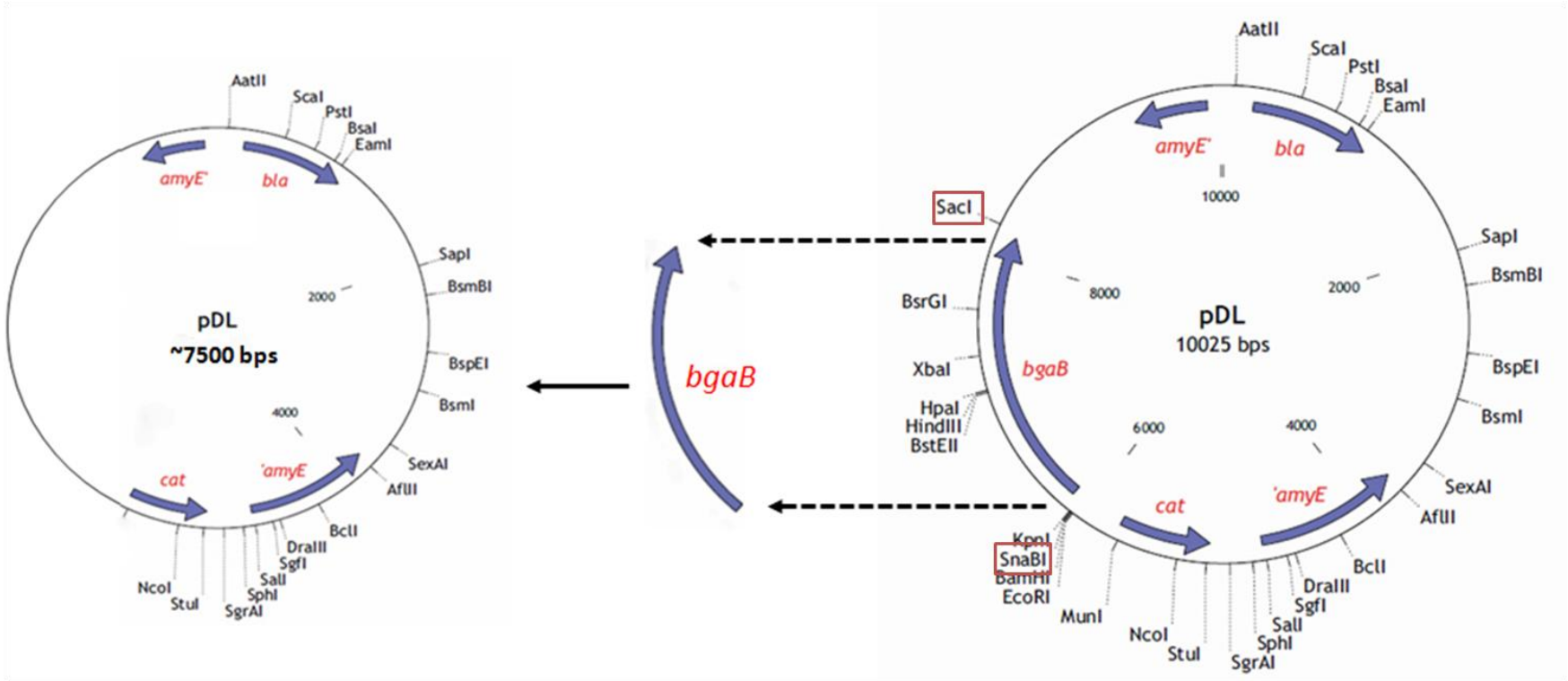

Figure 3.3 Construction of pDLΔ*bgaB* integration vector. *bgaB* gene was removed from pDL using restriction enzymes SacI and SnaBI (red boxes). The linearised fragment was ligated prior to transformation into *E. coli*.

3.2.7 Comparative growth curves

The growth curve assay was carried out by cultivating *B. subtilis* BS34A (contains wild type Tn*916*) and BS79A (contains Tn*916*Δ*orf12*) separately in 100 ml BHI broth in 250 ml Erlenmeyer flasks. The cultures were grown in a shaking incubator (200 rpm) at 37^{o}C. The growth was monitored by measuring the optical densities (OD) at 600 nm every 30 min up to 5 h. Tetracycline is added to two of the cultures in the overnight growth of the starter cultures and two of the cultures (one previously grown in tetracycline and one in antibiotic free media) at the start of the 5 h growth period following the overnight growth. Therefore one culture was grown in antibiotics media and then subcultured into antibiotic free (Tc-abf on Figures 3.4 and 3.5) and antibiotic containing media (Tc-Tc on Figures 3.4 and 3.5) and the other was initially grown in the absence of antibiotics and then similarly subcultured into antibiotic free (abf-abf on Figures 3.4 and 3.5) and antibiotic containing media (abf-Tc on Figure 3.4 and 3.5).

3.2.8 Competitive fitness assay

The relative fitness was assayed by cultivating the *B. subtilis* strains separately in BHI broth (free antibiotic) for 18 h to a density of 1 x 10^{9} cfu ml^{-1}. This is a preconditioning step ensuring both competitors were in comparable physiological states and cell densities prior to competition experiments. The two competitors

(0.1 ml of each strain) were then mixed in a 250 ml Erlenmeyer flask containing 100 ml BHI broth (free antibiotic or supplemented with tetracycline). Prior to incubation, 0.1 ml of the mixed culture was diluted to 1 x 10^{-4} and 1 x 10^{-5} in 1 ml BHI broth and plated on BHI agar supplemented with tetracycline (10 µg ml^{-1}) to select for *B. subtilis* strains BS34A (contains wild type Tn*916*) and BS79A (contains Tn*916*Δ*orf12*) and tetracycline plus chloramphenicol (5 µg ml^{-1}) to select for *B. subtilis* BS92A (BS34AΔ*amyE*, contains Tn*916*). The initial cell densities are calculated by subtracting the number of colonies on BHI agar supplemented with tetracycline and chloramphenicol from the BHI agar plus tetracycline. Incubation was carried out for 5 h in a shaking incubator (200 rpm) at 37^{o}C. At the end of the culture period, 0.1 ml of the mixed culture was diluted to 1 x 10^{-5} and 1 x 10^{-6}, followed by plating on BHI agar supplemented with the same antibiotics as mentioned previously. The final cell densities was then determined.

The fitness of one genotype relative to the other was elucidated, first by calculating the realised Malthusian parameter for each competitor and then by computing the ratio of their Malthusian parameters (Lenski *et al*., 1991). The following equations was used to determined the relative fitness of the competitors; (i) $m = \ln (N_1/N_0)$ (ii) $w = m1/m2$ and (iii) $s = 1-w$, where m is the Malthusian parameter, N_1 and N_0 are the final and initial densities during the pairwise, w is the relative fitness of each genotype and s is the selection coefficient or fitness effect.

3.2.9 Transfer experiment and transconjugants selection

Transfer of Tn*916* between *B. subtilis* strains [BS34A (contains wild type Tn*916*) and BS79A (contains Tn*916*Δ*orf12*)] and *C. difficile* CD37 was carried out using filter mating (Section 2.6). The nontoxinogenic *C. difficile* CD37 was used as a recipient in this experiment as it has been previously shown to be a good recipient for Tn*916* from *B. subtilis* strains (Mullany *et al*., 1990). The donor strains were grown in BHI broth supplemented with tetracycline whereas the recipient strain was grown in a pre-reduced BHI broth supplemented with rifampicin. The transconjugants were selected on BHI agar supplemented with tetracycline (10 µg ml^{-1}) and rifampicin (25 µg ml^{-1}) after 24-48 h incubation at 37^{o}C under anaerobic condition (Section 2.3).

3.3 Results

3.3.1 Construction of Tn*916*Δ*orf12* fragment

The involvement of *orf12* in the regulation of *tet*(M) in Tn*916* was investigated by constructing a 2 bp mutation in the start codon of *orf12*. Constructions of the mutated start codon was carried out by first, amplifying the Tn*916* fragment (from the end of *orf14* to *orf9*) using primers AJ1 and AJ4 (Figure 3.4 A). The amplified PCR product was cloned into pGEM-T Easy and subsequently transformed into *E. coli* α-select (bronze efficiency). The plasmid harbouring the correct sized insert (4.1 kb), designated pAPR108 (Figure 3.4 B) was used as the template in site directed mutagenesis, where a 2 bp mutation was introduced in the start codon of the *orf12* using primers AJ15 and AJ16. Amplification of the regulatory region and the entire plasmid gave rise to a 7.1 kb fragment as shown in Figure 3.4C. The mutated regulatory region was ligated and transformed into *E. coli*. Plasmid extraction was then carried out and sequenced. Figure 3.5 shows a multiple sequence alignment of Tn*916*Δ*orf12* and Tn*916* fragments. These data confirmed the mutation made in the start codon of *orf12* of Tn*916* (**AT**G→**GC**G).

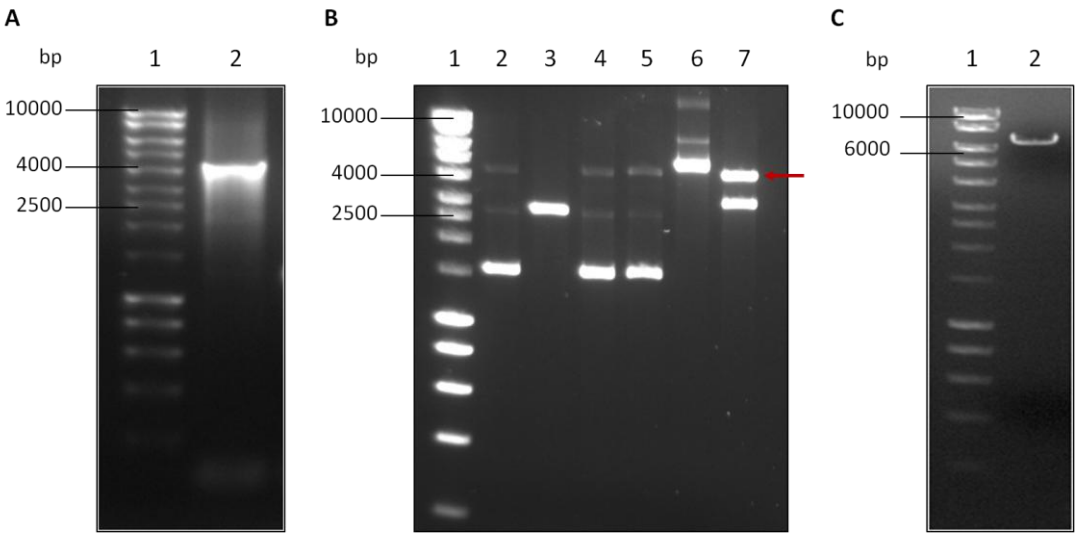

Figure 3.4 Analysis of Tn*916* and Tn*916*Δ*orf12* fragments. Panel A shows the amplified Tn*916* fragment. Lane 1: HyperLadder I; Lane 2: The 4.1 kb PCR product. Panel B shows the undigested and EcoRI-digested pGEM-T Easy. Lane 1: HyperLadder I; Lanes 2, 4, 5 and 6: Undigested plasmids; Lane 3: Digested plasmid with no insert; Lane 7: Digested plasmid with the correct sized insert. Arrows represent the 4.1 kb insert. Panel C shows the PCR product of Tn*916*Δ*orf12* fragment. Lane 1: HyperLadder I; Lane 2: The PCR product (7.1 kb).

Figure 3.5 Multiple sequence alignment of Tn*916* and Tn*916*Δ*orf12* fragments. The 2 bp start codon mutation of *orf12* is shown in the red box. The promoter P*tet*(M) is indicated by -35 and -10 underlined sequences. The dashed arrows represent the inverted repeats 5, 6, 7 and 8. The ribosome binding site (RBS) and the start codon of *tet*(M) are underlined.

3.3.2 Integration of Tn*916*Δ*orf12* fragment into *B. subtilis* BS59A

In *B. subtilis* BS59A (contains Tn*916*ΔE), the Tn*916*Δ*orf12* fragment is expected to replace *erm*(B) via allelic replacement as illustrated in Figure 3.6. The integration of Tn*916*Δ*orf12* fragment and an allelic replacement of *erm*(B) gene by the *tet*(M) gene will allow selection of *B. subtilis* transformants using tetracycline. The replaced gene [*erm*(B) to *tet*(M)] was confirmed by PCR. Two sets of primers (CTn9824F and O10R; CTn13562F and O14R) (Table 2.3) were used to amplify the integrated junctions as shown in Figure 3.7 A. The PCR products (Figure 3.7 B) were sent for sequencing. Another PCR amplification was carried out to confirm the presence of *tet*(M) in *B. subtilis* BS79A (contains Tn*916*Δ*orf12*) (Figure 3.7 C). The presence of *tet*(M) was further confirmed by the sequencing results.

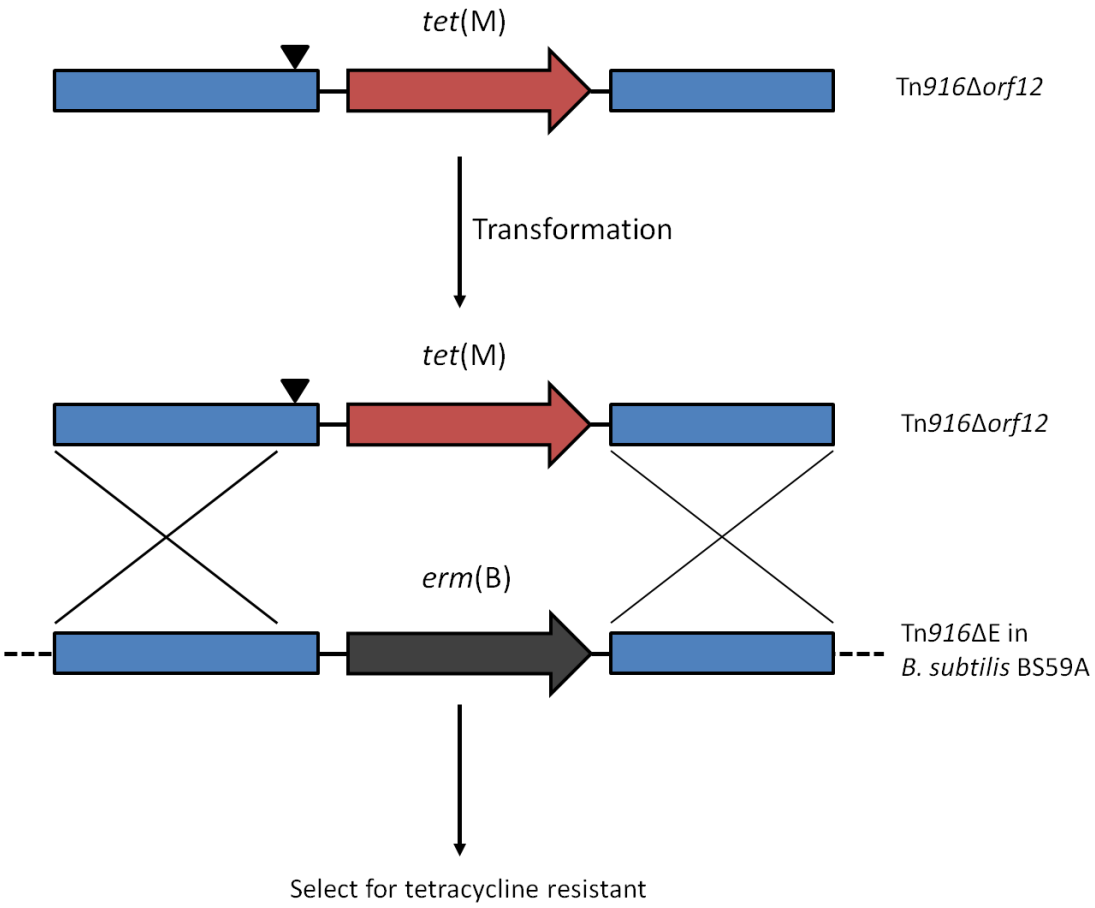

Figure 3.6 Double cross over recombination that is expected to occur in *B. subtilis* BS59A (contains Tn*916*ΔE). The black triangle represents the mutation in the start codon of *orf12*. The blue boxes represent the homologous region of Tn*916*. The *tet*(M) and *erm*(B) genes are represented by the red and black arrowed boxes, respectively.

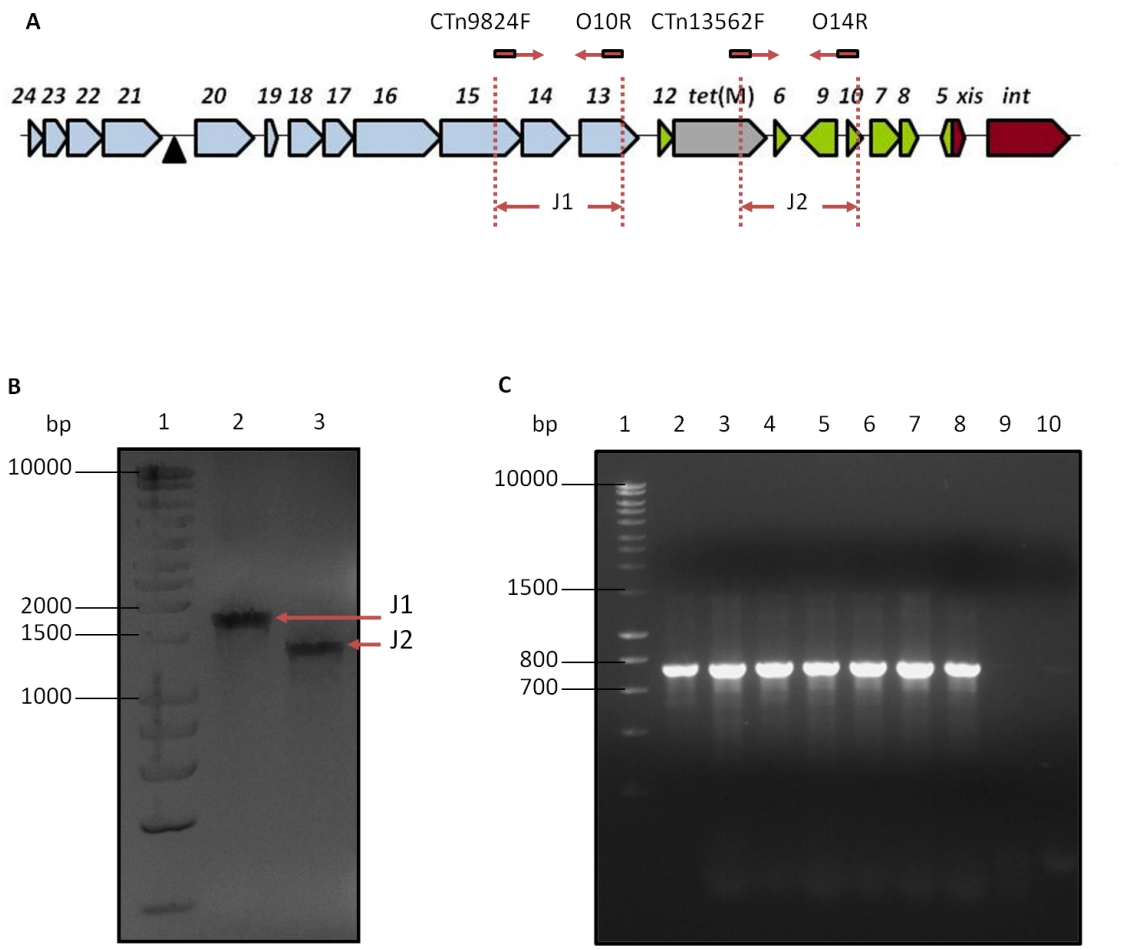

Figure 3.7 The amplified Tn*916* junctions in *B. subtilis* BS79A (contains Tn*916*Δ*orf12*). Panel A: Arrows represent the primers and direction of priming. Junction 1 (J1) is expected to be 1.7 kb in size whereas junction 2 (J2) is 1.4 kb in size. Panel B: The PCR products of J1 and J2. Panel C: The PCR products of *tet*(M) genes. Lane 1: HyperLadder I; Lane 2: Genomic DNA of *B. subtilis* BS34A (positive control); Lanes 3-8: Genomic DNA of *B. subtilis* BS79A (from 6 isolated colonies); Lane 9: Genomic DNA of *B. subtilis* BS59A (negative control); Lane 10: No DNA.

3.3.3 Confirmation of the removal of *bgaB* gene from pDL vector and construction of *B. subtilis* mutant carrying *cat* gene

The integration vector pDLΔ*bgaB* was successfully constructed by removing the *bgaB* gene from pDL. The *bgaB* was removed from the vector to avoid any background effect from this gene. Both pDL and pDLΔ*bgaB* were digested with PstI and a reduction in the size of pDLΔ*bgaB* compared to pDL indicates the absence of *bgaB* gene (Figure 3.8). Integration of pDLΔ*bgaB* into the *amyE* locus of *B. subtilis* BS34A (contains wild type Tn*916)* was carried out via transformation. In *B. subtilis* BS34A, the plasmid is expected to integrate into the genome via allelic exchange, causing disruption to the *amyE* gene (Figure 3.9). The constructed *B. subtilis* mutant was designated BS92A. pDLΔ*bgaB* contains the *cat* gene that encodes for chloramphenicol resistant hence allows selection during competitive fitness assays.

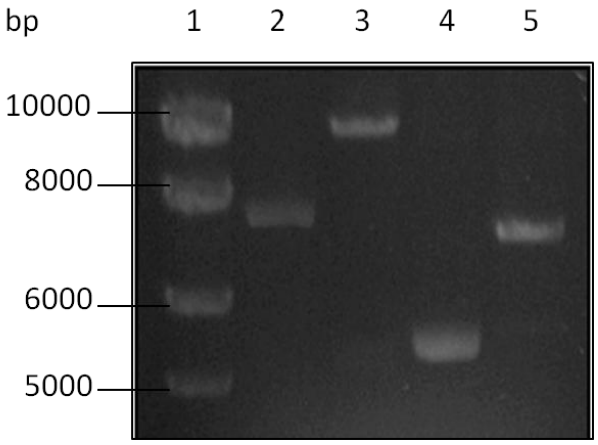

Figure 3.8 Confirmation of the removal of *bgaB* gene from pDL. The gel photo visualises the undigested and PstI-digested pDL and pDLΔ*bgaB*. Lane 1: HyperLadder I; Lane 2: Undigested pDL; Lane 3: Digested pDL; Lane 4: Undigested pDLΔ*bgaB*; Lane 5: PstI-digested pDLΔ*bgaB*. A reduction in the size of pDLΔ*bgaB* observed in Lane 5 compared to pDL on Lane 3 suggests the absence of *bgaB* gene.

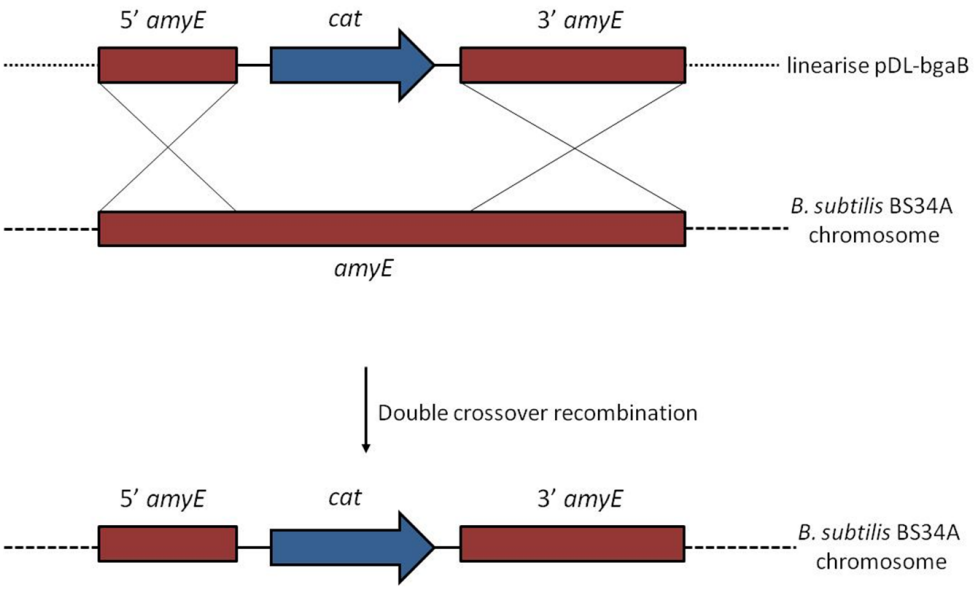

Figure 3.9 The expected double recombination of the integration vector in *B. subtilis* BS34A. Linearisation of the plasmid should lead to integration only by a double cross over mechanism.

3.3.4 Confirmation of double recombination and validation of the interrupted *amyE* gene in *B. subtilis* BS92A

The double recombination of the linearised pDLΔ*bgaB* in *B. subtilis* BS34A (contains wild type Tn*916*) was confirmed using PCR amplification. Two sets of primers were designed upstream and downstream of the integrated junctions, and overlapping the *cat* gene (Figure 3.10 A). The genomic DNA of one transformant designated *B. subtilis* BS92A (BS34AΔ*amyE*, contains Tn*916*) was used as template for the PCR reaction (Figure 3.10 B). In addition, the interruption of the *amyE* gene was confirmed phenotypically using starch agar. Upon interaction with the Gram's iodine, a clear zone was observed around the streaked BS34A (control) indicated the hydrolysis of starch by the extracellular amylase. Conversely, the absence of clear zone around the BS92A confirmed the interruption of *amyE* gene (Figure 3.11).

The constructed BS92A was subjected to a comparative growth curve against the wild type strain (BS34A) to ensure that the marker (*cat* gene) is stably maintained and its presence does not interfere with the growth rate of BS92A. In this experiment, BS34A and BS92A were grown separately for 5 h, and an OD_{600} was measured periodically every 0.5 h. Based on the results, BS92A displayed the same rate of growth as BS34A, hence is considered appropriate marker strain for competitive experiments (Figure 3.12).

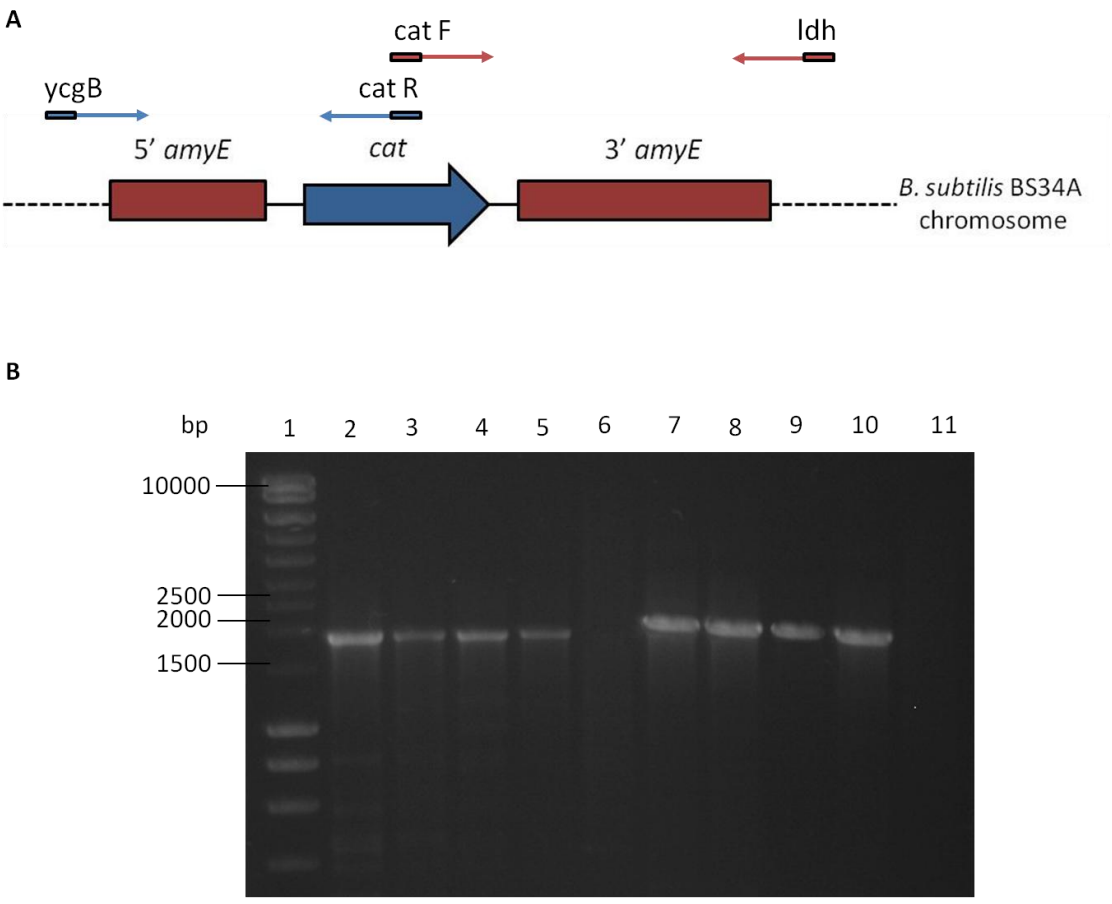

Figure 3.10 PCR amplification of the integrated junctions in *B. subtilis* BS34A (contains wild type Tn*916*). Panel A: Arrows represent the primers and direction of priming. Two sets of primers that overlapped the *cat* gene were used for the PCR amplification. Panel B: The PCR products of the integrated junctions. Four different colonies were used as template for the PCR amplification. Lane 1: HyperLadder I; Lanes 2-5: Amplified PCR products using primers ycgB and catR (Junction 1); Lane 7-10: Amplified PCR products using primers catF and ldh (Junction 2). Lanes 6 and 11: Negative control (genomic DNA of *B. subtilis* BS34A).

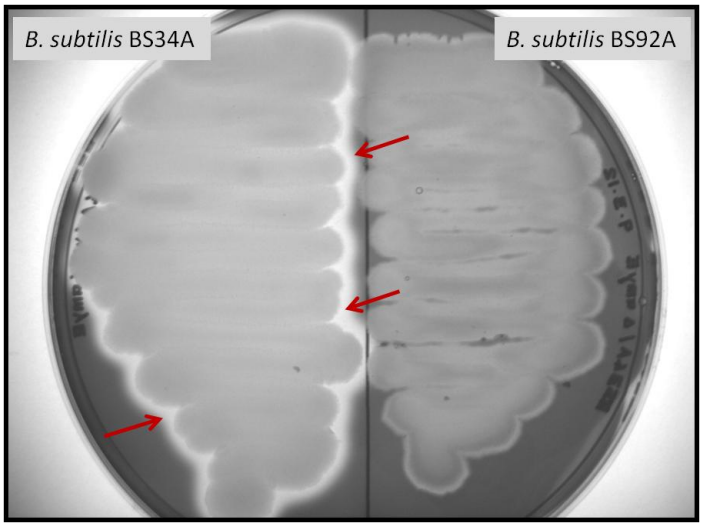

Figure 3.11 Observations on starch agar. The clearing zone indicates the hydrolysis of starch by the extracellular amylase whereas the absence of clearing zone indicated there is no hydrolysis of starch, presumably due to the interruption of *amyE* gene.

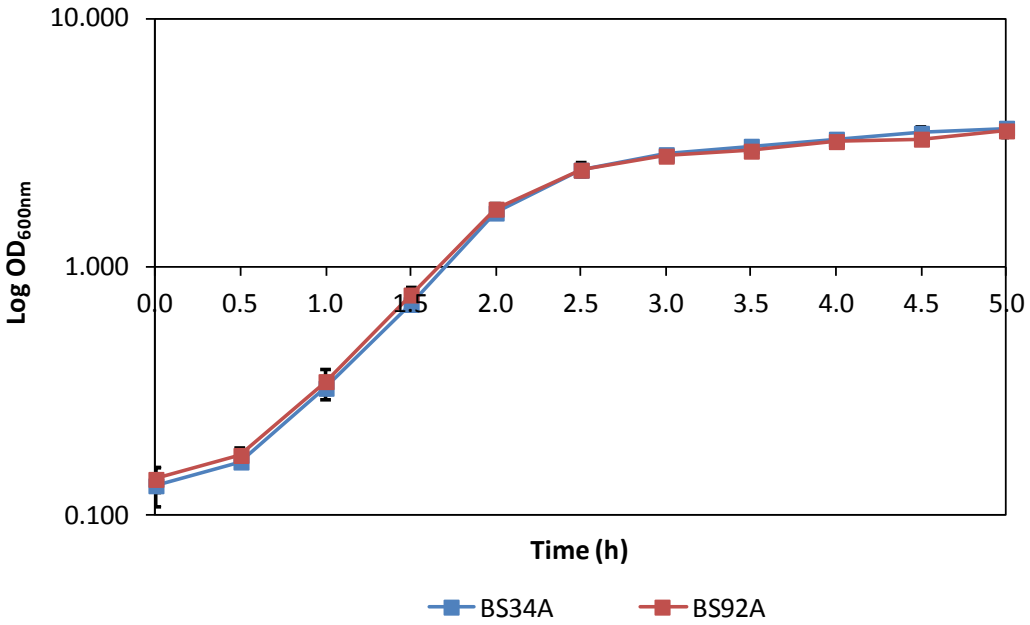

Figure 3.12 Comparative growth curve of *B. subtilis* strains BS34A (contains wild type Tn916) and BS92A (BS34AΔ*amyE*). Both strains demonstrated the same growth profile ($P>0.05$). Error bars represent standard deviation of three independent experiments.

3.3.5 Comparative growth curves of *B. subtilis* strains BS34A and BS79A

In this experiment, the effect of tetracycline to the growth of *B. subtilis* BS34A (contains wild type Tn*916*) and BS79A (contains Tn*916*Δ*orf12*) was investigated. Figure 3.13 and Figure 3.14 illustrate the growth profile of BS34A and BS79A, respectively, which were monitored under four different conditions; from overnight antibiotic free media to tetracycline (abf-Tc) and antibiotic free (abf-abf) media, and from overnight tetracycline containing media to antibiotic (Tc-Tc) and antibiotic free (Tc-abf) media. As shown in Figure 3.13, the abf-abf and Tc-abf cultures of BS34A showed a similar growth profile ($p>0.05$). A slightly delayed growth was observed for Tc-Tc culture, whereas the slowest growth rate was observed for abf-Tc culture. Towards the end of the logarithmic phase and the start of stationary phase, all cultures seemed to grow at the same rate. BS79A demonstrated a similar growth profile to BS34A (Figure 3.14). Despite the BS34A and BS79A being almost isogenic (the element may be in a different location) the growth kinetics are the same (Figure 3.15). Interestingly, when the abf-Tc cultures of both strains were compared, it was noted that BS79A had a significantly slower growth rate than BS34A (Figure 3.16) ($p<0.05$), particularly during the mid-exponential phase (2 h). However, both strains grow at the same rate after 4 h.

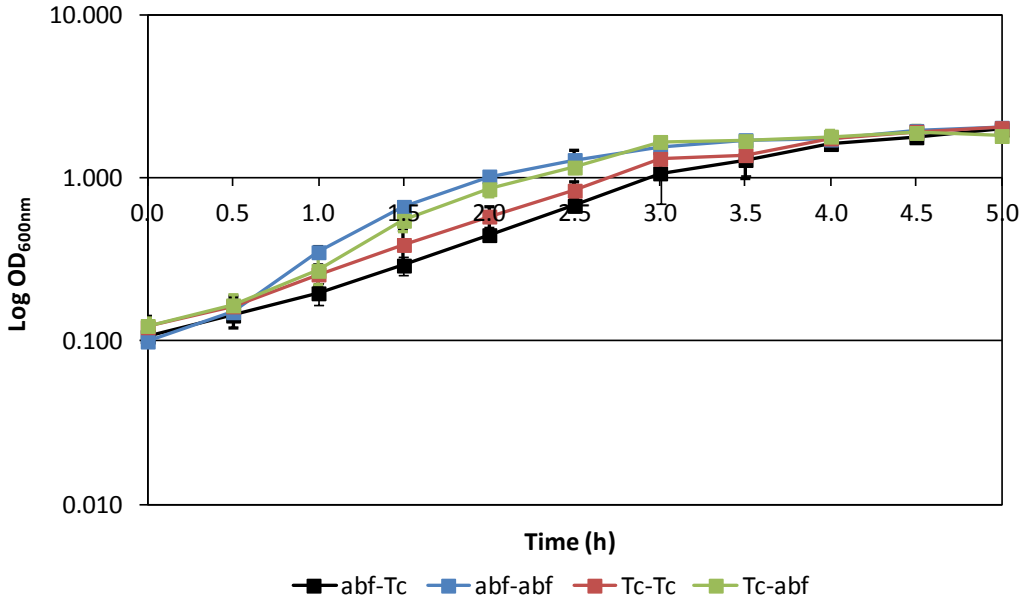

Figure 3.13 Comparative growth curve of BS34A. Colors indicate different treatments of each sample from the overnight culture to the tested culture. Black: antibiotic free to tetracycline; blue: antibiotic free; red: tetracycline and green: tetracycline to antibiotic free. Error bars represent standard deviation from three independent experiments.

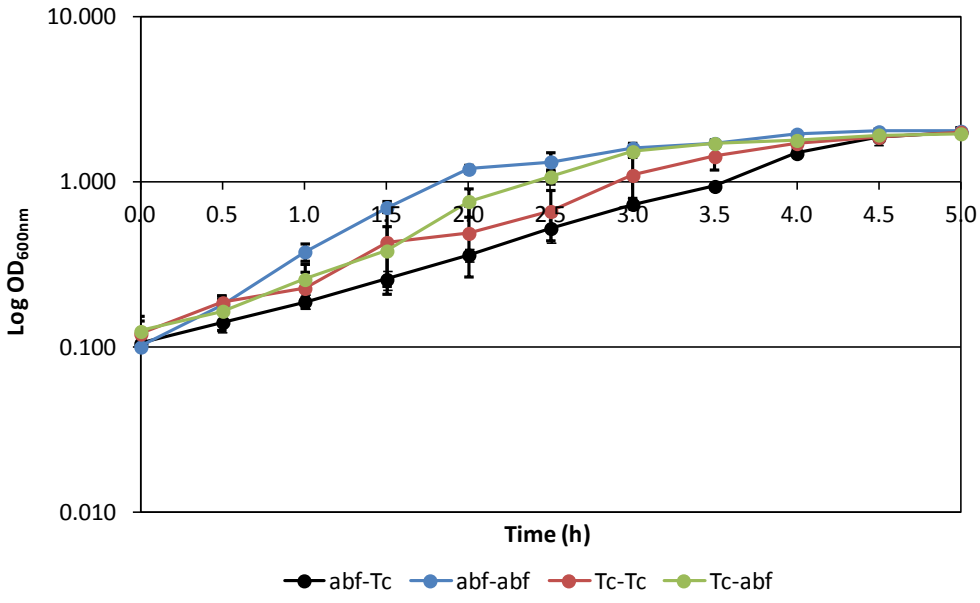

Figure 3.14 Comparative growth curve of BS79A. Colors indicate different treatments of each sample from the overnight culture to the tested culture. Black: antibiotic free to tetracycline; blue: antibiotic free; red: tetracycline and green: tetracycline to antibiotic free. Error bars represent standard deviation from three independent experiments.

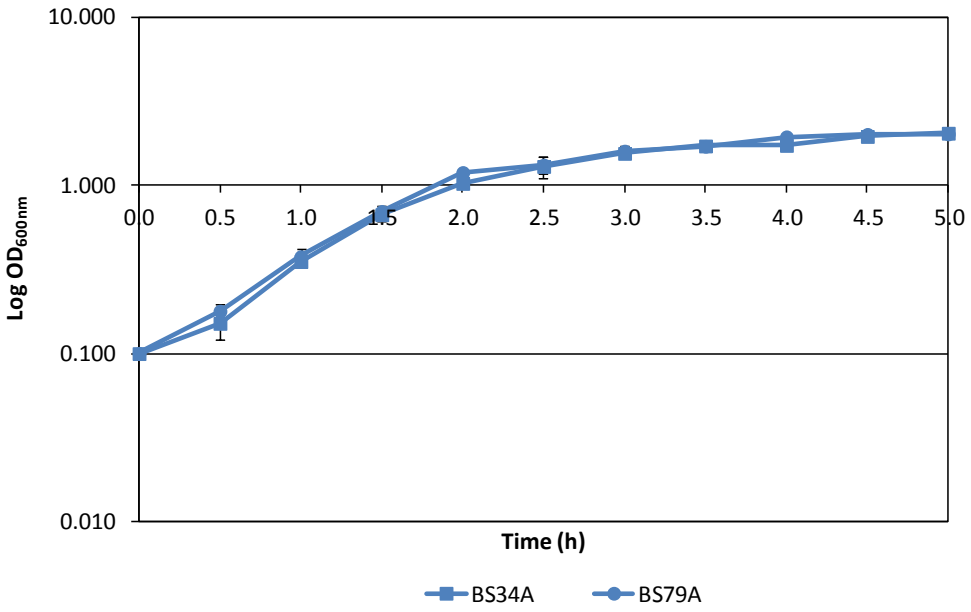

Figure 3.15 Comparative growth curve of *B. subtilis* strains BS34A and BS79A in antibiotic free medium (abf-abf). BS34A (■) and BS79A (●) demonstrate a similar growth rate (P>0.05). Error bars represent standard deviation from three independent experiments.

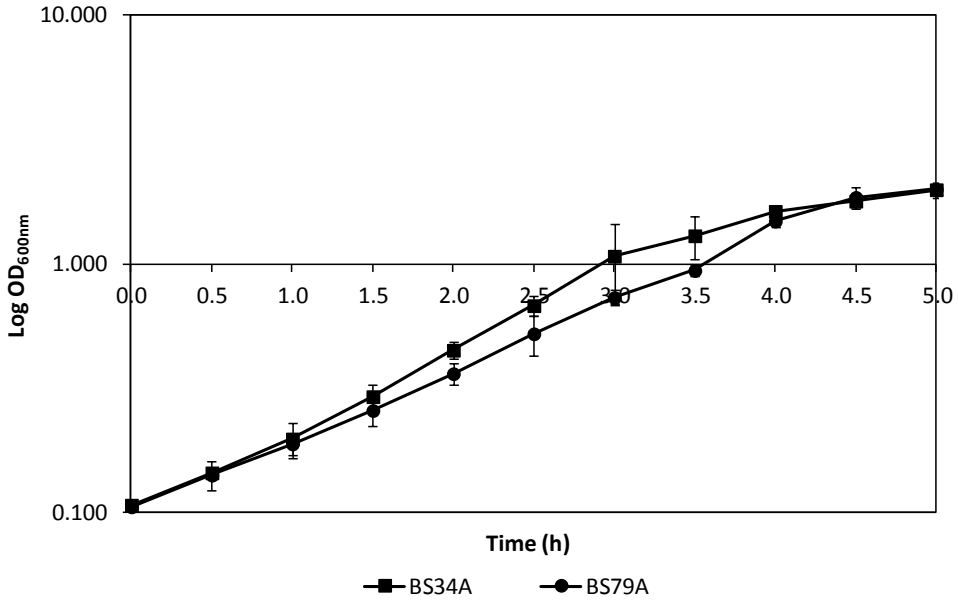

Figure 3.16 Comparative growth curve of *B. subtilis* strains BS34A and BS79A, challenged with tetracycline (abf-Tc). BS79A (●) exhibited a delayed growth relative to BS34A (■) (P<0.05) during the mid-exponential phase (2 h). Error bars represent standard deviation from three independent experiments.

3.3.6 Competitive fitness of *B. subtilis* BS34A, BS92A and BS79A

Estimation of the relative fitness between *B. subtilis* strains BS34A (contains wild type Tn*916*), BS92A (BS34AΔ*amyE*) and BS79A (contains Tn*916*Δ*orf12*) was carried out by competition experiments. In this experiment, BS92A carrying the *cat* gene was used as the marked competitor to distinguish between BS34A and BS79A (both strains carry *tet*(M) gene hence not directly competed). The relative fitness of the competitors was calculated using the equations described in Section 3.2.8. Results indicate that BS92A is 3% more fit than BS34A (Table 3.1). In contrast, BS79A is 4% more fit than BS92A (Table 3.2). The transitive fitness relation between these three strains is BS79A>BS92A>BS34A, which means BS79A>BS34A. As BS79A is 4% more fit than BS92A, and BS92A is 3% more fit than BS34A, therefore by using the transitive law, it is indicated that BS79A is 7.12% more fit than BS34A.

The competitive fitness between BS79A and BS92A was also determined in the presence of tetracycline. In this experiment, tetracycline was added at the beginning of the competition experiment. Table 3.3 illustrates the relative fitness of BS79A and BS92A, enumerated every 1 h up to 5 h of competition. BS79A is 10% more fit than BS92A during the first 1 h, however the fitness is reduced for the next 2 h of competition. At 4 h, BS79A demonstrated a more fitness effect (3%) than BS92A, whereupon it was again decrease at 5 h.

Table 3.1 Relative fitness of *B. subtilis* strains BS92A (BS34AΔ*amyE*) and BS34A (contains wild type Tn*916*). The relative fitness was elucidated using the realised Malthusion parameter; m = ln [N(1)/N(0]) and w =m1/m2 where m describing the exponential growth of each competitor, N(1) and N(0) are the final and initial cell densities during competition and w is the relative fitness of each genotype. The fitness effect (s) is calculated as s = w-1. Therefore, in this competition experiment, s = 1.03-1 = 0.03 which imply that strain A (BS92A) is 3% more fit than strain B (BS34A).

Strains	**Realised Malthusion parameter**[a]		**Relative fitness**[a] w=mA/mB	**Fitness effect** s=w-1
	mA=ln [A(1)/A(0)]	mB = ln [B(1)/B(0)]		
B. subtilis BS92A (A) vs. *B. subtilis* BS34A (B)	2.59 (± 0.03)	2.52 (± 0.05)	1.03 (± 0.11)	0.03 (3% ± 1%)

[a]Average of 3 independent experiments

Table 3.2 Relative fitness of *B. subtilis* strains BS79A (contains Tn*916*Δ*orf12*) and BS92A (BS34AΔ*amyE*). The relative fitness was elucidated as above. As fitness effect (s) is calculated as s = w-1, therefore, in this competition experiment, s = 1.04-1 = 0.04 which imply that strain A (BS79A) is 4% more fit than strain B (BS92A).

Strains	**Realised Malthusion parameter**[a]		**Relative fitness**[a] w=mA/mB	**Fitness effect** s=w-1
	mA=ln [A(1)/A(0)]	mB= ln [B(1)/B(0)]		
B. subtilis BS79A (A) vs. *B. subtilis* BS92A (B)	2.31 (± 0.14)	2.22 (± 0.16)	1.04 (± 0.02)	0.04 (4% ± 2%)

[a]Average of 3 independent experiments

Table 3.3 Relative fitness of *B. subtilis* strains BS79A (contains Tn*916*Δ*orf12*) and BS92A (BS34AΔ*amyE*) in tetracycline containing media. The relative fitness was elucidated as previously described. However, in this experiment, N(1) which is the final cell densities varies between 1-5 h. N(0) remains the initial cell densities. This experiment demonstrated a variation in the fitness effect, with an inconsistent fitness observed for BS79A throughout the 5 h competition experiments.

***B. subtilis* BS79A (A) vs. *B. subtilis* BS92A (B)**	**Realised Malthusion parameter[a]**		**Relative fitness[a]**
	mA=ln [A(1)/A(0)]	mB= ln [B(1)/B(0)]	w=mA/mB
1 h	0.64 (± 0.14)	0.58 (± 0.12)	1.10 (± 0.16)
2 h	1.22 (± 0.22)	1.30 (± 0.19)	0.94 (± 0.26)
3 h	2.49 (± 0.06)	2.56 (± 0.17)	0.97 (± 0.11)
4 h	3.25 (± 0.05)	3.15 (± 0.12)	1.03 (± 0.09)
5 h	0.94 (± 0.14)	1.51 (± 0.25)	0.62 (± 0.17)

[a]Average of 3 independent experiments

3.3.7 Transfer of Tn*916* from *B. subtilis* BS34A and BS79A to *C. difficile* CD37

This experiment was carried out to investigate the effect of the disruption of the start codon of *orf12* in the mobility of Tn*916*. In this filter mating experiment, *C. difficile* CD37 was used as the recipient. The frequency of transfer [± standard deviation (SD)] detected for BS34A (contains wild type Tn*916*) was 1.74 x 10^{-6} (± 2.28 x 10^{-6}) per recipient. As for BS79A which contains Tn*916*Δ*orf12*, the transfer frequency detected was 4.14 x 10^{-6} (± 4.07 x 10^{-6}) per recipient. From these results, it was concluded that the transfer of Tn*916*Δ*orf12* is not appreciably different to that of the wild type Tn*916*, despite the disruption of the start codon of *orf12*. The presence of Tn*916* in *C. difficile* CD37 was confirmed by PCR amplification of *tet*(M) gene (Figure 3.17).

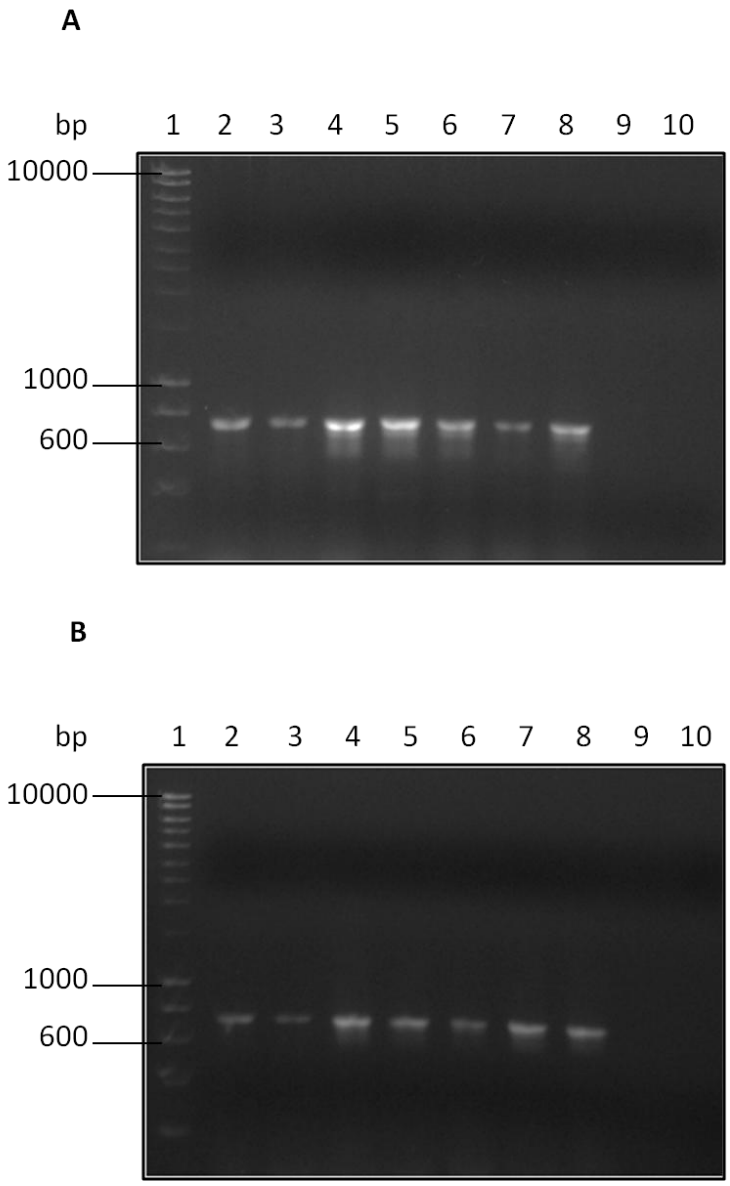

Figure 3.17 PCR amplification of *tet*(M) gene in *C. difficile* CD37. Panel A: *tet*(M) gene in CD37 transconjugants (BS34A x CD37). Panel B: *tet*(M) gene in CD37 transconjugants (BS79A x CD37). Lane 1: Hyperladder I; Lane 2: Genomic DNA of *B. subtilis* BS34A (positive control); Lane 3: Genomic DNA of *B. subtilis* BS79A (positive control); Lanes 4-8: Putative transconjugants carrying *tet*(M) gene; Lane 9: Genomic DNA of *C. difficile* CD37 (negative control); Lane 10: No DNA.

3.4 Discussion

In this study, an in-depth investigation concerning the role of *orf12* and its translation in regulating the transcription of Tn*916* was carried out using *B. subtilis* construct containing 2 bp mutation disrupting the start codon of *orf12*. The experiments were performed in the presence and absence of tetracycline, which was previously shown to be involved in the transcriptional regulation of this element (Su *et al*., 1992; Celli and Trieu-Cuot, 1998). In agreement with previous reports, the involvement of tetracycline in the transcriptional regulation of Tn*916* was again highlighted in this study. In growth conditions where tetracycline is present (abf-Tc and Tc-Tc), both the wild type (BS34A) and the mutated strain [BS79A (contains Tn*916*Δ*orf12*)] demonstrated a slower growth rate compared to their respective tetracycline-free culture (Tc-abf and abf-abf) counterparts, especially during the mid-logarithmic phase where cells were rapidly dividing (Figure 3.13 and Figure 3.14). It is possible that at this stage, the presence of tetracycline has partially inhibited the growth while Tet(M) takes time to protect enough ribosomes to allow increased translation of *tet*(M) gene. As this happens, the cells are able to grow normally, indicated by comparable growth rates with tetracycline-free cultures towards the end of the logarithmic phase and the start of stationary phase. The ability of Tet(M) to protect ribosomes was demonstrated by Burdett (1986) although it remains a matter of speculation of the average time required to complete the process.

Interestingly, results presented also suggests that tetracycline exerted a more pronounced effect to the growth profile when added to the cultures during monitoring of growth (abf-Tc) rather than exposure at the onset (Tc-Tc). Pre-exposing the cultures with tetracycline for overnight has assisted the cells to maintain the resistance during the second exposure, which led to a higher growth rate when compared with the non pre-exposed cells. The significance of pre-exposing the cells to tetracycline has been highlighted in a number of studies. For instance, Nesin *et al*. (1990) have demonstrated that pre-exposure of cells to tetracycline not only increase the tetracycline resistance but also caused an increase in the level of mRNA transcripts for *tet*(M). Pre-exposing the cultures with tetracycline has also been shown to enhance conjugal transfer of Tn*916* between *Bacillus* species as reported by Showsh and Andrews (1992).

In the presence of tetracycline, BS79A (contains Tn*916*Δ*orf12*) demonstrated a slower growth rate compared to the wild type BS34A (Figure 3.15), which is probably due to the defective start codon of *orf12*. The absence of the start codon is expected to permanently stop the translation of *orf12*, thus led to the maximal formation of the transcriptional terminator structures. Therefore minimal read-through of transcription is expected to occur into *tet*(M) gene, representing the basal level of transcription through these terminators. This hypothesis is supported by previous study by Burdett (1986) who demonstrated that the transcription into *tet*(M) without the translation of the leader peptide is possible as the ribosomes could still bind to the *tet*(M) Shine-Dalgarno site. The model proposed for *tet*(M)

regulation requires a basal level of Tet(M) to be produced in order to protect a few of the ribosomes in the cell in case of exposure to tetracycline. This basal level of expression is investigated in detail in the next chapter.

As comparison of the exponential growth rates was insufficient to detect any biological fitness cost of BS34A (contains wild type Tn*916*) and BS79A (contains Tn*916*Δ*orf12*), therefore a more sensitive and accurate evaluation was carried out using competition experiments. Results suggest that BS79A is 7.12% more fit than BS34A in the absence of selective pressure, indicating that the 2 bp mutation at the start codon of *orf12* does not confer any fitness cost to BS79A in the absence of antibiotic. In fact, it appears that there is a slight fitness benefit to this strain in the absence of antibiotic. Although the reasons for this remain elusive, we can hypothesise that the level of translation of *orf12* in the wild type will be more than zero, as it will be in BS79A therefore more terminator structures will be destroyed in the wild type when compared to BS79A. This means the wild type is likely producing a higher basal amount of Tet(M) and other Tn*916* proteins.

In the presence of tetracycline, the fitness of BS79A (contains Tn*916*Δ*orf12)* reduced relative to BS92A (BS34AΔ*amyE*) after 2-3 h of growth (Table 3.3). As synthesis of Tet(M) is limited in BS79A due to the defective start codon of *orf12*, therefore it is suspected that the ability of the cells to compete is substantially reduced especially during mid-logarithmic phase where cells are rapidly dividing, this is what we detected in our experiments.

Additionally, it was shown that in the presence of tetracycline, Tn*916*Δ*orf12* was transferred at a comparable frequency as the wild type Tn*916* despite the mutation in the start codon. It has been shown previously in this study that BS34A (contains wild type Tn*916*) and BS79A (contains Tn*916*Δ*orf12*) grow at different rate in the mid-exponential phase (Figure 3.16), hence transfer frequency was expected to be lower in the mutant, however this does not seems to be the case. The reason that contributed to this result are unclear, however it is suspected it could be due to the basal level of transcriptional read-through of *tet*(M) and the downstream genes (*xis* and *int*) is high enough for the transfer of the mutant Tn*916*Δ*orf12*, although this needs to be experimentally proven. It also suspected that the concentration of tetracycline might affect the frequency of transfer as shown in a number of studies. Although in this study tetracycline was used at a concentration of 10 μg ml^{-1}, which was previously shown to enhance the transfer of Tn*916* (Showsh and Andrews, 1992), in most cases, tetracycline was used at a sub-inhibitory concentration as reported by Doucet-Populaire *et al*. (1991) and Ammor *et al*. (2008). Another reason, and probably the correct one, is that the filter-mating experiments are not refined enough to detect small differences in the transfer frequency.

3.5 Conclusions

In this chapter the 2 bp mutation in the start codon of *orf12* of Tn*916* has been shown to have an effect on the growth of the cells [BS79A (contains Tn*916*Δ*orf12*)] compared to the strain carrying wild type Tn*916* (BS34A). However, no appreciable difference could be detected in the frequency of transfer to *C. difficile* CD37. Furthermore this is the first demonstration that the basal level of transcription of *tet(*M) and downstream genes is enough to provide resistance to inhibitory concentrations of the antibiotic (10 μg ml^{-1}) and enough to allow transfer.

Chapter 4.0

Quantitative analysis of *tet*(M) expression using a reporter gene system

4 Quantitative analysis of *tet*(M) expression using a reporter gene system

4.1 Introduction

Reporter gene systems have been widely used for analysis of gene regulation as it offers a rapid and sensitive quantification of gene expression. There are a number of reporter genes available including β-galactosidase (Helmer *et al*., 1984), luciferase (Slauch and Silhavy, 1991), green fluorescent protein (GFP) (Tsien, 1998) and β-glucuronidase (Jefferson *et al*., 1987). The β-glucuronidase gene, which originated from *E. coli*, was first used as a reporter gene for transformation of plants (Jefferson *et al*., 1987). β-glucuronidase (EC 3.2.1.31) encoded by *uidA* (Novel and Novel, 1973) belongs to the family of hydrolases that catalyses the cleavage of a wide variety of β-glucuronides. The expression of this enzyme is measured using colorimetric assays.

In this chapter, the transcriptional regulation of Tn*916* and Tn*5397* was investigated using the β-glucuronidase reporter gene system. The transcriptional activity initiated at the promoter upstream of *tet*(M); P*tet*(M) was quantified colorimetrically. P*tet*(M) is the promoter in Tn*916*, believed to be at the beginning of the regulatory network of Tn*916* (Su *et al*., 1992; Celli and Trieu-Cout, 1998). The activity of P*tet*(M) has been shown to be regulated by the presence of tetracycline (Celli and Trieu-Cout, 1998). This chapter also emphasises the functional roles of

the *orf12* of Tn*916* and the alternative orfs, *orf25* and *orf26* of Tn*5397* in the transcriptional regulation of these elements.

4.2 Materials and methods

4.2.1 Bacterial strains and plasmids

E. coli α-select (bronze efficiency) was used for transformation of pUC19-Pcwp2-GusA and pHCMCO5 (Table 2.2). *B. subtilis* BS34A (contains wild type Tn*916*) was used as a host for all promoter constructs. *E. coli* and *B. subtilis* were grown under the conditions described in Section 2.3.

4.2.2 Bacterial transformation

B. subtilis and *E. coli* transformation was carried out according to the protocol described in Section 2.5.10 and 2.5.11, respectively. The *E. coli* transformants were selected on LB agar after 18-24 h incubation at 37^{o}C. Conversely, selection of *B. subtilis* transformants were carried out on BHI agar after 24-48 h incubation at 37^{o}C. Agar plates were supplemented with ampicillin (100 µg ml^{-1}), tetracycline (10 µg ml^{-1}) or chloramphenicol (10 µg ml^{-1}) for selection of transformants.

4.2.3 Construction of P*tet*(M) promoter constructs of Tn*916* and Tn*5397*

The *orf12* of Tn*916* and *orf25* and *orf26* of Tn*5397* were amplified using primers (Tn*916*: Ptet(M) For/Rev; Tn*5397*: Ptet(M) For5397/Rev5397) (Table 2.3) that bound upstream of P*tet*(M) promoter and *tet*(M) gene (Figure 4.1 and Figure 4.2). The amplified PCR products were cloned into pUC19-Pcwp2-GusA, replacing the Pcwp2 using restriction enzymes KpnI and EcoRI (Figure 4.3). The plasmids were then transformed into *E. coli* and transformants were selected on LB agar supplemented with ampicillin. After 18-24 h incubation at 37^{o}C, the transformants were randomly picked and grown into LB/ampicillin broth. Plasmid extraction (Section 2.5.1) was carried out and the purified plasmids were then sequenced. These plasmids were used as template in site directed mutagenesis (Section 2.5.15) for mutant construction (Figure 4.4). The mutant amplicons were then ligated and transformed into *E. coli*. After 18-24 h incubation, the transformants were selected for plasmid extraction. The purified plasmids were then digested with restriction enzymes KpnI and BamHI. The GusA-P*tet*(M) fragments were cloned into pHCMCO5 replacing the lacO/Pspac fragment followed by transformation into *E. coli*. Subsequently, plasmid DNA (5 µg) was prepared for transformation into *B. subtilis* BS34A (Section 2.5.9). Transformants were selected on BHI agar supplemented with tetracycline and chloramphenicol after 24-48 h incubation at 37^{o}C.

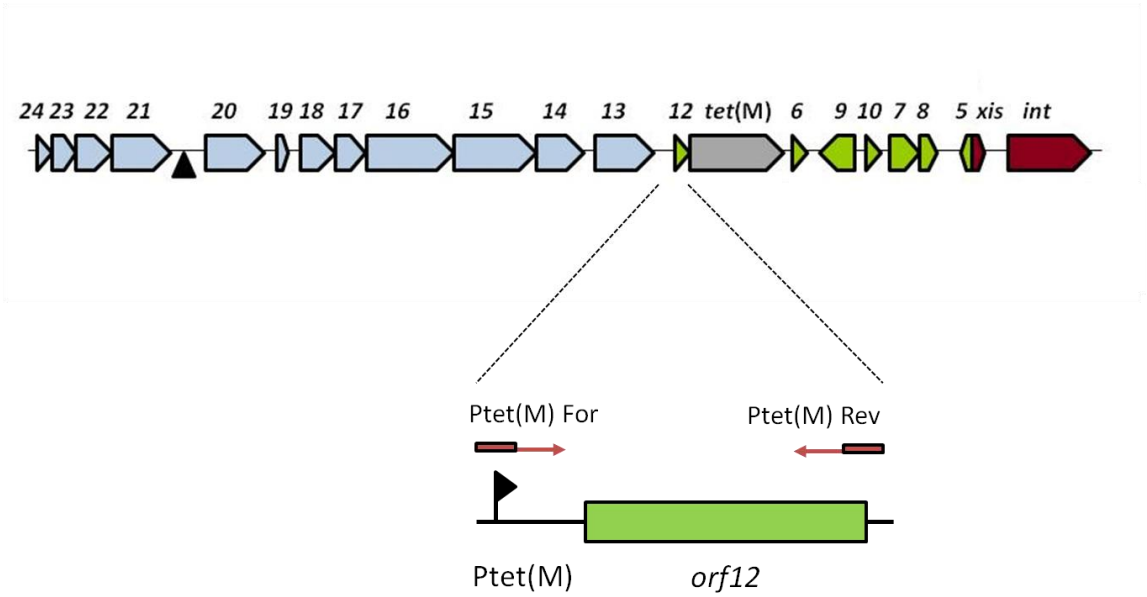

Figure 4.1 Amplification of the P*tet*(M) of Tn*916*. Primers P*tet*(M) For and P*tet*(M) Rev were designed to amplify 100 bp upstream of the *orf12* and *tet*(M) gene. The pointed 'P' indicates the P*tet*(M) promoter. The 450 bp amplified PCR product was cloned into the pUC19-GusA vector and transformed into *E. coli*.

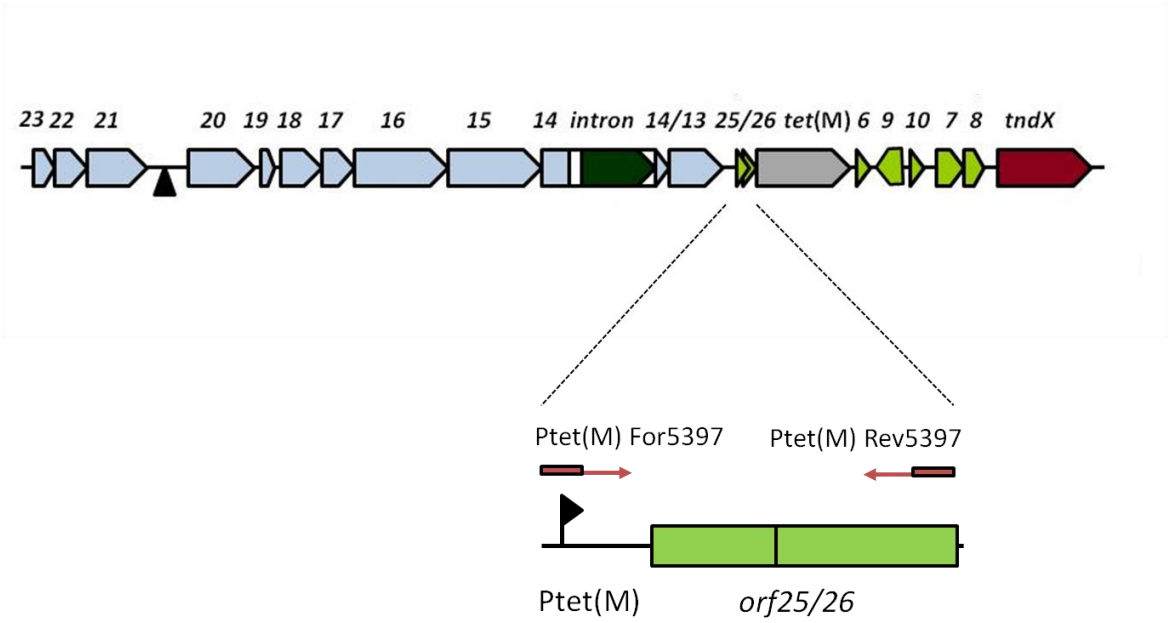

Figure 4.2 Amplification of the Ptet(M) of Tn*5397*. Primers Ptet(M) For5397 and Ptet(M) Rev5397 were designed to amplify 100 bp upstream of the *orf25/26* and *tet*(M) gene. The pointed 'P' indicates the P*tet*(M) promoter. The 358 bp amplified PCR product was cloned into the pUC19-Pcwp2-GusA vector and transformed into *E. coli*.

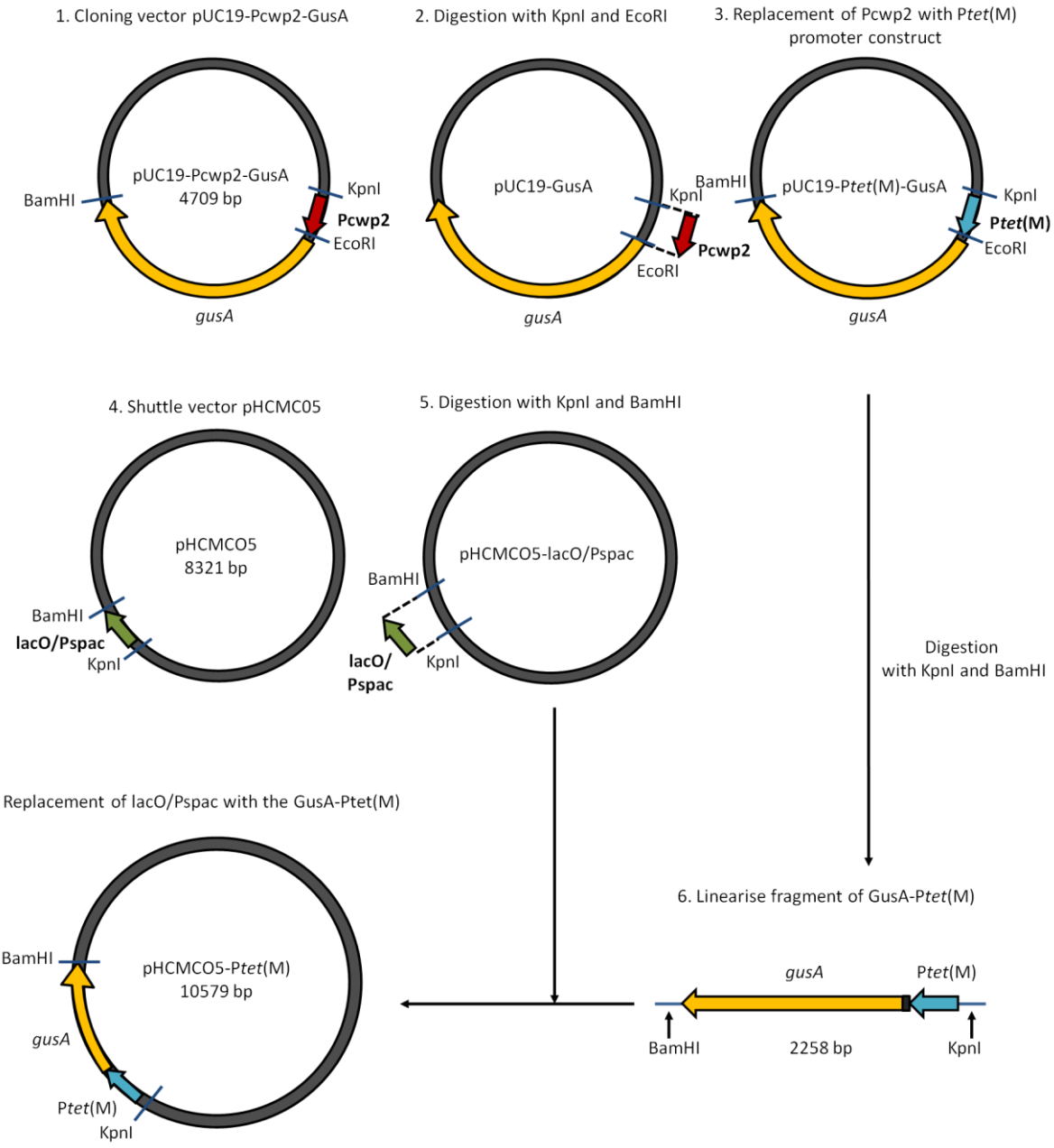

Figure 4.3 Construction of the transcriptional reporter construct, pHCMCO5-P*tet*(M). The P*tet*(M) construct was digested with restriction enzymes KpnI and EcoRI. The digested fragment was cloned into KpnI and EcoRI-digested pUC19-Pcwp2-GusA and transformed into *E. coli*. The prepared plasmid DNA was then digested with KpnI and BamHI, and the GusA-P*tet*(M) fragment was cloned into a shuttle vector pHCMCO5, replacing the lacO/Pspac. The constructed plasmid was then transformed into *E. coli* and subsequently into *B. subtilis* BS34A.

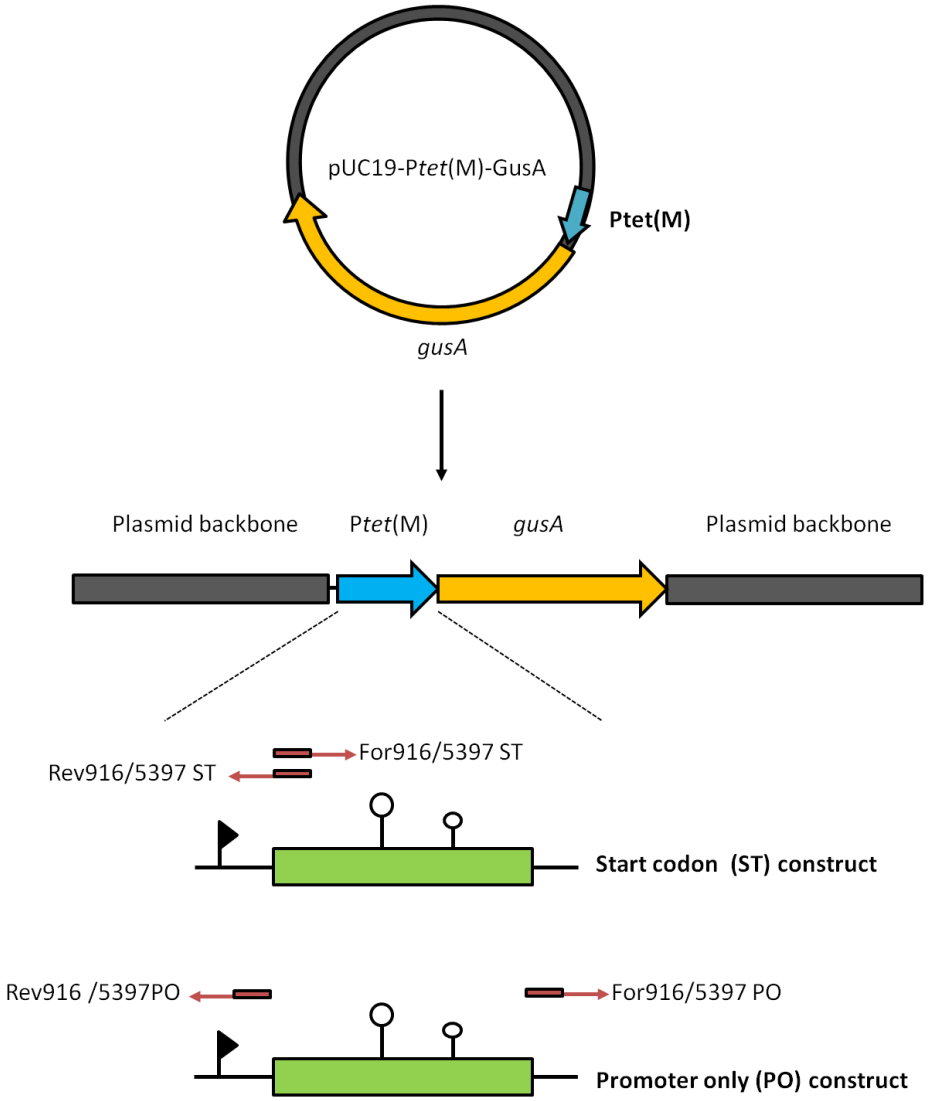

Figure 4.4 Site directed mutagenesis of P*tet*(M) Tn*916* and Tn*5397*. The blue box represents the P*tet*(M) constructs of Tn*916 and* Tn*5397,* green boxes represent *orf12* in Tn*916* and *orf25* and *orf26* in Tn*5397*, yellow box represents the *gusA* gene, grey box represents the plasmid backbone, red arrows represent the annealing position of the primers and the direction of priming. The pUC19-P*tet*(M)-GusA was used as template. Two sets of primers (For916 ST and Rev916 ST; For5397 ST and Rev5397 ST) were used to introduce 2 bp mutation in the start codon of *orf12* and *orf26* of Tn*916* and Tn*5397*, respectively. Primers For916 PO, Rev916 PO, For5397 PO and Rev5397 PO were used to construct the P*tet*(M) without the *orf12* of Tn*916*, and *orf25* and *orf26* of Tn*5397*. All PCR products were ligated and transformed into *E. coli*.

4.2.4 Measurement of reporter gene (*gusA*) expression

The β-glucuronidase activity was measured based on the method developed for *B. subtilis* (Belitsky *et al*., 1995) with slight modifications. The optical density of the overnight culture of *B. subtilis* containing the promoter constructs was measured at 600 nm using the spectrophotometer. This culture (20 ml) was then harvested by centrifugation (3000 x *g*, 25^{o}C, 10 min). The cell pellets were stored in the freezer (-70^{o}C) for 1 h. The pellet was then thawed at room temperature (25^{o}C) prior to resuspension in 0.8 ml of Z buffer (60 mM $Na_2HPO_4.7H_2O$, pH7; 40 mM NaH_2PO_4 H_2O; 10 mM KCl; 1mM $MgSO_4.7H_2O$; 50 mM 2-mercaptoethanol) and 0.8 µl of toluene. The mixture was transferred to 1.5 ml tube containing unwashed glass beads (150-212-µm-in diameter) and treated in a Ribolyser at setting 6.5 for 25 sec to lyse the cells. Treatment was repeated twice. The lysates were cooled on ice for 1 min and centrifuged (3000 x *g*, 4^{o}C, 3 min) to remove the glass beads. Next 0.4 ml of the supernatant was removed and mixed with 0.4 ml Z buffer in a microcentrifuge tube. The mixture was incubated at 37^{o}C for 5 min. The enzyme reaction was started by the addition of 0.16 ml of 6 mM ρ-nitrophenyl-β-D-glucuronide and incubated for 5 min at 37^{o}C. The enzyme reaction was stopped by the addition of 0.4 ml of 1 M Na_2CO_3 followed by centrifugation (3000 x *g*, 25^{o}C, 10 min) to remove the cell debris. The absorbance was read at 405 nm using the spectrophotometer. The β-glucuronidase units were calculated using the following equation: (A_{405} x 1000) / [OD_{600} x time (min) x 1.25 x volume (ml)] (Miller, 1972).

4.2.5 Investigating the freezing time in β-glucuronidase assay

Freezing at -70^{o}C and thawing at room temperature (Section 4.2.4) are important steps in β-glucuronidase assay as in theory, it assists the cell lysis via ice crystal formation. As we knew the freezing time of some of the samples was likely to vary in this study, we therefore investigated the influence of different freezing time on the enzyme activity. *B. subtilis* BS80A harbouring the pHCMCO5/Tn*916* P*tet*(M) WT (wild type) (Table 2.1) and BS83A harbouring pHCMCO5/(-)P*tet*(M) (promoterless construct) (Table 2.1) were grown in BHI broth for 18 h under shaking conditions (200 rpm). These cultures were diluted to OD_{600} ~0.1 using fresh pre-warmed BHI broths (100 ml) and left to grow for 5 h. Five ml of each culture was aliquoted into a 25 ml tube every 1 h intervals. The OD_{600} was measured followed by centrifugation (3000 x *g*, 25^{o}C, 10 min). The supernatant was discarded and the cell pellets frozen at -70^{o}C. The β-glucuronidase assay was carried out at the end of the 5 h incubation, meaning we had harvested cells incubated at -70^{o}C for varying lengths of time.

4.2.6 Investigating the freezing time in β-glucuronidase assay using an exponentially-grown cells at a single time point

As we saw a surprising result in the above assay, we wanted to determine if freezing time differences would matter on aliquots of the same cells harvested at exponential phase of growth. This culture was grown until OD_{600} ~0.2. Five ml of the culture was aliquoted into 3 separate 25 ml tubes and froze for 1, 3 and 5 h at -70^{o}C after centrifugation. The β-glucuronidase assay was subsequently carried out after the individual incubation times. This methodology corrected for extended growth. The specific activity was calculated using the equation described in Section 4.2.4.

4.2.7 Determination of the basal level expression of β-glucuronidase in Tn*916* and Tn*5397* wild type constructs

B. subtilis harbouring pHCMC05/P*tet*(M) wild type constructs of Tn*916* (BS80A) and Tn*5397* (BS84A) were grown separately in BHI broths containing chloramphenicol 10 μg ml^{-1}) for 18 h (37^{o}C, 200 rpm). The cultures were diluted to an OD_{600} of ~0.1 in 500 ml Erlenmeyer flasks containing 100 ml fresh pre-warmed antibiotic-free BHI broths. Cultures were incubated at 37^{o}C under shaking conditions (200 rpm). Five ml of samples were collected every 30 min intervals up to 8 h. The OD_{600} of the collected samples were measured prior to harvesting by centrifugation (3000 x *g*,

4°C, 10 min). The pelleted cells were stored at -70°C until used for the enzyme assay.

4.2.8 Measurement of the effect of tetracycline on the expression of β-glucuronidase in Tn*916* and Tn*5397* P*tet*(M) wild type constructs

B. subtilis BS80A [P*tet*(M) Tn*916* (wild type)] and BS84A [P*tet*(M) Tn*5397* (wild type)] were prepared as described previously in Section 4.2.7. However, in this experiment tetracycline (10 μg ml^{-1}) was added to the diluted cultures after 2 h (mid-logarithmic phase) and 5 h (stationary phase) of growth. Cultures were grown for an additional 2 h after the addition of tetracycline. Samples were collected every 30 min intervals during that 4 h and 7 h of growth and treated as described previously.

4.2.9 Measurement of the effect of tetracycline and biocides on the expression of β-glucuronidase in Tn*916* and Tn*5397* P*tet*(M) constructs

In experiments to investigate the effect of tetracycline on the expression of β-glucuronidase, all P*tet*(M) Tn*916* [wild type (BS80A); promoter only (BS81A); start codon (BS82A]) and Tn*5397* [wild type (BS84A); promoter only (BS85A); start codon (BS86A]) constructs were prepared as mentioned in Section 4.2.7. The diluted cultures of all P*tet*(M) constructs were grown for 4 h at 37^{o}C with shaking (200 rpm). Tetracycline (10 μg ml^{-1}) was added to the cultures after 2 h of growth. A control culture which was not challenged with tetracycline was grown in parallel for each construct. The expression detected in this control culture was taken as 100% expression for that time point and the expression of the challenged culture was compared to it and percentage difference calculated. Samples were collected every 30 min intervals and treated as previously described.

The effect of biocides on the expression of β-glucuronidase was investigated using BS80A [P*tet*(M) Tn*916*/wild type)]. The experiment was carried out as above however the basal level of expression before challenge was used as the control. Biocides (chlorhexidine digluconate (CHX), hydrogen peroxide (HP), sodium hypochlorite (SH) and ethanol (EtOH) were added to the cultures after 2 h of

growth. All biocides were used at sub-inhibitory concentrations as determined by our collaborators from the Technical University of Denmark (MIC/4).

4.2.10 Plasmid stability test

B. subtilis harbouring P*tet*(M) promoter constructs of Tn*916* and Tn*5397* were grown separately in BHI broths supplemented with chloramphenicol (10 µg ml^{-1}) for 18 h (37^{o}C, 200 rpm). The grown cultures were diluted to an OD_{600} of ~0.1 in 50 ml tube containing 20 ml fresh pre-warmed antibiotic-free BHI broth. Cultures were incubated at 37^{o}C under shaking conditions (200 rpm). One hundred µl of the cultures were collected every 30 min intervals and diluted into a total of 1 ml (900 µl of BHI broth + 100 µl culture) to dilution factors of 10^4, 10^5 and 10^6. One hundred µl of cultures from each dilution were plated onto antibiotic free-BHI agar and BHI agar supplemented with chloramphenicol (10 µg ml^{-1}). Plates were incubated at 37^{o}C for 18 h. The number of colonies on each plate was counted. Cells that grow on antibiotic free-BHI agar represents the total viable cells whereas cells grown on BHI agar supplemented with chloramphenicol (10 µg ml^{-1}) represents the number of cells that still carry the plasmid.

4.3 Results

4.3.1 Generation of P*tet*(M) Tn*916* promoter fusions

The plasmid-based promoter P*tet*(M) constructs of Tn*916* were successfully transformed into *B. subtilis* BS34A (contains wild type Tn*916*). P*tet*(M) indicated by -35 and -10 (Su *et al*., 1992) which was located upstream of the *orf12* was fused with the promoterless *gusA* gene (Novel and Novel, 1973) in the shuttle vector pHCMCO5. The constructed gene fusion plasmid allows the expression of the reporter gene, initiated at P*tet*(M) promoter to be quantitated. The three P*tet*(M) Tn*916* constructs comprise either the entire *orf12* [wild type, WT (BS80A)], Δ*orf12* with a 2 bp mutation in the start codon of *orf12* [start codon, ST (BS82A)] or the deletion of the entire *orf12* [promoter only, PO (BS81A)] as indicated in Figure 4.5. In BS82A construct, the start codon of *orf12* (ATG) was mutated to GCG.

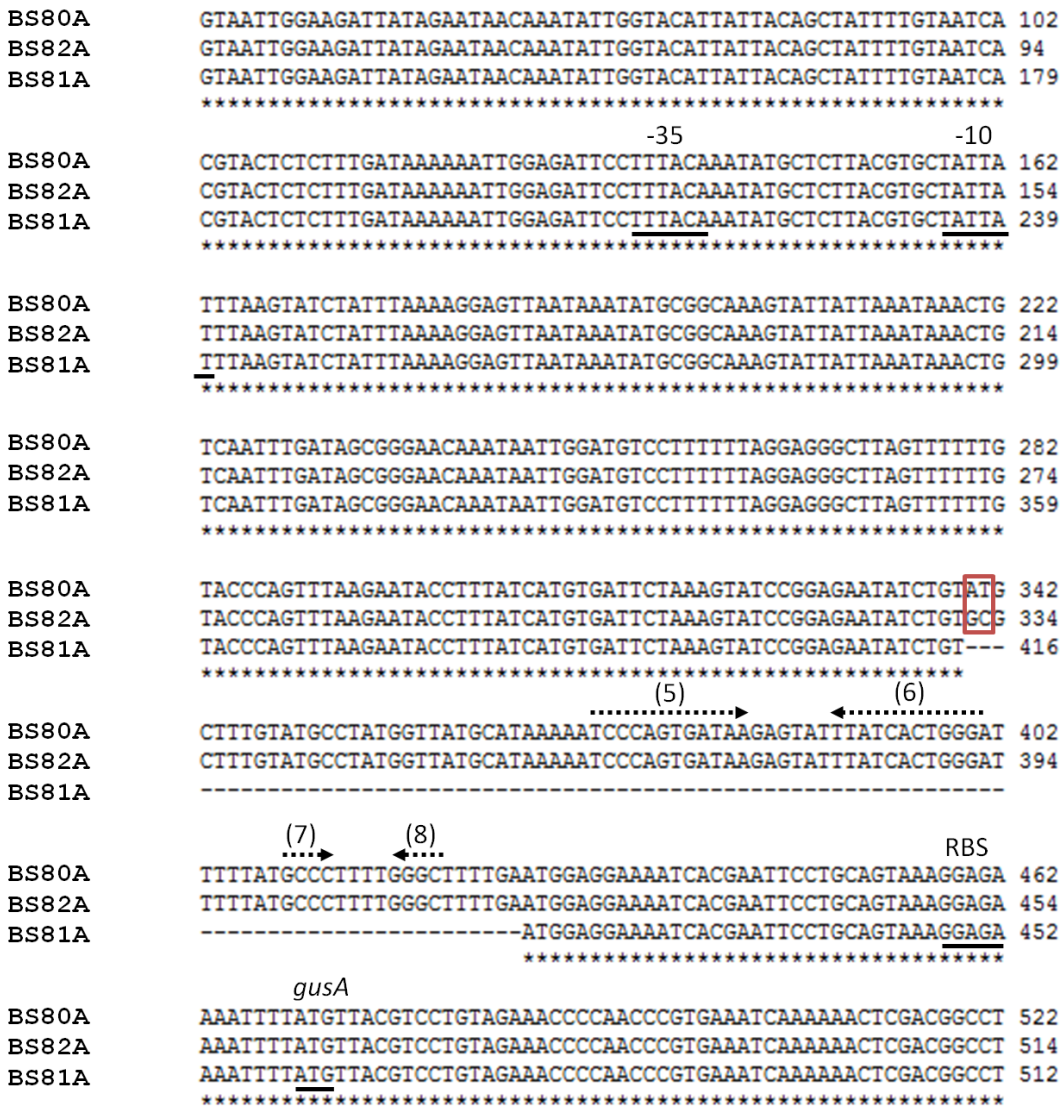

Figure 4.5 Sequence alignment of P*tet*(M) Tn*916* constructs. The -35 and -10 sequences of P*tet*(M) promoter are underlined. The 2 bp start codon mutation of *orf12* is shown in red box (**AT**G ---> **GC**G). The dashed line illustrates the deletion of *orf12*. The dashed arrows represent the inverted repeats 5, 6, 7 and 8. The ribosome binding site (RBS) and the start codon of *gusA* are underlined. BS80A; P*tet*(M) Tn*916* wild type (WT), BS82A; start codon mutant (ST), BS81A; promoter only (PO).

4.3.2 Generation of P*tet*(M) Tn*5397* promoter fusions

The plasmid-based promoter P*tet*(M) constructs of Tn*5397* were successfully transformed into *B. subtilis* BS34A. In Tn*5397*, a deletion of 84 bp upstream of *tet*(M) compared to Tn*916* has generated alternative orfs; *orf26* and *orf25*. The three P*tet*(M) constructs of Tn*5397* comprise either both *orf25* and *orf26* [wild type, WT (BS84A)], Δ*orf26* with a 2 bp mutation in the start codon of *orf26* [start codon, ST (BS86A)] or the deletion of *orf25* and *orf26* [promoter only, PO (BS85A)] as illustrated in Figure 4.6.

Figure 4.6 Sequence alignment of P*tet*(M) Tn*5397* constructs. The -35 and -10 sequences of P*tet*(M) promoter are underlined. The 2 bp start codon mutation of *orf26* is shown in red box (**TT**G ---> **GC**G). The dashed line illustrates the deletion of *orf25* and *orf26*. The dashed arrows represent the inverted repeats 3, 4, 5 and 6. The ribosome binding site (RBS) and the start codon of *gusA* are underlined. BS84A; P*tet*(M) Tn*5397* wild type (WT), BS86A; start codon mutant (ST), BS85A; promoter only (PO).

4.3.3 Effect of freezing time on the activity of β-glucuronidase

In this experiment, the effect of freezing time on the activity of β-glucuronidase was investigated on cells which were frozen for 1-5 h at -70^{o}C. This was carried out as we predicted there may be differences in the freezing times of the samples harvested throughout the experiments. As illustrated in Figure 4.7, the highest β-glucuronidase activity (1419.69 ± 108.90 Miller Unit) was detected when *B. subtilis* BS80A [P*tet*(M) Tn*916* (wild type)] was frozen for 5 h. The enzyme activity decreased gradually with the decrease of freezing time. *B. subtilis* BS83A (promoterless construct) which was included as the control demonstrated a constant enzyme activity despite the differences in the freezing time. This led us to believe there may be a relationship with expression from this promoter and growth of the cells.

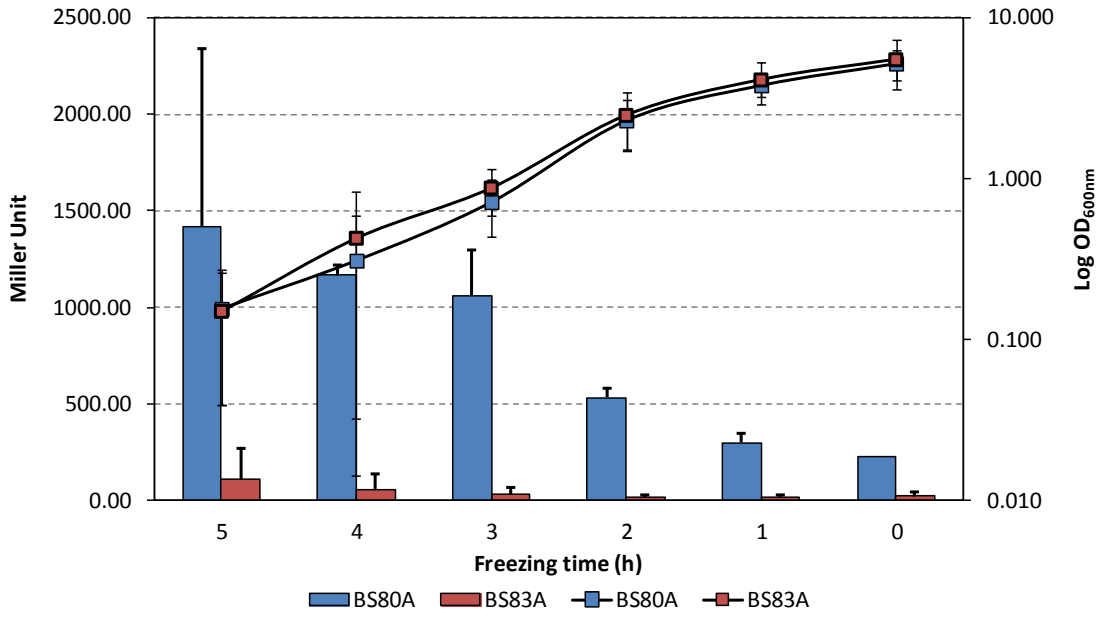

Figure 4.7 Enzymatic activity as a function of freezing time at -70°C. The *B. subtilis* strains BS80A [P*tet*(M) Tn*916* (wild type)] and BS83A (promoterless construct) were grown for 5 h in BHI broth. Samples were taken every 1 h intervals and froze for 1-5 h prior to enzyme assay. The bars represent the enzyme activity whereas the lines represent the growth rates of both strains. Error bars indicate the standard deviation of three independent experiments.

Therefore, another enzymatic assay was carried out to investigate if the β-glucuronidase activity we observed was growth-dependent. In this experiment, *B. subtilis* BS80A [P*tet*(M) Tn*916* (wild type)] and BS83A (promoterless construct) were left to grow for 2 h (OD_{600} ~ 0.2) prior to being frozen at -70^{o}C for 1, 3 and 5 h. Assays were carried out after each of the different incubation periods were finished (i.e. at 1 h, at 3 h and at 5 h). Results are illustrated in Figure 4.8. Although frozen for different lengths of time, the enzyme activity was comparable. These results suggest that the β-glucuronidase activity is growth-dependent and is not affected by the length of freezing time during the assay.

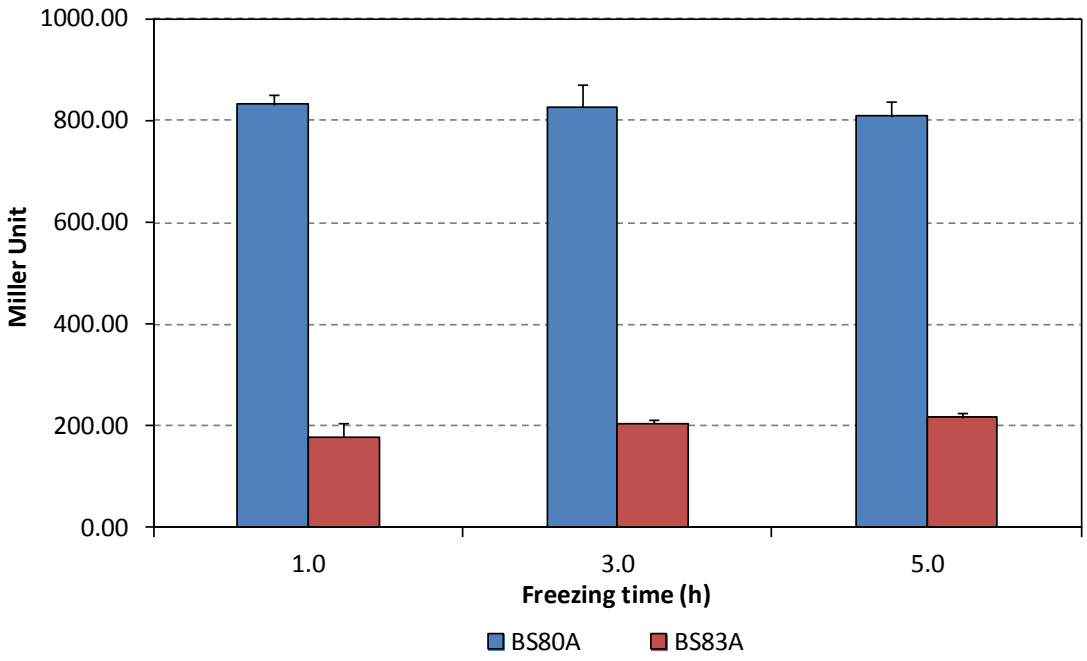

Figure 4.8 Relationship between freezing time and β-glucuronidase activity. *B. subtilis* strains BS80A [P*tet*(M) Tn*916* (wild type)] and BS83A (promoterless construct) were grown to 2 h prior freezing at -70^{o}C for 1, 3 and 5 h. Enzyme assay was subsequently carried out. Error bars indicate the standard deviation of three independent experiments.

4.3.4 Basal level expression of β-glucuronidase in Tn*916* and Tn*5397* promoter constructs

In this experiment, the basal expression of β-glucuronidase by P*tet*(M) Tn*916* and Tn*5397* wild type constructs was investigated as the previous experiments had indicated that this may in fact change during the growth phase of the bacteria host. *B. subtilis* BS80A [P*tet*(M) Tn*916* (wild type)] and BS84A [P*tet*(M) Tn*5397* (wild type)] were grown up to 8 h, and the enzyme activity was quantified. High expression level of β-glucuronidase were observed in both constructs during lag and exponential phases (Figure 4.9). The highest activity recorded for BS80A and BS84A was at mid-exponential phase (4.5 h) before it reduced at 5 h and was generally constant thereafter. The enzyme activity profile observed for BS80A and BS84A confirmed that the expression of β-glucuronidase initiated at P*tet*(M) promoter of Tn*916* and Tn*5397* is growth-dependent.

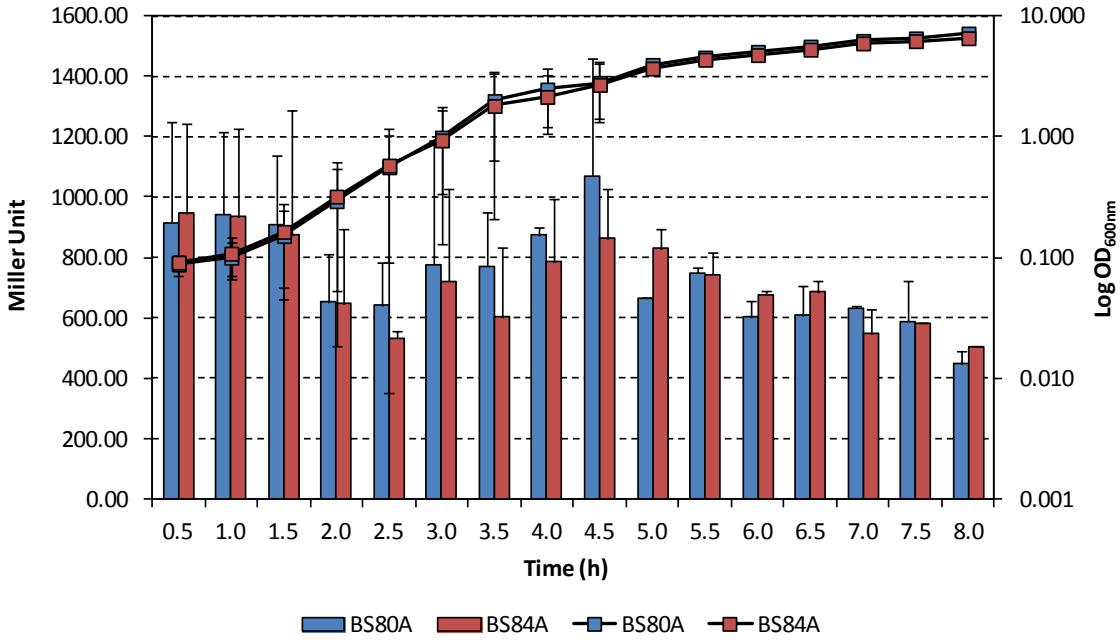

Figure 4.9 β-glucuronidase activity of *B. subtilis* BS80A [P*tet*(M) Tn*916* (wild type)] and *B. subtilis* BS84A [P*tet*(M) Tn*5397* (wild type)]. The bars represent the enzyme activity whereas the lines represent the growth of the two constructs. BS80A and BS84A were grown for 8 h prior to the enzyme assay. Error bars indicate the standard deviation of three independent experiments.

4.3.5 Effect of tetracycline on the expression of β-glucuronidase by P*tet*(M) Tn*916* and Tn*5397* constructs

The effect of tetracycline on the activity of β-glucuronidase was investigated at 2 growth points; one in exponential and one in stationary. This experiment was carried out using *B. subtilis* BS80A [P*tet*(M) Tn*916* (wild type)] and BS84A [P*tet*(M) Tn*5397* (wild type)]. In the exponential phase, both strains were grown up to 2 h prior to addition of an inhibitory concentration of tetracycline (10 μg ml^{-1}). BS80A demonstrated an increase in the enzyme activity (62% ± 21%) after 1 h of exposure to tetracycline, and activity was maintained up to 2 h after exposure (Figure 4.10).

In contrast, no significant increase in the enzyme activity of BS84A was detected when cells were challenged with tetracycline (Figure 4.11). This result suggests that the enzyme activity initiated from P*tet*(M) of Tn*5397* was not upregulated by tetracycline as observed for P*tet*(M) of Tn*916*.

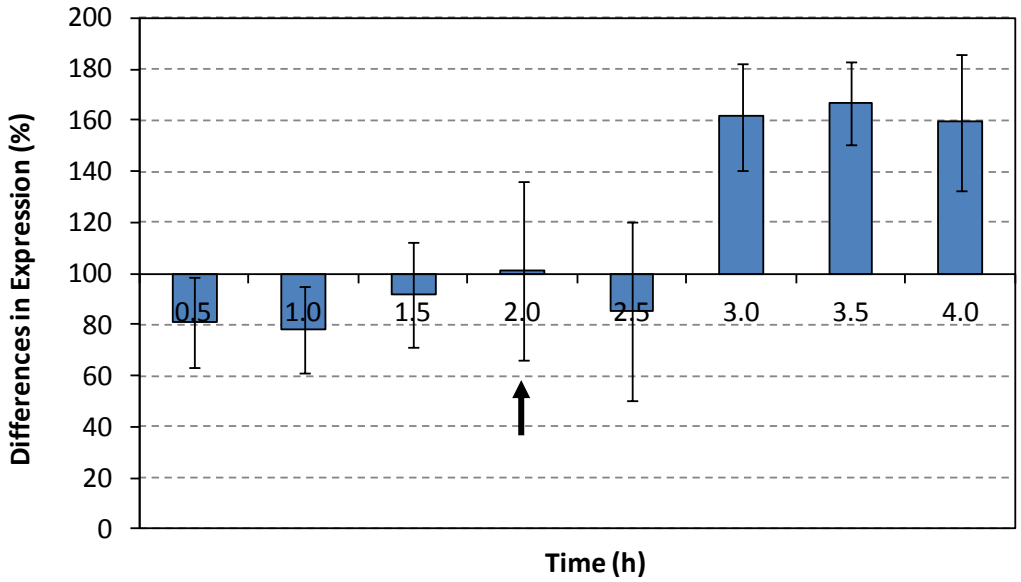

Figure 4.10 β-glucuronidase activity of the P*tet*(M) Tn*916* construct at exponential phase compared to an unchallenged culture. The black arrow shows the time point where *B. subtilis* BS80A [P*tet*(M) Tn*916* (wild type)] was exposed to tetracycline. Results presented are the average of three independent experiments.

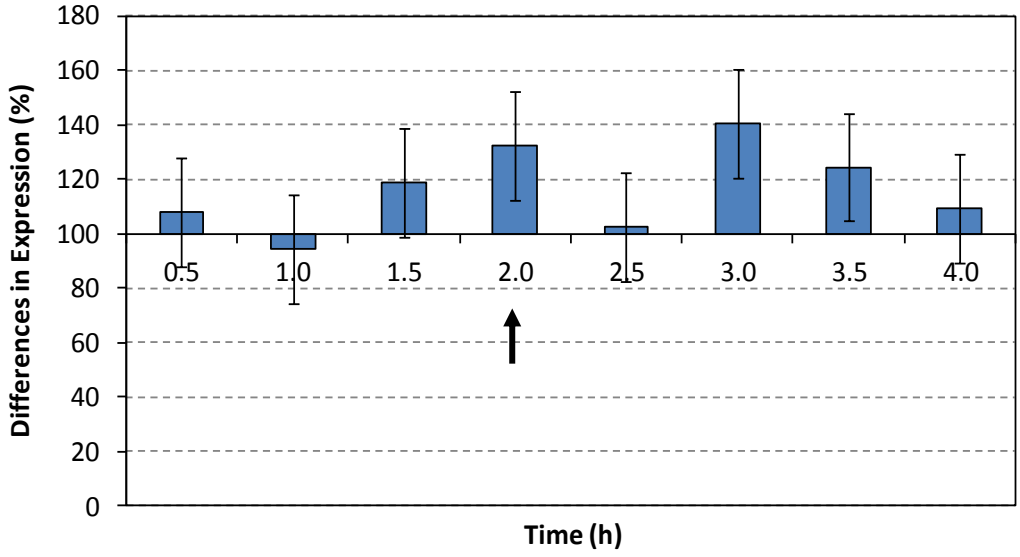

Figure 4.11 β-glucuronidase activity of the P*tet*(M) Tn*5397* construct at exponential phase. The black arrow shows the time point where *B. subtilis* BS84A [P*tet*(M) Tn*5397* (wild type)] was exposed to tetracycline. Results presented are the average of three independent experiments.

In the stationary phase, BS80A [P*tet*(M) Tn*916* (wild type)] were grown for 5 h before being exposed to tetracycline. The effect of tetracycline to the expression of β-glucuronidase was measured up to 2 h after exposure. The tetracycline downregulated the transcriptional activity of P*tet*(M) Tn*916* after 1 h of exposure. A slight increase in enzyme activity was later observed (Figure 4.12). As we do not observe any upregulation in the expression of β-glucuronidase during the stationary phase for BS80A, therefore expression of BS84A [P*tet*(M) Tn*5397* (wild type)] at this phase is not tested.

An increase in the enzyme activity during exponential phase and not during the stationary phase revealed that the tetracycline-based transcriptional regulation at P*tet*(M) of Tn*916* is growth phase-dependent.

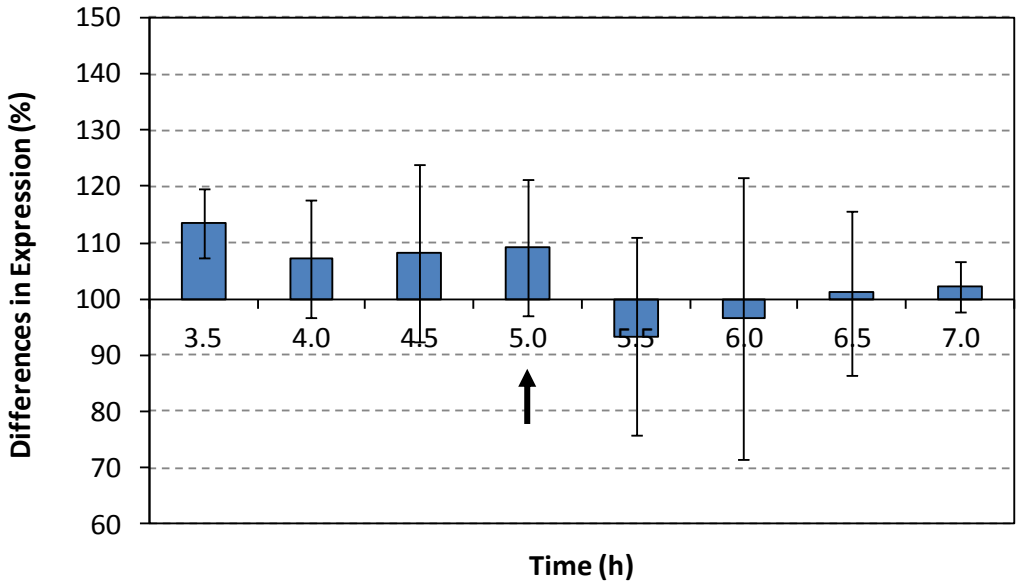

Figure 4.12 β-glucuronidase activity of the P*tet*(M) Tn*916* construct at stationary phase. The black arrow shows the time point where *B. subtilis* BS80A [P*tet*(M) Tn*916* (wild type)] was exposed to tetracycline. Results presented are the average of three independent experiments.

4.3.6 The functional role of *orf12* and *orf26* in the regulation of Tn*916* and Tn*5397*

The involvement of *orf12* and *orf26* in the regulation of Tn*916* and Tn*5397*, respectively was further investigated. In this experiment, a total of 3 P*tet*(M) promoter constructs for each conjugative transposons were tested;

Tn*916*: BS80A [P*tet*(M) Tn*916* (wild type)]; BS82A, with a 2 bp mutation in the start codon of *orf12* [P*tet*(M) Tn*916* (start codon)]; BS81A, with the deletion of the entire *orf12* [P*tet*(M) Tn*916* (promoter only)], and

Tn*5397*: BS84A, consists of *orf25* and *orf26* [P*tet*(M) Tn*5397* (wild type)]; BS86A, with a 2 bp mutation in the start codon of *orf26* [P*tet*(M) Tn*5397* (start codon)] and BS85A, with the deletion of *orf25* and *orf26* [P*tet*(M) Tn*5397* (promoter only)].

All constructs were grown for 4 h with an exposure to tetracycline at 2 h. Figure 4.13 illustrates the enzyme activity observed for P*tet*(M) Tn*916* constructs. All constructs demonstrated highest enzyme activities during the first 1 h of growth, before the activities decline by 1.5 h. A marked increase in the activity of BS80A [P*tet*(M) Tn*916* (wild type)] and BS81A [P*tet*(M) Tn*916* (promoter only)] was observed when tetracycline was added to the culture. However, BS82A [P*tet*(M) Tn*916* (start codon)] show an indistinguishable activity.

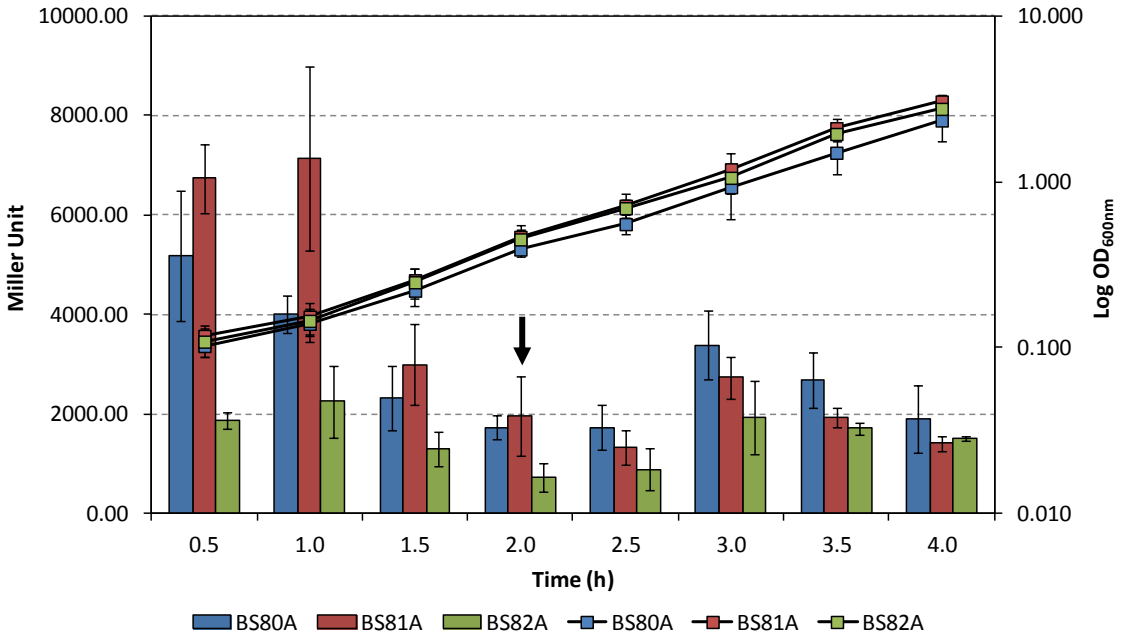

Figure 4.13 The β-glucuronidase activity of the P*tet*(M) Tn*916* promoter constructs. The bars represent the enzyme activity whereas the lines represent the growth rates of the three constructs. The *B. subtilis* constructs were grown up to 4 h with exposure to tetracycline (shown in black arrow) at mid-exponential phase (2 h). Error bars indicate the standard deviation of three independent experiments.

Figure 4.14 show the enzyme activity observed for P*tet*(M) constructs of Tn*5397*. In BS85A [P*tet*(M) Tn*5397* (promoter only)], highest enzyme activity was observed during the first 1 h of growth before it went down thereafter despite the presence of tetracycline at 2 h. In contrast, the enzyme activities observed for BS84A [P*tet*(M) Tn*5397* (wild type)] and BS86A [P*tet*(M) Tn*5397* (start codon)] are generally constant throughout the 4 h growth and the presence of tetracycline does not seem to upregulate the expression of β-glucuronidase in these constructs. At this point, it is difficult to interpret the result. Therefore, a plasmid stability test was carried out to investigate if the instability of plasmid has led to the results we observed.

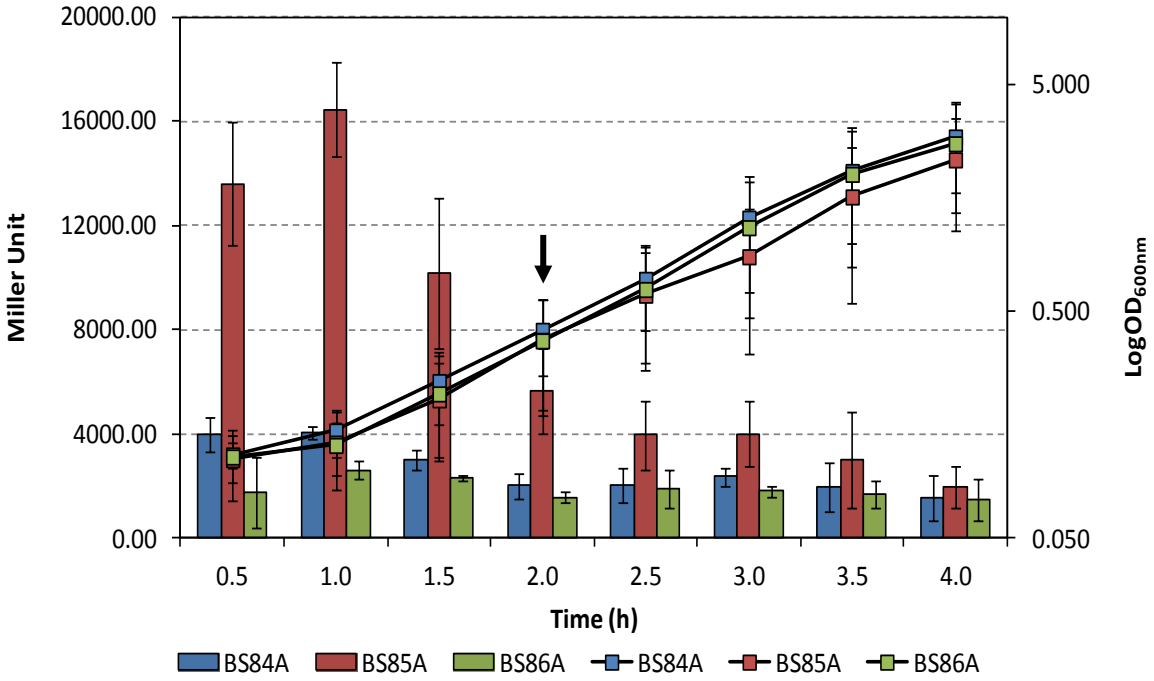

Figure 4.14 The β-glucuronidase activity of the P*tet*(M) Tn*5397* promoter constructs. The bars represent the enzyme activity whereas the lines represent the growth rates of the three constructs. The *B. subtilis* constructs were grown up to 4 h with exposure to tetracycline (shown in black arrow) at mid-exponential phase (2 h). Error bars indicate the standard deviation of three independent experiments. BS84A [P*tet*(M) Tn*5397* (wild type)]; BS85A: [P*tet*(M) Tn*5397* (promoter only)]; BS86A [P*tet*(M) Tn*5397* (start codon)].

4.3.7 Plasmid stability of P*tet*(M) promoter constructs

Plasmid stability test was carried out on all P*tet*(M) constructs of Tn*916* and Tn*5397*, mainly to determine if the instabilities of plasmid, pHCMCO5 which carries the promoter constructs has resulted to a low enzyme activity observed . Based on the results (raw data is included in Appendix A), it can be concluded that pHCMCO5 carrying Tn*916* promoter constructs are stable throughout the first 2 h growth hence the low activity observed is not due to the plasmid instability. However, each construct in the Tn*916* group showed instability after this time and therefore the data was corrected for this instability and is presented in Figure 4.15. The Tn*5397* construct were stable throughout the experiment.

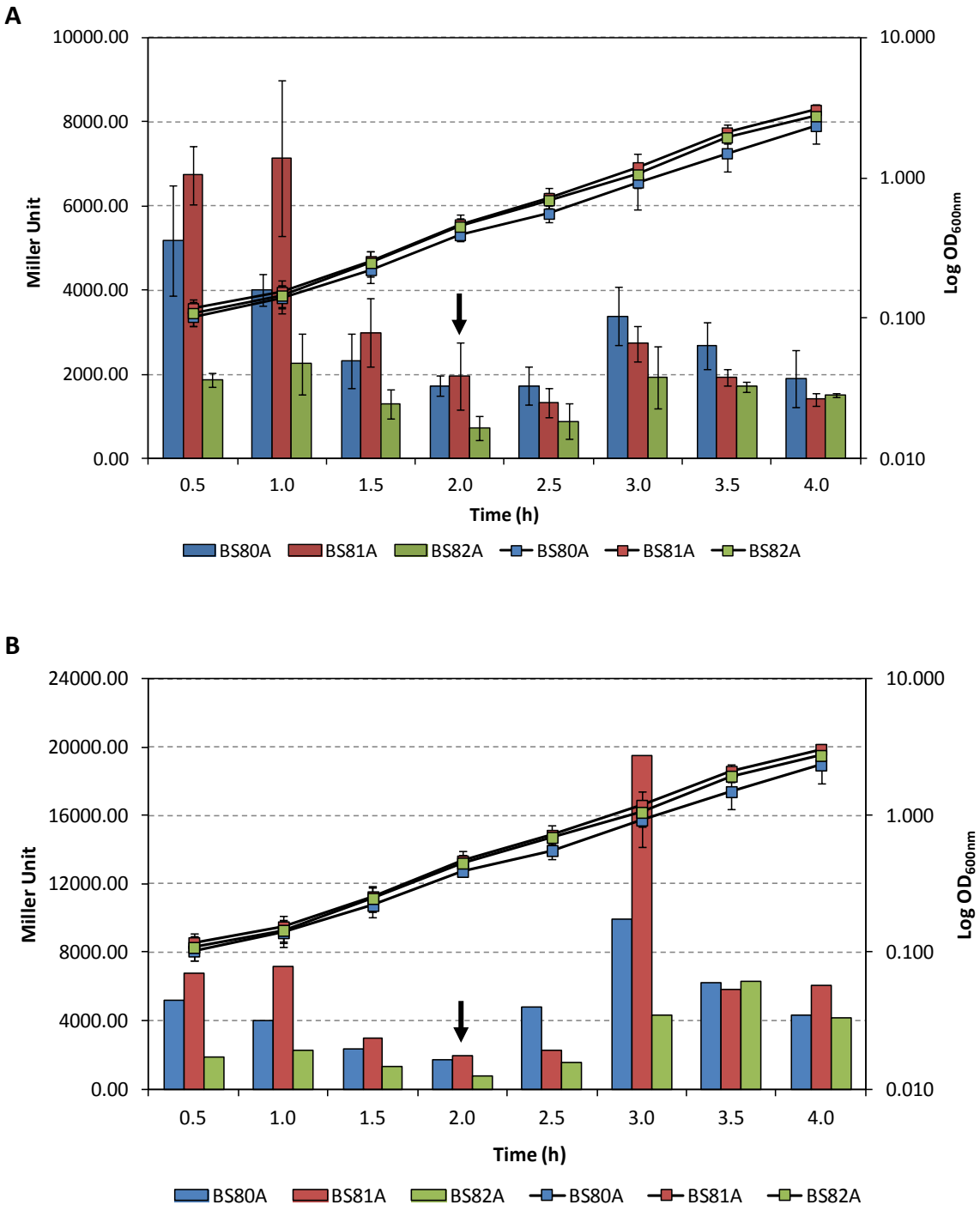

Figure 4.15 The corrected data of β-glucuronidase activity of the P*tet*(M) Tn*916* promoter constructs based on plasmid stability. Panel A shows the original data whereas Panel B shows the corrected data.

4.3.8 Biocides upregulate the expression of β-glucuronidase

This experiment was carried out to test the hypothesis that the regulation of Tn*916* is dependent on the rate of transcription (charged tRNA level) rather than the presence of tetracycline (Roberts and Mullany, 2009). In this collaborative work between our laboratory and the Research group for Microbial Genomics and Antimicrobial Resistance, Technical University of Denmark, the effect of biocides on the expression of β-glucuronidase of BS80A [P*tet*(M) Tn*916* (wild type)] was investigated. Four biocides; ethanol (EtOH), hydrogen peroxide (HP), chlorhexidine digluconate (CHX) and sodium hypochlorite (SH) at sub-lethal concentrations (MIC/4) were tested. Cultures were grown up to 4 h, and exposed to the tested compounds after 2 h of incubation. EtoH upregulated the expression of β-glucuronidase after 2 h of exposure, with 46-54% increase in transcription compared to the basal level before exposure. This is somewhat different to the other three biocides, where the activity increases as early as 1 h after exposure. The highest activity recorded for HP was 42%, as compared to the CHX and SH with 15% and 24%, respectively (Figure 4.16). All enzyme activities were standardised to the control sample (non-exposed sample) to adjust for the basal level expression.

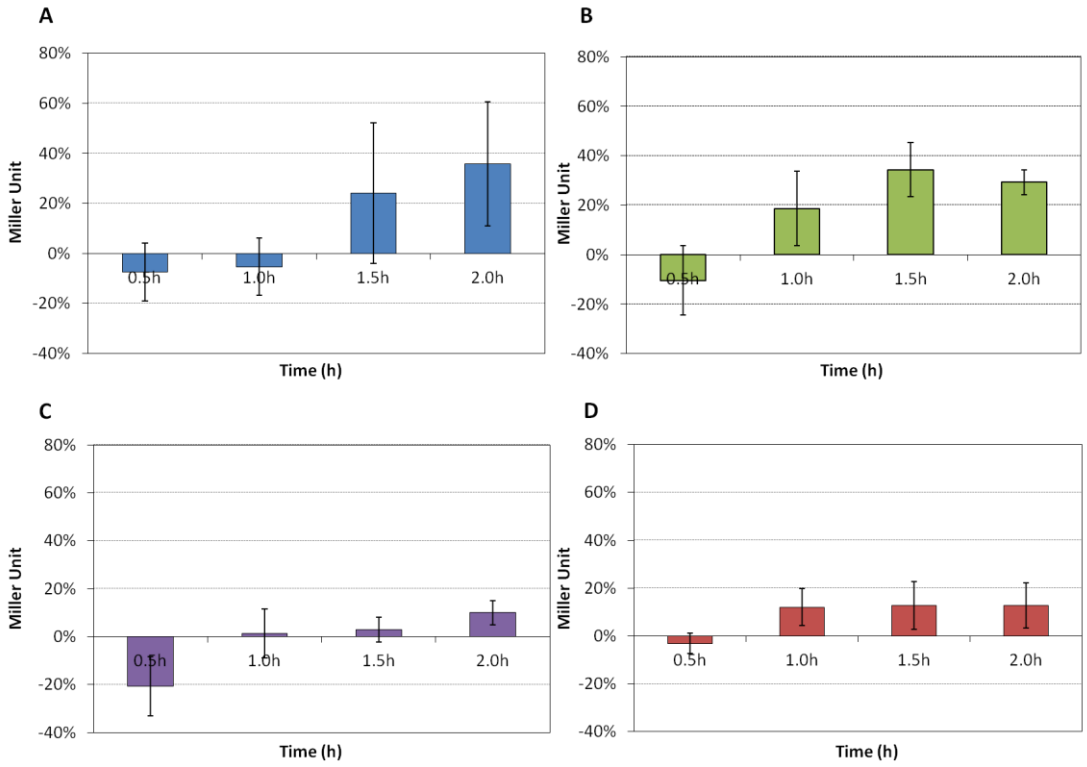

Figure 4.16 Effect of biocides on the activity of β-glucuronidase of the P*tet*(M) Tn*916* promoter construct. The construct, designated BS80A [P*tet*(M) Tn*916* (wild type)] was grown up to 4 h, with exposure to sub-lethal concentrations of biocides after 2 h of growth. Four biocides were tested; panel A represents the ethanol, panel B represents the hydrogen peroxide, panel C represents the chlorhexidine digluconate and panel D represents the sodium hypochlorite. The Y-axis represents the enzyme activity (Miller Unit) whereas the X-axis indicates the time in hours after exposure to biocides. Data presented with permission by Seier-Petersen, M. A.

4.4 Discussion

This study was designed to gain an insight into the functional role of *orf12* and *orf26* in the transcriptional regulation of Tn*916* and Tn*5397*, respectively. In order to do this, a β-glucuronidase gene was used as a reporter gene system to quantitatively measure the read-through activity of *orf12* and *orf26* under the control of P*tet*(M) promoter. Expression of β-glucuronidase is measured using fluorometric assay for *B. subtilis* which was developed by Belitsky *et al*. (1995). As this assay involves a freezing step at -70^{o}C, which was identified to assist the cell lysis, therefore an investigation into the effect of different freezing time to the enzyme activity was carried out. This was essential considering that throughout the experiments, samples are taken and frozen at different time points prior to enzyme assay at the end. Although the results suggested that the enzyme activity increased as the length of freezing time increased (Figure 4.7), it was unclear, however, whether the increase in the activity was due to the freezing time or the continuing growth of the cells. To verify this, another enzymatic assay was carried out on cells grown for 2 h and frozen for different times (1, 3 and 5 h). Interestingly, the enzyme activity observed were indistinguishable despite the variation in their freezing time, which strongly implies that the activity of β-glucuronidase is growth-dependent and is not affected by the length of freezing time during the assay. This is a novel finding as it shows, for the first time, that expression from the P*tet*(M) is growth-dependent.

Further to this, an experiment to measure the basal level expression of β-glucuronidase was carried out, mainly to investigate if the growth-dependent enzyme activity previously observed in the initial experiments described above is reproducible. Generally, basal level expression is a minimum expression of a gene ensuring that there is always a minimal amount of protein present in the cell in the absence of an inducer (Krebs *et al*., 2010). In this experiment, the enzyme activity of *B. subtilis* strains BS80A [P*tet*(M) Tn*916* (wild type)] and BS84A [P*tet*(M) Tn*5397* (wild type)] which were grown for 8 h was quantified. Our finding that the enzyme activities are maximal during the lag and mid-exponential phases reinforces our previous data that the enzyme activity is growth-dependent. It is postulated that during the lag phase, the rate of protein translation increases in response to the adaption of the cells to the new environment (fresh growth media). Additionally the cells are likely to have high levels of tRNA, having previously been in stationary phase. This would conceivably allow them to react quickly in the presence of nutrients. However, as the protein translation continues, the amount of charged tRNA (especially the rare ones in the leader peptide) in the cells become limited, thus led to the reduction of protein translation. The activity appears to remain low during exponential phase, presumably due to the low amount of tRNA, as a result of high protein translation. In stationary phase, the activity increase and this may be due to the fact that as nutrients are becoming limited protein production is slowing down and therefore tRNA pool is increasing allowing the ribosome to once again catch up with the RNA polymerase leading to expression of the reporter. As the amount of charged tRNA decreases through stationary phase, a lowering of the

enzyme activity is observed. At this phase, however, it is also possible that the low activity observed is due to the dying cells and consequent degradation of proteins. For a mobile genetic element to be able to detect when nutrients are running out in the environment of its host cell would be advantageous as it would be a good time for it to transfer. Upon entering stationary phase the host cells are also at high density (at least in the laboratory culture) and this may provide better opportunity for the element to gain access to a suitable recipient. It is possible that this situation may also occur in nature e.g. in the gut.

A number of studies illustrated a growth phase-associated gene expression (Wanner *et al*., 1977; Liang *et al*., 1999) which shows variations in the expression profile in response to growth-phases. For instance, the expression of the excision genes from the *Bacteroides* mobilisable transposon NBU1 is constant at the early growth-phase, and increase at the beginning of the late exponential phase (Song *et al*., 2009). Conversely, enterotoxin (*cpe*)-*gusA* expression in *C. perfringens* was undetectable throughout the exponential phase but is shown to increase by 3-fold at the beginning of the stationary phase (Mellville *et al*., 1994).

Further investigation was done by measuring the expression level of β-glucuronidase in the presence of tetracycline using BS80A [P*tet*(M) Tn*916* (wild type)] and BS84A [P*tet*(M) Tn*5397* (wild type)] constructs. BS80A demonstrated an increase in the expression level after 1 h of exposure to tetracycline (Figure 4.10). In the presence of tetracycline, most ribosomes are inactivated, which resulted in a

build up of charged tRNA molecules. As there are a few ribosomes that are protected by Tet(M) these ribosomes start translating the *orf12* using the accumulated tRNAs. A rapid translation of *orf12* prevents the formation of the terminators within the *orf12* and leads to a high expression level of the reporter gene located downstream of *orf12*. This data highlights the central role of the *orf12* region in the transcriptional response of Tn*916* to tetracycline, and is therefore consistent with the previously proposed transcriptional attenuation model by Su *et al*. (1992). The expression level of β-glucuronidase in the presence of tetracycline was also tested at stationary phase, however there is no increase in the enzyme activity observed. These results imply that the enzyme activity is not only upregulated in the presence of tetracycline, but it is also a growth-dependent. The expression level of BS84A (Tn*5397* WT construct) does not show the same increase in the presence of tetracycline as observed for the Tn*916* construct. This result is in contrast to the reported data by Roberts (2001) which demonstrated an inducible expression of this element by comparative growth curve and reverse transcriptase PCR, however this was not quantified so the actual level of increase in transcription is not known. At 1 h after addition of tetracycline the Tn*5397* reporter construct gave high expression compared to the control, however this high level of expression compared to the control was also seen before addition of tetracycline. It is difficult to interpret this data but there is a feature in the sequence of the terminator in Tn*5397* which is described in the following chapter.

To further understand the system, therefore P*tet*(M) promoter mutants were constructed which was described in Section 4.3.1 and Section 4.3.2. These constructs consist of a 2 bp mutation in the start codon of *orf12* (BS82A) and *orf26* (BS86A), and a deletion of the entire *orf12* (BS81A) and *orf25* and *orf26* (BS85A). The expression level of all promoter mutants were quantitated and compared to the wild type constructs (BS80A and BS84A). As all the constructs were plasmids, we also wanted to ensure that the stability of the plasmids did not affect the expression levels that we observed. Therefore, dilutions were plated out from each time point onto antibiotic free and chloramphenicol containing agar plates. The percentage growing on chloramphenicol compared to the total cell count on the antibiotic free was taken as the percentage stability. It was noticed that in the Tn*916* constructs the stability of the plasmids reduced after 2 h and therefore the data presented in Figure 4.13 was corrected e.g. at time point x, if culture A had 50% plasmid containing cells and gave a reading of 500 Miller Units this would be correct to 1000 Miller Units (assuming a 100% plasmid maintenance). This data is presented in Figure 4.15. The wild type expression levels (BS80A) reduced as the culture progressed through exponential phase as expected from the data from the previous chapter. Following addition of tetracycline at 2 h, we observed an increase in the expression until 1 h following addition of tetracycline. Then the expression levels go down, presumably as the pool of charged tRNAs are being used up.

The construct containing the start codon mutation (BS82A) show a similar level before addition of tetracycline, again representing the basal level of expression.

However when tetracycline was added it showed an increase. This could be due to the fact that the *B. subtilis* host BS34A contains a copy of Tn*916* in its chromosome (required as we were challenging with tetracycline). Therefore the ribosomes of the cell are likely to become protected by Tet(M) which will lead to an increase in overall gene expression. This will include our reporter construct. Again, as the levels of tRNA are expected to reduce a reduction is seen in the expression of BS82A [P*tet*(M) Tn*916* (start codon)]. Therefore, we can say that the effect seen in BS80A [P*tet*(M) Tn*916* (wild type)] is due to the attenuation system located within *orf12* and the profile seen with BS82A most likely represents the background expression pattern for rest of the chromosome which is being actively transcribed.

The promoter only construct (BS81A) shows an unexpected profile in that it is not constant as we could predict. It is higher in expression compared to the wild type and the start codon mutation which strongly suggests that the predicted terminators in this region are actively terminating transcription. This is investigated fully in the next chapter. It does reduce during growth of the culture which again suggests that the activity of this promoter is growth phase dependant. This is in agreement with the experiments in Chapter 3. Following addition of tetracycline the is an unexpected increase in activity, however this is due to the correction we have applied for the low stability of this plasmid. It could be that the plasmid is simply too unstable because it contains such a strong promoter and therefore when the tRNA levels are high (after exposure to tetracycline) its activity increases dramatically, which may also explain its instability.

Although Tn*916* and Tn*5397* are closely related, results presented in this study revealed that the presence of tetracycline does not upregulate the expression of β-glucuronidase initiated at P*tet*(M) of all Tn*5397* constructs. It is interesting to note that the plasmid constructs were all 100% stable throughout the experiment (Appendix A). The wild type expression (BS84A) gradually decreases with exponential growth, however upon exposure to tetracycline there is a modest increase. This could simply be due to the protected ribosomes resulting from the expression of Tet(M) from the chromosomal copy of Tn*916*. This is different to what we expected and an explanation is put forward to explain this in the next chapter.

The *orf26* start codon mutant (BS86A) showed no real change throughout the experiment. This was as expected and most likely represents the basal level of expression through the predicted terminators. The promoter only construct (BS85A) shows relatively high levels of expression compared to the other two constructs and decrease with the growth of the cells again suggesting this promoter is a growth phase-dependant promoter. It is possible that a specific sigma factor is produced during the early stages of growth and this is responsible for the differential expression of the terminator.

In a collaborative work between our laboratory and the Research group for Microbial Genomics and Antimicrobial Resistance, Technical University of Denmark, the effect of biocides on the transcriptional regulation of Tn*916* was investigated

using the reporter system constructed here. Results showed that the exposure of cells to biocides has upregulated the expression of β-glucuronidase, which is observed at an average of 1.5-2 h after exposure. As biocides are known for their ability to cause multiple damages to the biological system of bacteria (McDonnell and Russell, 1999), therefore it is suspected that this damage could result in the accumulation of charged tRNA molecules in the cells, due to the disruption of protein synthesis, which in turn results in the upregulation of β-glucuronidase expression. This result supports the hypothesis that the regulation of Tn*916* does not necessarily depend on the presence of tetracycline, but any event or process that could possibly increase the amount of charged tRNA molecules (Roberts and Mullany, 2009). This makes evolutionary sense as it will benefit the element if it can detect multiple stresses on the host which lead to transfer.

4.5 Conclusion

This study highlights the role of the leader peptide *orf12* in the transcriptional regulation of Tn*916*. More work will be necessary to determine the functional role of *orf26* in the transcriptional regulation of Tn*5397* as the response, if any, was weaker. The data in this chapter also supports the theory that the promoter is differentially expressed with high expression in the early growth phase. The work with the biocides shows that multiple stresses can affect the expression from the P*tet*(M) of Tn*916*.

Chapter 5.0

Investigation into the efficiency of terminators located upstream of *tet*(M) in Tn*916*

5 Investigation into the efficiency of terminators located upstream of *tet*(M) in Tn*916*

5.1 Introduction

Regulation of gene expression at the level of transcription in bacteria involves four identifiable steps; promoter recognition, initiation of transcription, transcript elongation and transcription termination (Turner *et al*., 2000). The efficiency of regulation of gene expression at this level is associated with the efficacy of the system in promoting as well as terminating the transcriptional processes. A terminator consists of two complementary sequences, capped by a short loop and followed by thymidine (T)-rich stretches. Studies have shown that the transcriptional terminators can be located within as well as at the end of an operon (Yanofsky, 1981). Over the years, many studies have been carried out focusing on the prediction of the transcriptional terminators in bacterial genomes (Hess and Graham, 1990; d' Aubenton Carafa *et al*., 1990). Further work has focused on evaluating the efficiency of the terminators in terminating the transcription process using an algorithm (d' Aubenton Carafa *et al*., 1990; Ermolaeva *et al*., 2000).

In this study, the efficiency of the terminators located within *orf12* of Tn*916* were evaluated using the *gusA* reporter system employed in Chapter 4. There are two terminators within this regulatory region; one large which will be known as the large terminator (LT) and one smaller which will be known as the small

terminator(ST). These terminators consists of two complementary sequences separated by 4-6 bases and followed by 4-5 T residues (Figure 5.1). Having a common structural similarity with the reported terminators, the transcriptional termination in this region of Tn*916* is therefore expected to occur according to the established model by Farnham and Platt (1980); the RNA stem loop that forms induces the RNA polymerase to pause, and the unstable rU-dA hybrid (Martin and Tinoco, 1980) between the nascent RNA and the transcribed DNA strand releases the transcript and leads to the dissociation of the RNA polymerase from the DNA and terminates the transcription process. In this study, various terminator constructs were designed to allow the efficiency of each terminator to be evaluated individually. Following the in vitro enzymatic reporter assays, an analysis of the predicted termination efficiency was carried out using algorithms developed by d' Aubenton Carafa *et al*. (1990) and these were compared to the experimental data.

Figure 5.1 The predicted stem loop structures and terminator sequences in the mRNA of *orf12* of Tn*916*. The red-shaded area represents the *orf12*. The free-energy values (ΔG) of each structure are shown in kcal mol^{-1}. The run of U residues are underlined and the terminator structures are labeled LT (large terminator) and ST (small terminator). (Taken from Roberts and Mullany, 2009)

5.2 Materials and methods

5.2.1 Bacterial strains and plasmid

E. coli α-select (bronze efficiency) was used for transformation of pHCMCO5 (Table 2.2) containing the terminator constructs. This plasmid was subsequently transformed into *B. subtilis* BS34A (contains wild type Tn*916*). *E. coli* and *B. subtilis* were grown under the conditions described in Section 2.3.

5.2.2 Bacterial transformation

E. coli and *B. subtilis* transformation were carried out according to the protocol described in Section 2.5.11 and 2.5.10, respectively. The *E. coli* transformants were selected on LB agar after 18-24 h incubation at 37^{o}C. Selection of *B. subtilis* transformants was carried out on BHI agar after 24-48 h incubation at 37^{o}C. Agar plates were supplemented with ampicillin (100 μg ml^{-1}), tetracycline (10 μg ml^{-1}) or chloramphenicol (10 μg ml^{-1}) for selection of transformants.

5.2.3 Construction of Tn*916* terminator constructs

The efficiency of the transcriptional terminators within *orf12* of Tn*916* was investigated using two sets of plasmid-based terminator constructs, which were constructed using the site directed mutagenesis approach described in detail in Chapter 4. Primers used to amplify all terminator constructs are listed in Table 2.3. In both sets, the terminators were fused with the reporter gene, *gusA* encoding for β-glucuronidase. The efficiency of the terminators was determined using the β-glucuronidase assay.

5.2.3.1 Construction of terminator construct set I

In the first set of terminator constructs (referred to as terminator construct set I), the upstream and the downstream sequences of the terminators were deleted, leaving the test terminator structure alone as shown in Figure 5.2. This construct allows the termination efficiency of each terminator to be tested while eliminating the background effect of the other terminator.

Terminator Construct Set I	
A. Wild type (WT) 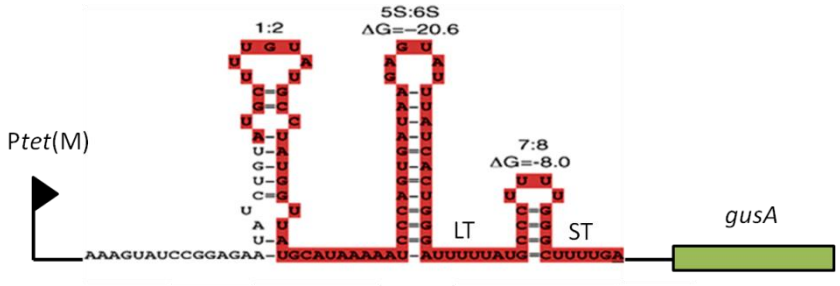	**B. Large terminator (LT)** 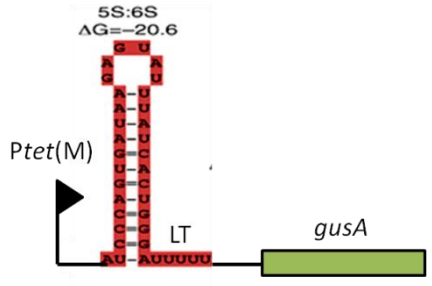
C. Small terminator (ST) 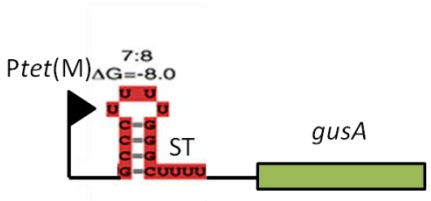	**D. Promoter only (PO)** 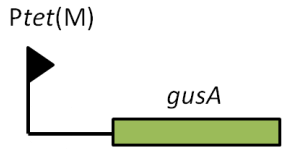

Figure 5.2 Schematic diagram of the transcriptional terminator constructs set I. All constructs were cloned into pHCMCO5 and transformed into *B. subtilis* BS34A. The pointed 'P' indicates the P*tet*(M) promoter. The red-shaded area represents *orf12* of Tn*916*. The free-energy values (ΔG) of each structure are shown in kcal mol^{-1}. The green box represents the reporter gene *gusA*. In wild type construct (WT), both terminators are present. In constructs with the large (LT) and small (ST) terminators, the upstream and downstream sequences were deleted, thus leaving only the test terminator alone. Both terminators were absent in promoter only (PO) construct.

5.2.3.2 Construction of terminator construct set II

In another set of terminator constructs (referred to as terminator construct set II), the T residues downstream of the stem loop structure were mutated into a series of G and C residues as illustrated in Figure 5.3. The GC nucleotides that substitute the poly-T residues is expected to overcome the weak interaction between the nascent RNA transcript and the DNA strand (rU-dA) that leads to the dissociation of the RNA polymerase and thus terminates the transcription.

Terminator Construct Set II

A. Wild type (WT)

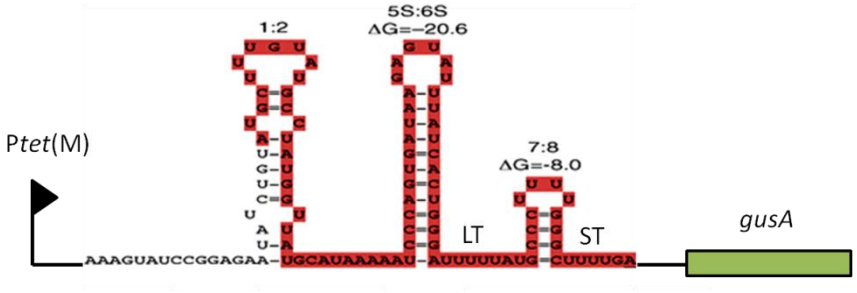

B. Large terminator (LT)

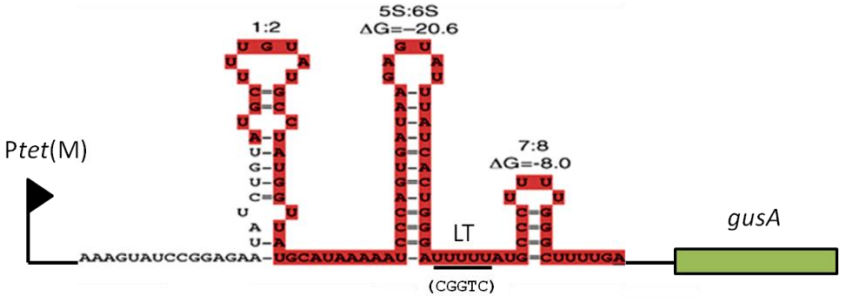

C. Small terminator (ST)

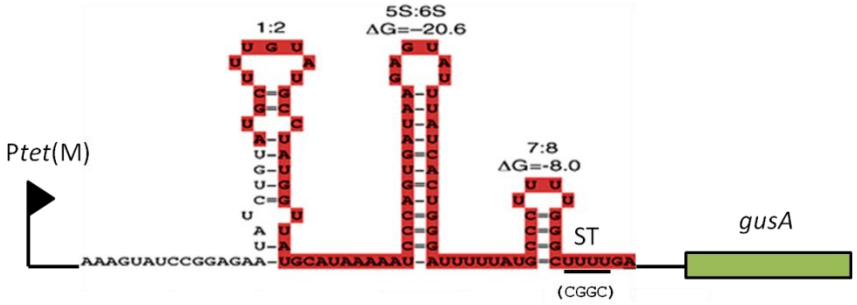

D. Large and small terminator (LTST)

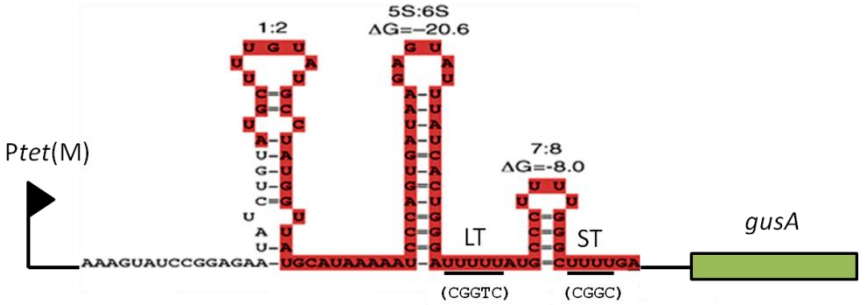

Figure 5.3 Schematic diagram of the transcriptional terminator constructs set II. All constructs were cloned into pHCMCO5 and transformed into *B. subtilis* BS34A. The pointed 'P' indicates the P*tet*(M) promoter. The red-shaded area represents *orf12* of Tn*916*. The free-energy values (ΔG) of each structure are shown in kcal mol^{-1}. The green box represents the reporter gene *gusA*. In wild type construct (WT), both terminators are present. In large (LT), small (ST) as well as large and small (LTST) terminator constructs, the underlined T residues were mutated into GC nucleotides as shown in brackets.

5.2.4 Prediction of the termination efficiency using an algorithm

An algorithm developed by d' Aubenton Carafa *et al*. (1990) was used to predict the termination efficiency of the transcription terminators located in *orf12* of Tn*916*. This algorithm was constructed based on two parameters that defined the putative terminator structures. The first parameter is n_T, defined as the total counts of the stretch of T residues, following the double stranded stem of the terminator. The calculations are as follows:

$\chi_n = \chi_{n-1} \times 0.9$ if the *n*th nucleotide is a T

$\chi_n = \chi_{n-1} \times 0.6$ if the *n*th nucleotide is other than T

The value for the first T is: $\chi_1 = 0.9$, and χ_n is calculated as the sum of the T residues only, therefore;

Equation 5.1 $n_T = \Sigma \chi_n$ for all T residues in the terminator.

For example, in hexanucleotide TTATTT, the n_T is calculated as follows:

T: 0.9
T: 0.9 x 0.9 = 0.81
A: 0.81 x 0.6 = 0.486
T: 0.486 x 0.9 = 0.437
T: 0.437 x 0.9 = 0.394
T: 0.394 x 0.9 = 0.354

Therefore n_T = 0.9 + 0.81 + 0.437 + 0.394 + 0.354 = 2.895 (n_T counts only the T residues). The value 0.2895 is considered as the minimum value possible for the stretch of T residues of a real terminator and values less than 2.895 are therefore rejected (d' Aubenton Carafa *et al*., 1990).

The second parameter for the algorithm is the Y value, which is the function of the Gibbs free energy (ΔG) against the number of nucleotides between the 5' end of the stem and the first U in the stretch (LH). Y value is calculated as follows:

Equation 5.2 $Y = (-\Delta G)/LH$

By using the value from the defined parameters n_T and Y, d' Aubenton Carafa *et al*. (1990) has plotted a two dimensional diagram to distinguish the real transcriptional terminators from intracistronic or random structures. Line D was drawn to obtain the best separation between the two structures (Figure 5.4). From the diagram, the distance between a point (a structure) and the line D was indicated. Based on the computational analysis, the following equation was derived;

Equation 5.3 $d = n_T \times 18.16 + Y \times 96.59 - 116.87$, where condition $d>0$ is applied to all terminator structures.

The correlation between the *d* value (Equation 5.3) and the percentage of the termination efficiency was empirically estimated and is shown in Figure 5.5 (d' Aubenton Carafa *et al*., 1990).

Figure 5.4 A two dimensional diagram showing the separation of the real transcriptional terminators from the intracistronic or random structures in *E. coli*. (●) represents the real transcriptional terminators whereas (○) represents either the intracistronic or random structures. The n_T and *Y* (-ΔG)/LH) values for each structure were plotted on abscissa (x-coordinate) and on ordinate (y-coordinate), respectively. A best separation between the two structures was obtained using line D. The distance between a point (a structure) and the line D was indicated. (Taken from d' Aubenton Carafa *et al*., 1991)

Figure 5.5 The correlation between the score *d* and the percentage of the termination efficiency of some rho-independent terminators in *E. coli*. The terminators are named based on the preceding gene or operon: (□) *rrnB T1*, bacteriophage T7 *Te*; (▲) *ampL* attenuator and *ampL35A* mutant; (○) *infC*, *pheS* attenuator, *his* attenuator, *trpt* and *trpC301* and *trpC302* mutants, bacteriophage T3 *Te*; (Δ) *tonB* (both directions), *rplT*; (●) *trp* attenuator, *trp a1419* and *trp a135* mutants, *trpL77*, *trpL78*, *trpL80*, *trpL153* mutants; (■) thr attenuator and *T2*, *T3*, *T4*, *T5*, *T6*, *T8* mutants in the poly (U) stretch; (⧦) *thr* attenuator stem mutants *L135U*, *L138U*, *L139U*, *L140A*, *L151A*, *L151U*, *L153A*, *L153U*, *L153 + G*, *L153 – G*, *L156U*; (**X**) rnpB; (**+**) intracistronic signals in *cca*. (Taken from d' Aubenton Carafa *et al*., 1991)

5.3 Results

5.3.1 Generations of Tn*916* terminator constructs

Construction of set I and set II terminator constructs was carried out as described in Sections 5.3.2.1 and 5.3.2.2, and this was verified by DNA sequencing. As shown in Figure 5.6, set I constructs constitute only the desired terminator regions. In the wild type construct (BS80A), the large and small terminators are both present. In the following two constructs (BS87A and BS88A), either the large or small terminator is present. Conversely, both terminators are absent in the BS81A construct. All constructs were fused with the reporter gene *gusA* which encodes for β-glucuronidase.

Set II constructs contain the entire *orf12* sequence as illustrated in Figure 5.7. However, other than the wild type (BS80A), the T residues downstream of the stem loop structure of all constructs were substituted with a series of G and C residues. In BS89A and BS90A constructs, the T residues were mutated to CGGTC and CGGC, respectively. Conversely, no terminator is present in BS91A construct as both of the poly-T residues are mutated.

Figure 5.6 Sequence alignment of the P*tet*(M) Tn*916* terminator constructs set I. The -35 and -10 of the P*tet*(M) promoter are underlined. The start codon of *orf12* is labeled and underlined. The dotted arrows represent the large (LT) and small (ST) terminators. The dashed line illustrates the deletion of the terminator in each constructs. The ribosome binding site (RBS) and the start codon of *gusA* are underlined. BS80A; wild type, BS87A; Δ small terminator, BS88A; Δ large terminator, BS81A; Δ large and small terminators.

Figure 5.7 Sequence alignment of the P*tet*(M) Tn*916* terminator constructs set II. The -35 and -10 of the P*tet*(M) promoter are underlined. The start codon of *orf12* is labeled and underlined. The dotted arrows represent the large (LT) and small (ST) terminators. The mutated T residues are shown in red boxes. The ribosome binding site (RBS) and the start codon of *gusA* are underlined. BS80A; wild type, BS89A; Δ small terminator, BS90A; Δ large terminator, BS91A; Δ large and small terminators.

5.3.2 Estimation of the termination efficiency of the terminators using an *in vitro* reporter gene assay

The efficiency of the Tn*916* terminators in terminating the transcription was investigated using β-glucuronidase assay. Figure 5.8 illustrates the enzyme activity observed for the terminator constructs in set I. In the absence of the small terminator (BS87A), the enzyme activity increased up to 53% as compared to the wild type (BS80A). The enzyme activity is more pronounced (77%) when the large terminator (BS88A) is absent. As the enzyme activity is considered reciprocal to the termination efficiency, these results suggest that the large terminator is more efficient than the small terminator in terminating the transcription initiated at the P*tet*(M) of Tn*916*. Surprisingly the construct without either terminator (BS81A) demonstrated a lower activity when compared to BS87A (Δ small terminator) and BS88A (Δ large terminator) although it is expected that the absence of these terminators will result in the highest enzyme activity due to it having the lowest (presumably zero) termination efficiency.

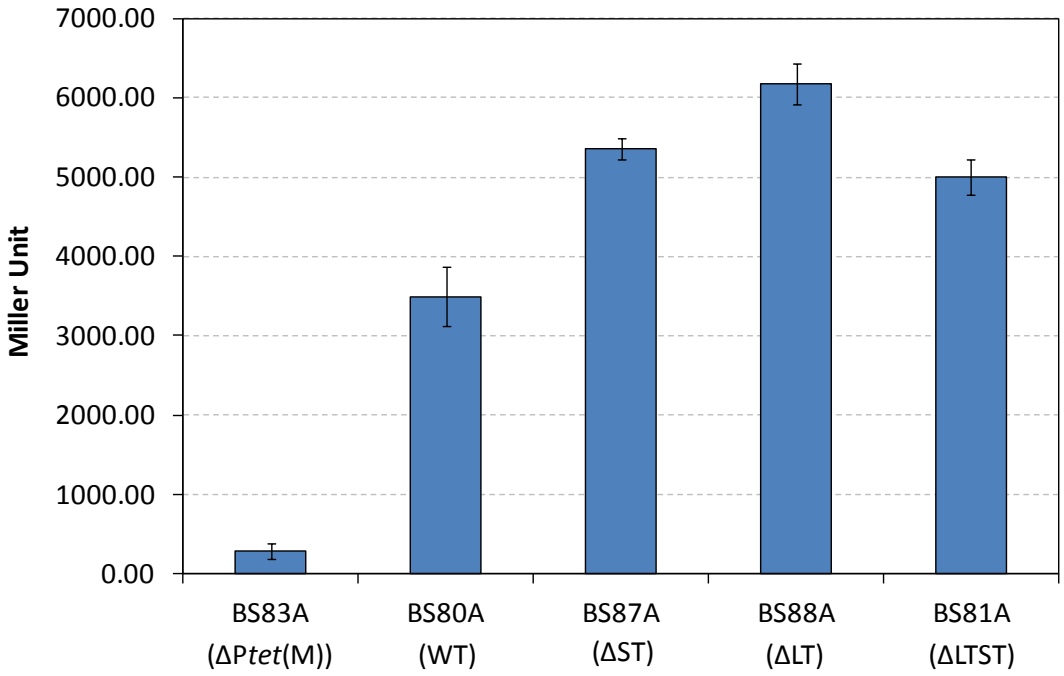

Figure 5.8 β-glucuronidase activity of the Tn*916* terminator constructs in set I. The enzyme activity was measured after 2 h of growth. Error bars indicate the standard deviation of three independent experiments.

We hypothesised that we may have altered the secondary structures by carrying out deletions in these constructs. Therefore, in order to make sure that no alternative secondary structures had formed in the RNA, the terminator constructs set I were re-designed by restoring the sequences located upstream of the stem loop and downstream of the T residues. Similarly, the termination efficiency of the terminators in these constructs (set II) was determined using β-glucuronidase assay. As shown in Figure 5.9, BS90A (Δ large terminator) which comprises the mutated T residues following the large stem loop structure demonstrated an increase in the enzyme activity as compared to the wild type (BS80A). On the contrary, a reduction in the enzyme activities was observed for BS89A (Δ small terminator) and BS91A (Δ small and large terminators).

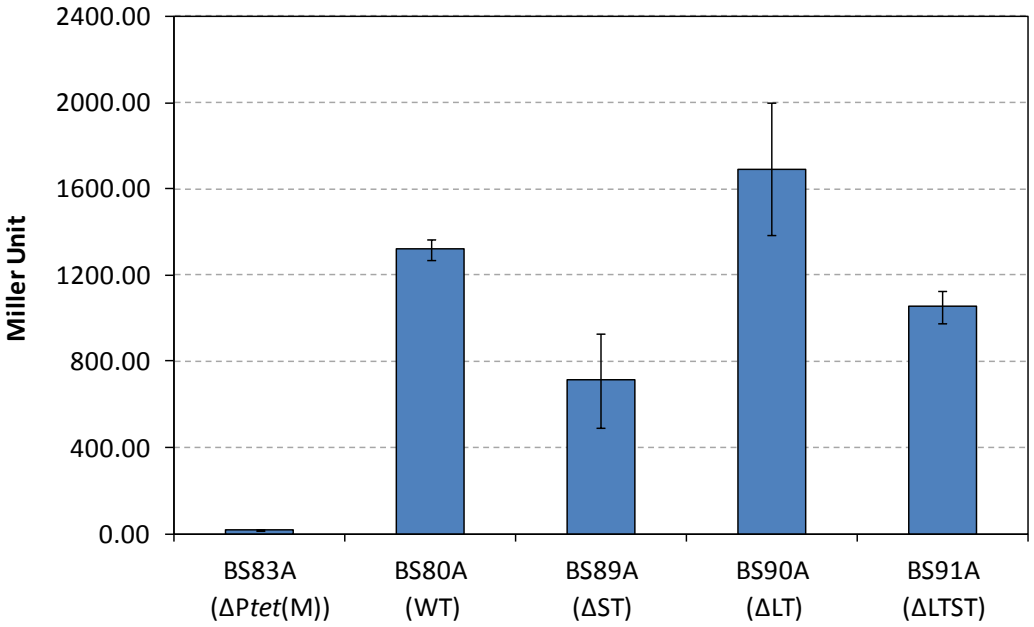

Figure 5.9 β-glucuronidase activity of the Tn*916* terminator constructs II. The enzyme activity was measured after 2 h of growth. Error bars indicate the standard deviation of three independent experiments.

5.3.3 Mfold analysis of the terminator structures in set II

The mfold program developed by Zuker (2003) is a web server that uses computational approach to predict the RNA secondary structure. This program was applied in this study to investigate the predicted RNA structure of the terminator constructs in set II as we found it difficult to interpret the results. This step was performed mainly to observe if the Shine-Dalgarno sequence of the reporter gene is occluded which would lead to a decrease enzyme activity of the terminator constructs [BS89A (Δ small terminator) and BS91A (Δ small and large terminators)]. Results presented suggest that although the RBS and the start codon of β-glucuronidase did appear to be occluded in the most energetically favourable folds (Figure 5.10), the RNA structures of the terminator constructs in set II are all conserved despite an extra binding region following the large terminator in two of the constructs (BS90A and BS91A). However, it is not certain if this has an effect. There is nothing specific to BS89A and BS91A in terms of predicted folding compared to the other constructs, therefore, the unexpected low activities observed are not likely to be due to the changes in the RNA secondary structure.

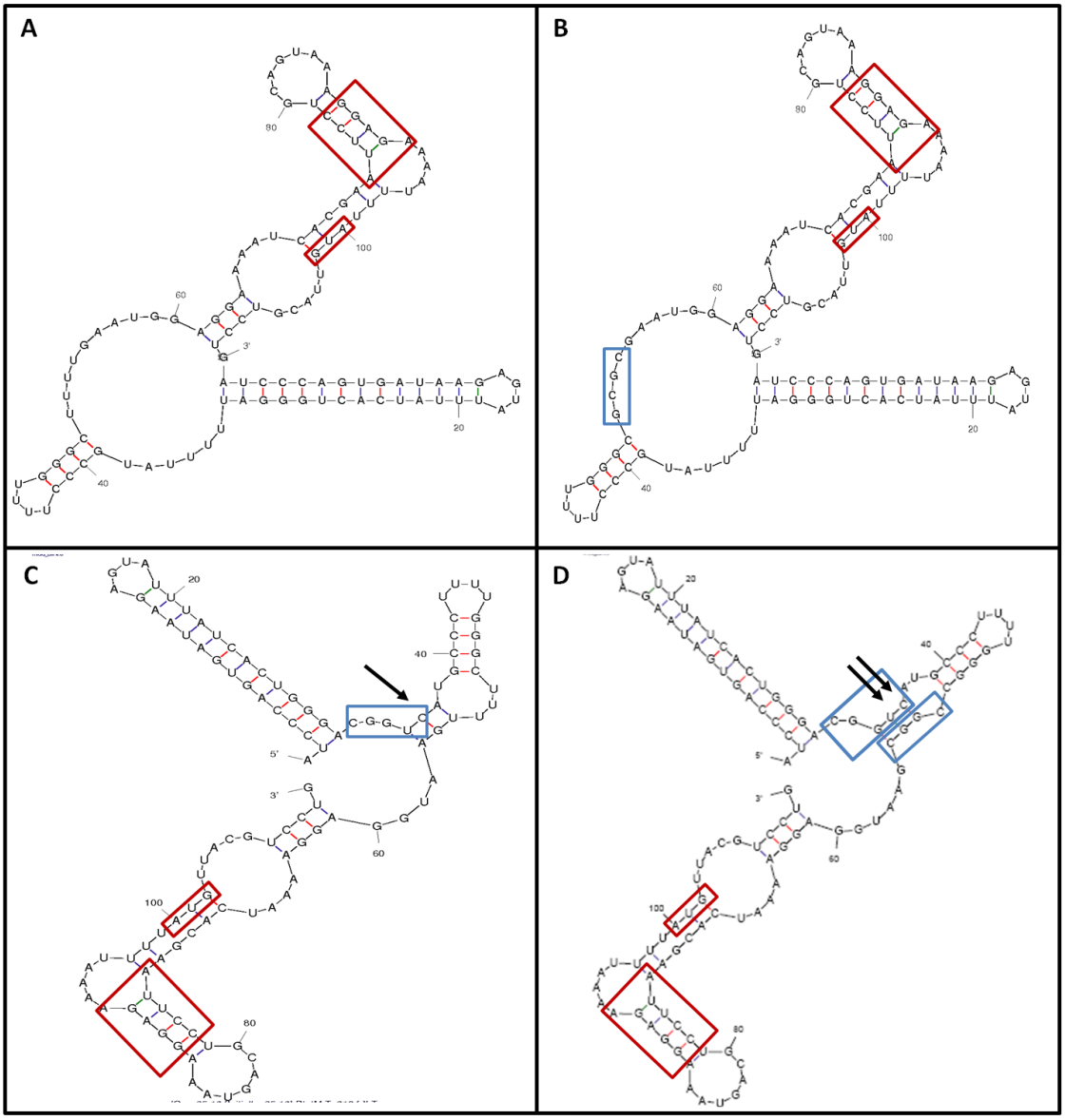

Figure 5.10 Structure of terminator constructs set II as predicted by mfold. The expected stem loop structures were visible in the predicted folds in all constructs despite the mutated T residues (shown in blue boxes). The start codon and the ribosome binding site (RBS) of β-glucuronidase are shown in red boxes. Black arrows show the extra binding regions following the large terminator. Panel A represents the wild type (BS80A), panel B represents the mutated small terminator (BS89A), panel C represents the mutated large terminator (BS90A) and panel D represents the mutated large and small terminators (BS91A). (Zuker, 2003)

5.3.4 Estimation of the termination efficiency of the terminators using an algorithm

The termination efficiency of the terminators in Tn*916* was estimated using an algorithm developed previously by d' Aubenton Carafa *et al*. (1990) (Section 5.2.4). The calculations are as follows;

As the $n_T = \Sigma \chi_n$ and the large terminator are pentanucleotides TTTTT, therefore:

T: 0.9
T: 0.9 x 0.9 = 0.81
T: 0.81 x 0.9 = 0.729
T: 0.729 x 0.9 = 0.656
T: 0.656 x 0.9 = 0.590

Therefore n_T = 0.9 + 0.81 + 0.729 + 0.656 + 0.590 = 3.685, and as

Y = (-ΔG)/LH, therefore

Y = 20.6/30

Y = 0.69

d value of the large terminator therefore equals:

$d = n_T \times 18.16 + Y \times 96.59 - 116.87$

d = 3.685 x 18.16 + 0.69 x 96.59 – 116.87

d = 16.7

On the other hand, as the small terminator are tetranucleotides TTTT, therefore:

T: 0.9
T: 0.9 x 0.9 = 0.81
T: 0.81 x 0.9 = 0.729
T: 0.729 x 0.9 = 0.656

Therefore $n_T = 0.9 + 0.81 + 0.729 + 0.656 = 3.095$, and as Y value is calculated as:

$Y = 8/12$

$Y = 0.67$

d value of the small terminator is therefore equals to:

$d = n_T \times 18.16 + Y \times 96.59 - 116.87$

$d = 3.095 \times 18.16 + 0.67 \times 96.59 - 116.87$

$d = 4.05$

Using the defined parameters, the *d* scores were plotted on the diagram in Figure 5.11 to estimate the termination efficiency of the terminators. The correlated termination efficiencies estimated for the large and small terminators are 58% and 28%, respectively. The estimation of the termination efficiency was then compared with the results of the in vitro assays of the terminator constructs in set I (Figure 5.12). Having termination efficiencies of 47% (±18) (large terminator) and 23% (±15) (small terminator), these results are therefore in good agreement with the measured efficiencies using an algorithm.

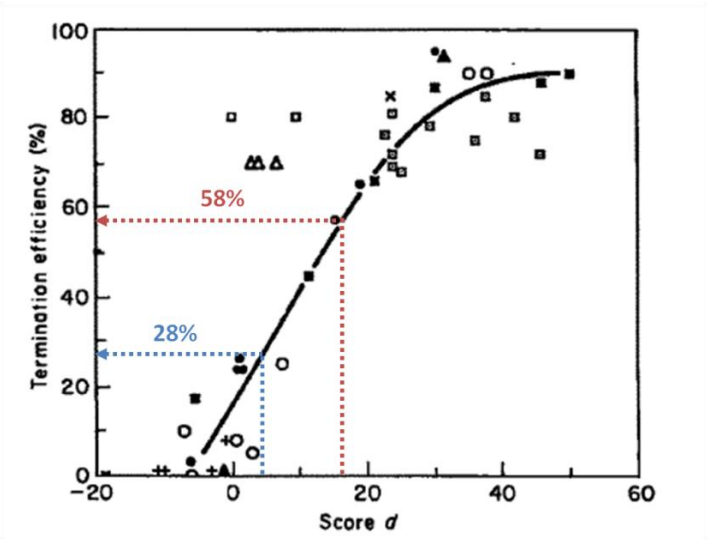

Figure 5.11 Correlation between the score d of some rho-independent terminators and their efficiency in vitro (d' Aubenton Carafa *et al*., 1990). The *d* values of the large terminator (16.7) and the small terminator (4.05) were plotted on the x-axis and correlated with 58% (red dotted line) and 28% (blue dotted line) of termination efficiencies, respectively.

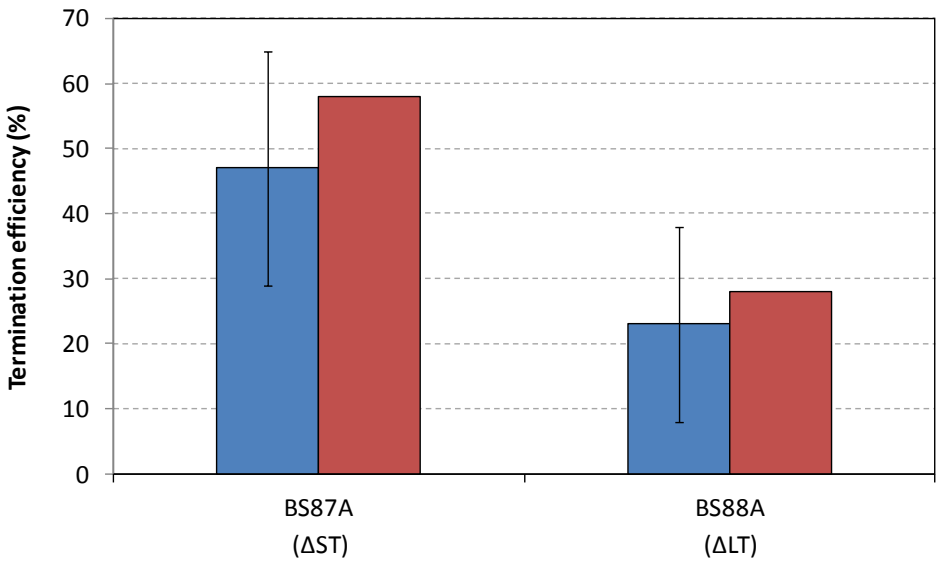

Figure 5.12 The termination efficiency of the large (BS87A) and small (BS88A) terminators set I. The termination efficiencies were determined by in vitro assays (blue) and an algorithm (red).

5.4 Discussion

The two terminators located within *orf12* of Tn*916* are shown to satisfy the minimal conditions of a rho-independent transcription terminator; GC rich stem (Sugimoto *et al*., 1987; Tuerk *et al*., 1988), small loop (≤ 6 nucleotides) (Gralla and Crothers, 1973; Groebe and Uhlenbeck, 1988) followed by a series of uridine residues (Stroynowski *et al*., 1983; Lynn *et al*., 1988) in the RNA. Having a variation in the number of GC content as well as the number of U residues, both terminators are expected to demonstrate different termination efficiencies. Results presented in this study demonstrated that the large terminator is more efficient than the small terminator and this result is consistent with the predicted *in silico* termination efficiency (experimental value is 91% of the predicted value). This result is highly expected as the large terminator consists of more GC content as well as the U residues than the small terminator. The preference of the GC nucleotides as the most energetically favorable base pair for the formation of a stable RNA stem loop and its association with the T residues, which are responsible for the efficiency of the termination process have been reported in a number of studies (Christie *et al*., 1981; Stroynowski *et al*., 1983; Tuerk *et al*., 1988). In fact, it was suggested that high GC content (>75%) is necessary for the formation of RNA stem loop and a rapid disruption of the RNA-DNA duplex during the termination process (d' Aubenton Carafa *et al*., 1990). Additionally, studies by Jeng *et al*. (1997) indicated that the termination efficiency increases by the number of T residues.

In a system where both terminators are present, it is predicted that the transcription could be efficiently reduced by up to 69.76%. This value corresponds to ~30% of transcriptional read-through, therefore when both terminators are absent, it is estimated that the transcriptional read-through could lead to as high as 11646 units of enzyme activity. The experimental data seen in Chapter 4 does show high levels of activity for the promoter only construct (Figure 4.13 and Figure 4.14). The predicted value suggests that P*tet*(M) is an exceptionally strong promoter and needs to be controlled as rapid transcription from this promoter would likely be deleterious for both the element as well as the host therefore it is not surprising that this regulatory system is conserved. Also in this study, it has been shown that the small terminator can independently cause termination without the synergistic presence of the large terminator. This result appears to contradict the previous hypothesis by Hippel and Yager (1991), which according to their kinetic and thermodynamic analyses, the small terminator with a free energy value of -8 kcal mol^{-1} is considered as a weak terminator and not normally capable of causing termination on its own.

Although the large terminator constitutes more GC content and T residues than the small terminator, these characteristics are not the only factors that contribute to the measured efficiencies. In some terminators, the sequences of the promoter regions can strongly affect the termination efficiency (Golliger *et al*., 1989) by allowing substantial read-through of strong termination signals in a phenomenon known as factor-independent antitermination (Telesnitsky and Chamberlin, 1989).

Additionally, d'Aubenton Carafa and co-workers (1991) suggested that various protein factors might contribute to the efficiency of terminators, which is in fact a restriction to the constructed algorithm which is unable to correlate the sensitivity of the terminators to these proteins. They also suggested that the sequences situated upstream to the stem loop structure and downstream of the stretch of T residues might play a role in determining the efficiency of the terminators, although the mechanism remains elusive. This prediction is relevant to our results which indicate that the restoration of the upstream and downstream sequence (terminator construct set II) may have led to different termination efficiencies as compared to the terminator constructs in set I. Interestingly, the enzyme activities of BS89A (Δ small terminator) and BS91A (Δ small and large terminators) decrease as compared to the wild type (BS80A) when the U residues following the small terminator are mutated. It is unclear if the mutation introduced in this region has led to the reduced enzyme activity considering that the predicted secondary structures of both constructs are consistent with the wild type. Further investigation is therefore necessary particularly to understand the significant of these T residues in the transcriptional termination of Tn*916*.

Although Tn*916* and Tn*5397* have an almost identical terminator structure, despite those two nucleotides different in the large stem (Roberts and Mullany, 2009), the termination efficiency of the large terminator in Tn*5397* cannot be estimated using an algorithm as the minimal value of the parameter (n_T) is not fulfilled. This is because there is a single base (A residue) separation between the 3'-end of the

stem and the poly-T residues which led to the rejected n_T value (<2.895). However, the small terminator in Tn*5397* has been estimated to share the same termination efficiency (28%) with the small terminator in Tn*916*. This may explain the lack of differential transcriptional activity we have seen in Chapter 4 for Tn*5397*. If the predicted large terminator does not actually function as a terminator, we would not see a very large change in expression due to the presence of tetracycline, or indeed at the beginning of the growth phase as 72% of transcripts would be predicted to read-through the attenuator. However, the efficiency of the large terminator in Tn*5397* requires experimental verification.

5.5 Conclusion

The efficiency of the terminators within the *orf12* of Tn*916* was successfully predicted using an algorithm and validated using the *in vitro* reporter assays. The large terminator is more efficient than the small terminator as indicated by both analyses. This is also the first demonstration that the small terminator can act alone.

Chapter 6.0

Transfer of Tn*5397* between *C. difficile* and *E. faecalis*

6 Transfer of Tn*5397* between *C. difficile* and *E. faecalis*

6.1 Introduction

E. faecalis and *C. difficile* are the leading pathogens of nosocomial infections in humans in which they inhabit the same niche (Poduval *et al*., 2000; Donskey *et al*., 2003). For the last ten years, the emergence of vancomycin resistant enterococci (VRE) as nosocomial pathogens has caused considerable public concern as it leads to multiple infections that cause serious or life threatening illnesses (Mundy *et al*., 2000). However, the greatest concern is the co-infection of *C. difficile* in patients with VRE (Donskey *et al*., 2003) where the possible genetic exchanges between the two pathogens could possibly disseminate the vancomycin resistant determinants, *vanA* and *vanB* (Arthur *et al*., 1996) to *C. difficile*. This might cause major challenges in the treatment of *C. difficile* infections (CDI) as metronidazole and vancomycin are the conventional treatments of CDI despite the newly introduced antibiotic fidaxomicin (Cornely *et al*., 2012).

In this chapter, transfer of the conjugative transposon Tn*5397* conferring tetracycline resistance gene *tet*(M) from *C. difficile* 630 to *E. faecalis* JH2-2 was investigated. This experiment was carried out to investigate if there is a barrier to genetic exchange between *C. difficile* and *E. faecalis*. This observation is crucial as it highlights the need for continual monitoring of emerging resistances in both *C. difficile* and *E. faecalis*.

6.2 Materials and methods

6.2.1 Bacterial strains

In filter mating experiments, *C. difficile* 630 and *E. faecalis* EF20A were used as the donor strains of Tn*5397*, whereas the recipient strains were *E. faecalis* JH2-2 and *C. difficile* R20291. The characteristics of each strain are listed in Table 2.1. All strains were grown under the conditions described in Section 2.3.

6.2.2 Transfer experiments and transconjugants selection

Transfer of Tn*5397* between *C. difficile* and *E. faecalis* was demonstrated by filter mating (Section 2.6). The *E. faecalis* transconjugants were selected on BHI agar supplemented with tetracycline (10 μg ml^{-1}), fusidic acid (5 μg ml^{-1}) and rifampicin (25 μg ml^{-1}) after 24 h of incubation at 37^{o}C. In contrast, the *C. difficile* transconjugants were selected on BHI agar supplemented with tetracycline (10 μg ml^{-1}) and erythromycin (10 μg ml^{-1}) after 24-48 h incubation at 37^{o}C in an anaerobic atmosphere (80% N_2, 10% H_2 and 10% CO_2).

6.2.3 Electrophoresis and Southern blotting

The genomic DNA (3 μg) of *E. faecalis* transconjugants from 5 independent experiments was digested with a 6 bp cutter restriction enzyme, XmnI. Digestion was carried out for 12 h at 37^{o}C. The digested genomic DNA was then electrophoresed on 1% (w/v) agarose gel in 1X TAE buffer for 1 h at 50 V. The insertion profile and the copy number of Tn*5397* in *E. faecalis* transconjugants was subsequently determined using Southern blot analysis (Section 2.7). A 300 bp probe derived from *tndX* gene was used for hybridisation (Figure 6.1).

6.2.4 Single specific primer PCR (SSP-PCR)

SSP-PCR was used to determine the integration site of Tn*5397* in *E. faecalis* EF20A. Genomic DNA of *E. faecalis* (3 μg) and pUC19 (0.1 μg) were digested with either EcoRI or BamHI at 37^{o}C for 2 h. The digested DNA and the dephosphorylated pUC19 were purified using QIAprep Spin Miniprep column. Ligations were carried out at 4^{o}C for 18 h with T4 DNA ligase. The ligation mixture (approximately 0.2 ng μl^{-1}) was used as template in PCR. Amplification was carried out using Tn*5397* specific primers (LEO or REO) and either M13 For or M13 Rev primers (situated in pUC19). Sequences of each primer were listed in Table 2.3. The schematic representation of SSP-PCR is shown in Figure 6.2.

Figure 6.1 A schematic representation of Tn*5397.* Arrow represents the location of the 300 bp probe derived from *tndX* gene which was used for hybridisation. (Adapted from Roberts and Mullany, 2009)

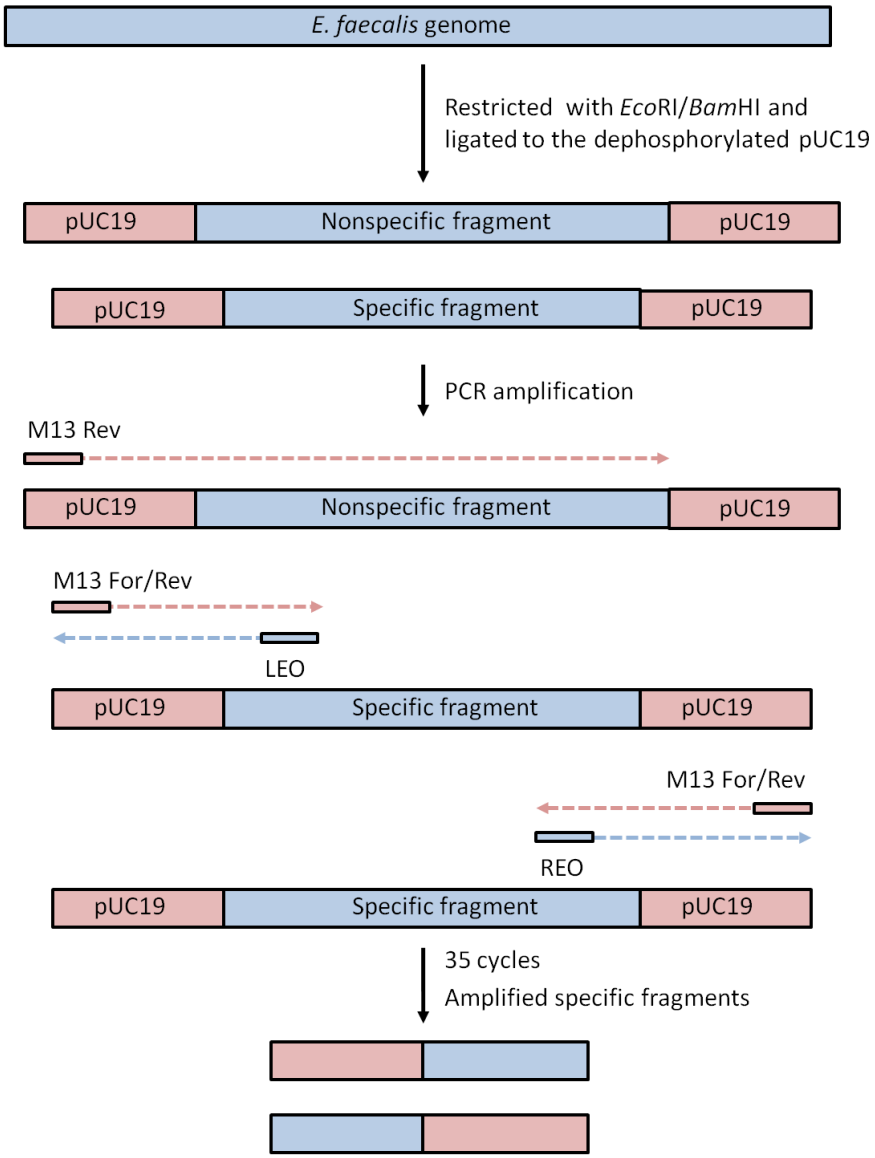

Figure 6.2 Schematic representation of SSP-PCR. *E. faecalis* genome was restricted with EcoRI and BamHI prior to ligation with the dephosphorylated pUC19. The ligated products which consist of non-specific and specific fragments were used as template in PCR using primers M13 For and M13 Rev (Table 2.3). Dashed arrows represent the primers and the direction of priming. Template that consists of specific fragments are amplified in the PCR reaction.

6.3 Results

6.3.1 Transfer of Tn*5397* from *C. difficile* 630 to *E. faecalis* JH2-2

Transfer of Tn*5397* from *C. difficile* 630 to *E. faecalis* JH2-2 was demonstrated. The mean transfer frequency [± standard deviation (SD)] was 8.85×10^{-8} ($\pm 2.14 \times 10^{-7}$) transconjugants per recipient (average of 5 independent filter mating experiments). The presence of this element in *E. faecalis* transconjugants was confirmed by PCR amplification of *tndX* gene with the expected products of 1.6 kb (Figure 6.3). DNA from the donor strain (*C. difficile* 630) was included as positive control for the PCR. All transconjugants analysed were generated independently from different filter mating experiments to exclude the possibility of analysing siblings. Sequence analysis showed that all the amplified PCR products are *tndX* (accession no. AF333235). One transconjugant was chosen for further study and was designated EF20A.

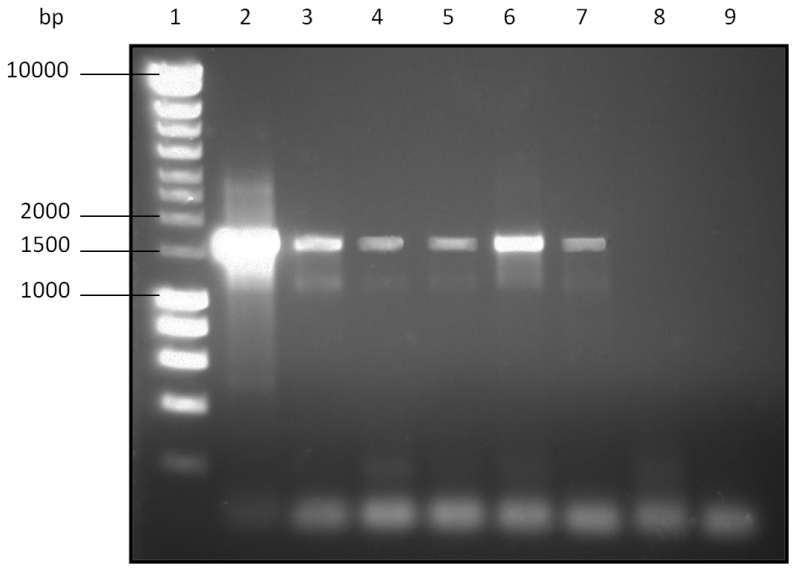

Figure 6.3 Amplification of *tndX* gene in *E. faecalis* transconjugants. Lane 1: HyperLadder I; Lane 2: Genomic DNA of *C. difficile* 630 (positive control); Lanes 3-7: Genomic DNA of *E. faecalis* transconjugants from 5 independent filter mating experiments; Lane 8: Genomic DNA of *E. faecalis* JH2-2 (negative control); Lane 9: No DNA.

6.3.2 Transfer of Tn*5397* from *E. faecalis* EF20A to *C. difficile* R20291

This experiment was carried out to investigate if Tn*5397* can be transferred from *E. faecalis* back to *C. difficile*, hence demonstrate a two-way genetic exchange between these two bacteria. Results show that Tn*5397* was transferred from *E. faecalis* EF20A to *C. difficile* R20291 with a transfer frequency [± standard deviation (SD)] of 4.44×10^{-6} ($\pm 1.15 \times 10^{-6}$) transconjugants per recipient or 6.15×10^{-8} ($\pm 1.27 \times 10^{-8}$) transconjugants per donor (average of 3 independent filter mating experiments). Tn*5397* has been shown to occupy 2 target sites in *C. difficile* R20291 (Hussain *et al*., unpublished data), namely *fic1* and *fic2* (filamentation induced by cAMP) genes. PCR amplification was carried out using combination of primers that flanked both target sites to confirm the presence as well as the orientation of Tn*5397* in *C. difficile* R20291 (Figure 6.4). *C. difficile* R20291 (recipient) was included as a negative control. PCR amplification and sequencing results confirmed the presence of Tn*5397* in these two sites (Figure 6.5). These results confirmed the reciprocal genetic exchange between *E. faecalis* and *C. difficile*.

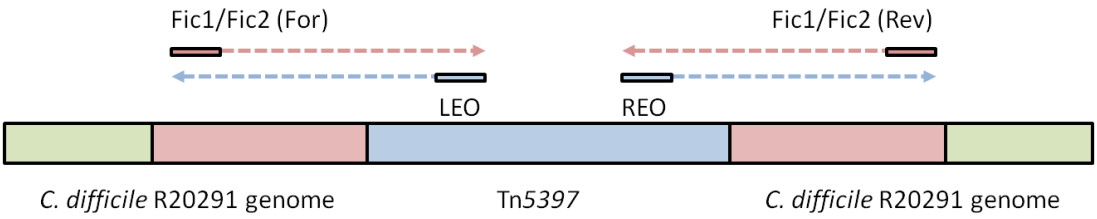

Figure 6.4 Schematic diagram showing the position of the primers used to amplify the 2 target sites of Tn*5397* in the *C. difficile* R20291 genome. PCR amplification was carried out using combinations of primers (Fic1 For and LEO; Fic2 For and LEO; Fic1 Rev and REO; Fic2 Rev and REO) (Table 2.3) flanking the insertion sites and the transposon. Red boxes represent the Fic1/Fic2 regions. Green boxes represent the *C. difficile* genome. Dashed arrows represent the primers and the direction of priming.

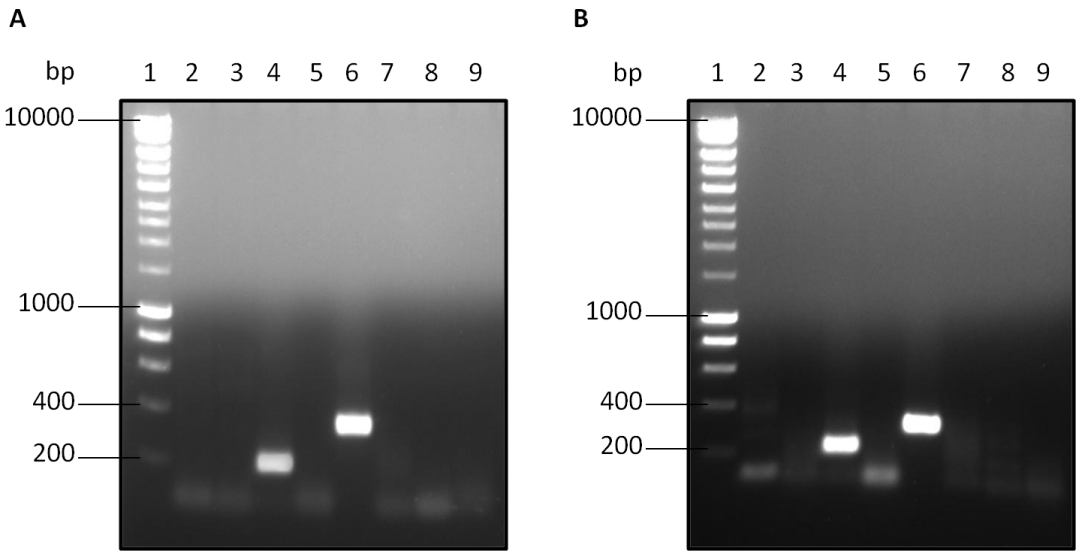

Figure 6.5 PCR results showing the presence of Tn*5397* in two sites of *C. difficile* R20291. panel A: Amplification of the first target site, Fic1: Lane 1: HyperLadder I; Lane 2: Fic1 For + Leo (transconjugant); Lane 3: Fic1 For + Leo (negative control); Lane 4: Fic1 For + Reo (transconjugant); Lane 5: Fic1 For + Reo (negative control); Lane 6: Fic1 Rev + Leo (transconjugant); Lane 7: Fic1 Rev + Leo (negative control); Lane 8: Fic1 Rev + Reo (transconjugant); Lane 9: Fic1 Rev + Reo (negative control). Panel B: Amplification of the

second target site, Fic2: Lane 1: HyperLadder I; Lane 2: Fic2 For + Leo (transconjugant); Lane 3: Fic2 For + Leo (negative control); Lane 4: Fic2 For + Reo (transconjugant); Lane 5: Fic2 For + Reo (negative control); Lane 6: Fic2 Rev + Leo (transconjugant); Lane 7: Fic2 Rev + Leo (negative control); Lane 8: Fic2 Rev + Reo (transconjugant); Lane 9: Fic2 Rev + Reo (negative control). The negative control for this PCR reaction was *C. difficile* strain R20291 (recipient).

6.3.3 Determination of the number of copies of Tn*5397* in *E. faecalis* transconjugants

Southern hybridisation was carried out to determine the number of copies of Tn*5397* in *E. faecalis*. Genomic DNA of *E. faecalis* JH2-2 and *E. faecalis* EF20A from 5 independent experiments were digested with XmnI and probed with a 300 bp amplicon of *tndX*. The cutting sites of XmnI in the *tndX* sequence were mapped and the presence of a single band (approximately 1300 bp) in all transconjugants after the Southern blotting suggests that a single copy of Tn*5397* has integrated into the genome of all the *E. faecalis* transconjugants at a single conserved site (Figure 6.6 and Figure 6.7).

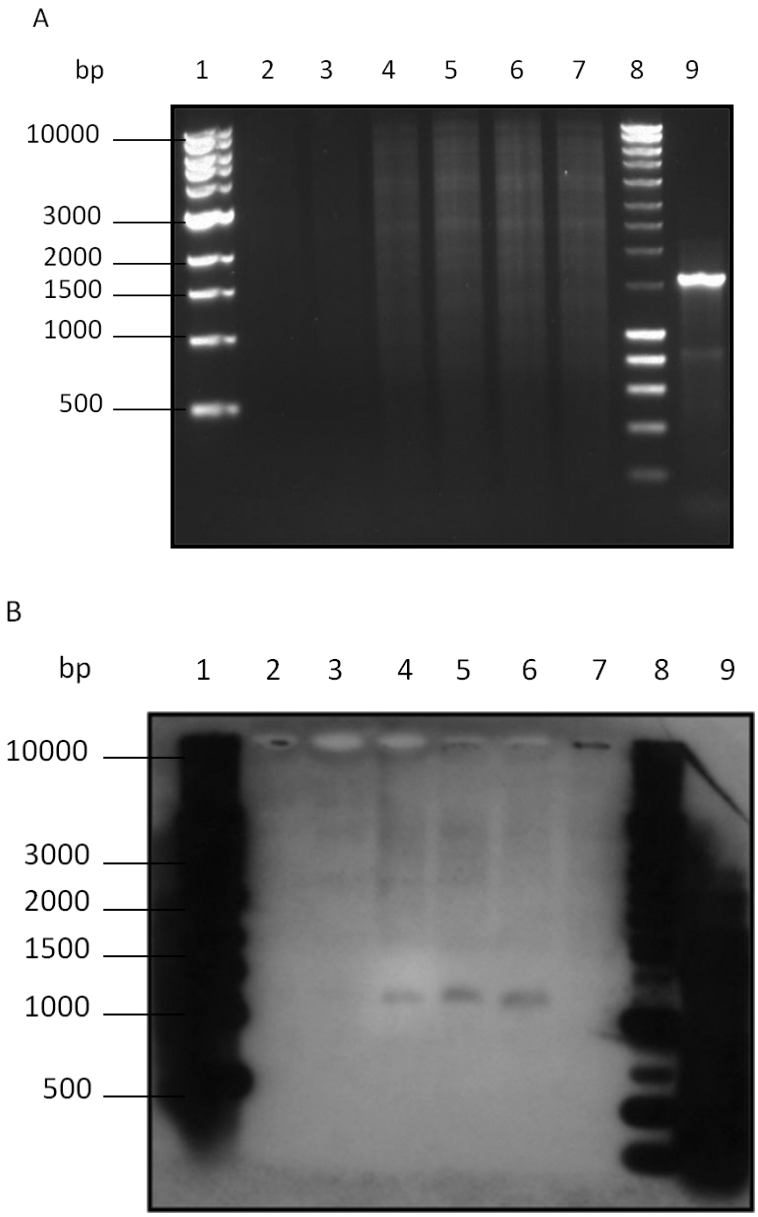

Figure 6.6 Southern blot analysis using *tndX* probe**.** Insertion profile of Tn*5397* in *E. faecalis*. Panel A shows the genomic DNA digested with XmnI and electrophoresed on 1% agarose gel. Panel B shows the Southern blotting performed on this gel. The single hybridizing band for each transconjugant is shown (30 min exposure). Lane 1: 1 kb DNA ladder; Lanes 2-6: XmnI-digested genomic DNA of transconjugants; Lane 7: *E. faecalis* JH2-2 (negative control); Lane 8: HyperLadder I; Lane 9: *tndX* fragment.

A

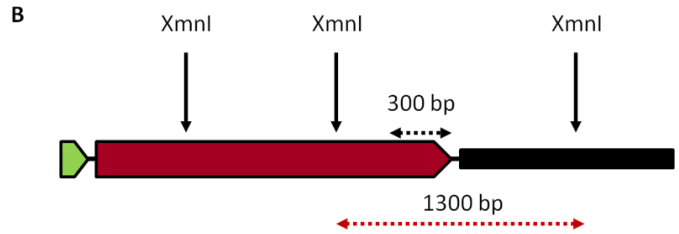

Figure 6.7 Cutting sites of XmnI within *tndX* gene and *E. faecalis* genome. Panel A represents Tn*5397*, with *tndX* gene circled. Panel B represents the cutting sites of XmnI (black arrows) within *tndX* gene (red arrowed box) and *E. faecalis* genome (black bar). The black dotted arrow represents the location of the probe used for hybridisation. A product of 1300 bp, which consists of *tndX* gene and *E. faecalis* genome (black bar), was observed on the blot (red dotted arrow).

6.3.4 Determination of the target site of Tn*5397* in *E. faecalis*

The nucleotide sequence of the target site of Tn*5397* in *E. faecalis* was determined using SSP-PCR (Figure 6.8A). Amplicons were cloned into pGEM-T Easy and after transformation into *E. coli*, plasmids which contained different sizes of inserts were sequenced (Figure 6.8B). Analysis of the sequence showed that Tn*5397* has inserted within the chromosome at a region which is identical to an open reading frame from *E. faecalis* V583 encoding the IIA component of a mannose/sorbose specific sugar phosphotransferase system (Accession number: NP_814245) involved in the uptake and phosphorylation of carbohydrates.

Based on the sequence of PTS system IIA component of *E. faecalis* V583, amplification of the genome:transposon junction was carried out using primers (PTS For and PTS Rev) flanking the insertion site (Figure 6.9). The sequencing results showed the presence of a GA dinucleotide flanking both the genome:transposon junctions (Figure 6.10).

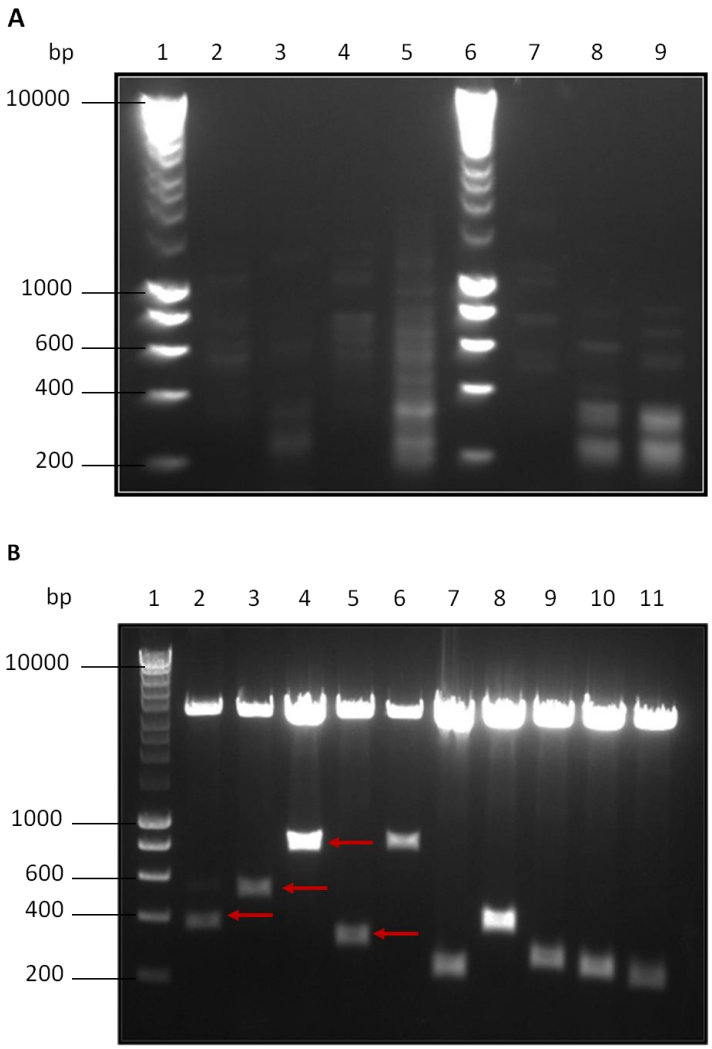

Figure 6.8 Characterization of the target sites of Tn*5397* in *E. faecalis*. Panel A: Visualization of amplified products from SSP-PCR. Lane 1: HyperLadder I; Lanes 2 and 7: Leo + M13 For; Lanes 3 and 8: Reo + M13 For; Lanes 4 and 9: Leo + M13 Rev; Lane 5: Reo + M13 Rev. PCR products from Leo + M13 For (Lanes 2 and 7) were chosen and cloned into pGEM-T Easy. Panel B: XmnI-digested plasmids containing different sizes of inserts. The inserts from the plasmids in Lanes 2-5 (arrows) were sequenced.

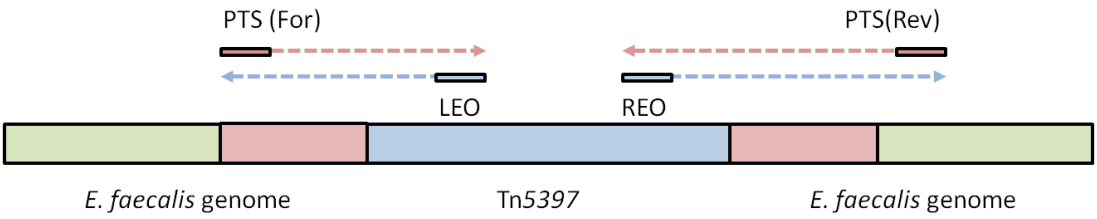

Figure 6.9 Schematic diagram showing the position of the primers used to amplify the target site of Tn*5397* in the *E. faecalis* genome. PCR amplification was carried out using combination of primers (PTS For and LEO; PTS Rev and REO) (Table 2.3) flanking the insertion site and the transposon. Red boxes represent the PTS IIA component gene. Green boxes represent the flanking *E. faecalis* genome. Dashed arrows represent the primers and the direction of priming.

Target site in JH2-2	GACGCTTGTATTAGCT **GA** CTGATTTAAAAGGAG
Left end in transconjugant	GACGCTTGTATTAGCT **GA** TGGAAATGTACCATC
Right end in transconjugant	CATTGATACATTCTCT **GA** CTGATTTAAAAGGAG
Empty target site in transconjugant	GACGCTTGTATTAGCT **GA** CTGATTTAAAAGGAG
Target site in CD630	TGTTCATCCTTTTAGT **GA** TGGTAATGGAAGAAC

Figure 6.10 DNA sequence of the target site-transposon junctions. The GA dinucleotide that flanks Tn*5397* is shown in boldface. The target site in *C. difficile* 630 was included as reference comparison. The conserved hexamer TGATTT was observed in both target site of *E. faecalis* JH2-2 and *C. difficile* 630 (underlined).

6.3.5 PCR amplification for the joint of the circular form of Tn*5397* in *E. faecalis*

Circularisation of the conjugative transposon Tn*5397* was first demonstrated by Wang *et al*. (2000). PCR amplification was carried out using outward firing primers, LEO and REO (Figure 6.11). A PCR product of 280 bp is expected if the left and right ends of the transposon were ligated together following excision from the chromosome. Figure 6.12 shows the amplified products from both the *C. difficile* 630 (donor) and the *E. faecalis* transconjugants. No products were observed for *E. faecalis* JH2-2 (recipient) (negative control).

6.3.6 Effect of acquisition of Tn*5397* on the growth of *E. faecalis*

The effect of the acquisition of Tn*5397* to the growth of the *E. faecalis* EF20A was investigated using comparative growth curve. Results demonstrate that the acquisition of Tn*5397* had caused a small fitness burden to *E. faecalis* EF20A, which is presented by a delayed growth rate compared to the wild type *E. faecalis* JH2-2 (Figure 6.13).

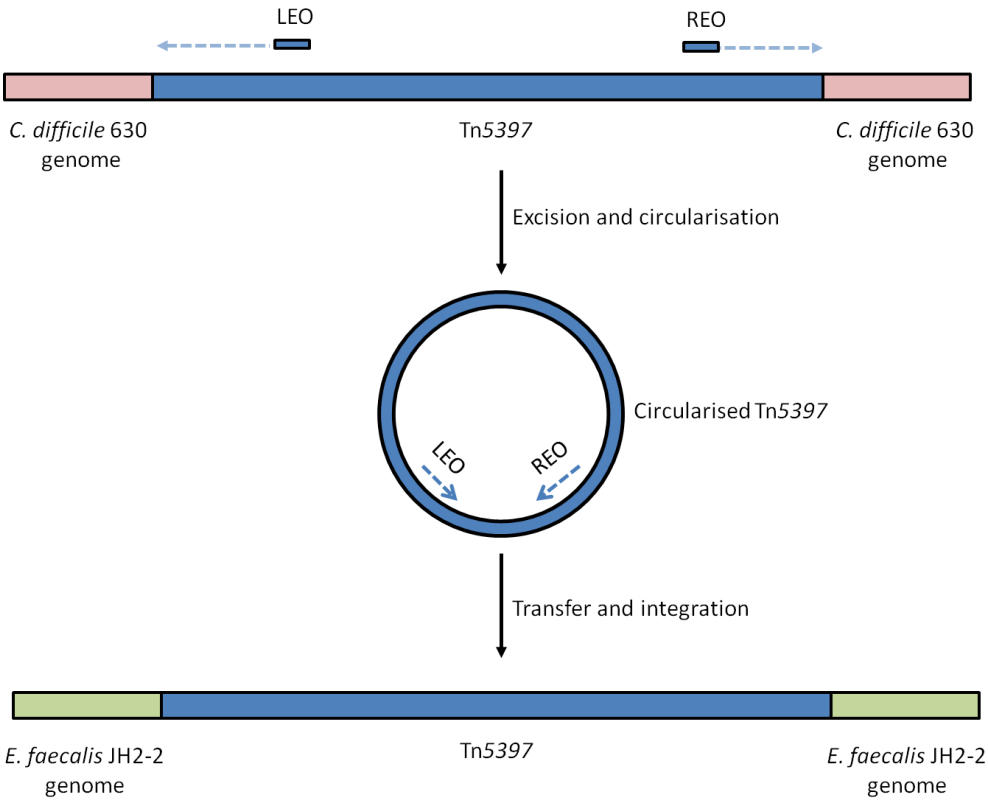

Figure 6.11 Circularisation of Tn*5397.* Primers LEO and REO (Table 2.3) are designed to bind to the sequence of Tn*5397* in an outward position. These primers are able to amplify the region in Tn*5397* if this element excises and form a circular intermediate prior to integration.

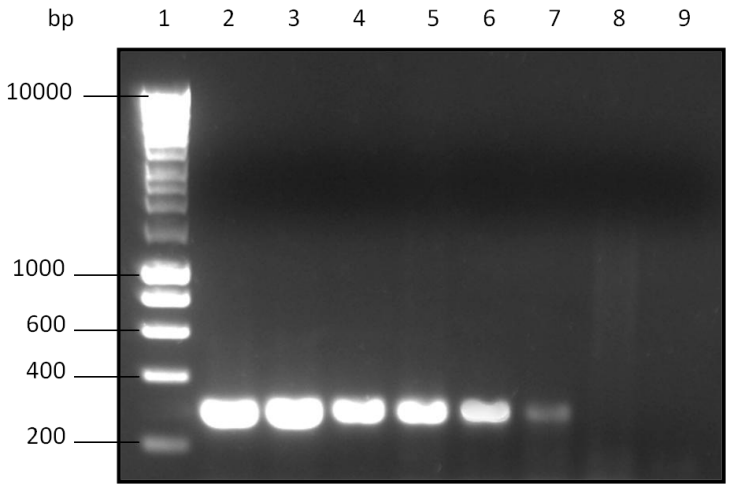

Figure 6.12 PCR results revealing the presence of circular form of Tn*5397* in *E. faecalis* transconjugants. Lane 1: HyperLadder I; Lane 2: Genomic DNA of *C. difficile* 630 as template (positive control); Lanes 3-7: Genomic DNA of *E. faecalis* as template (transconjugants from five independent experiments); Lane 8: Genomic DNA of *E. faecalis* JH2-2 as template (negative control); Lane 9: No DNA.

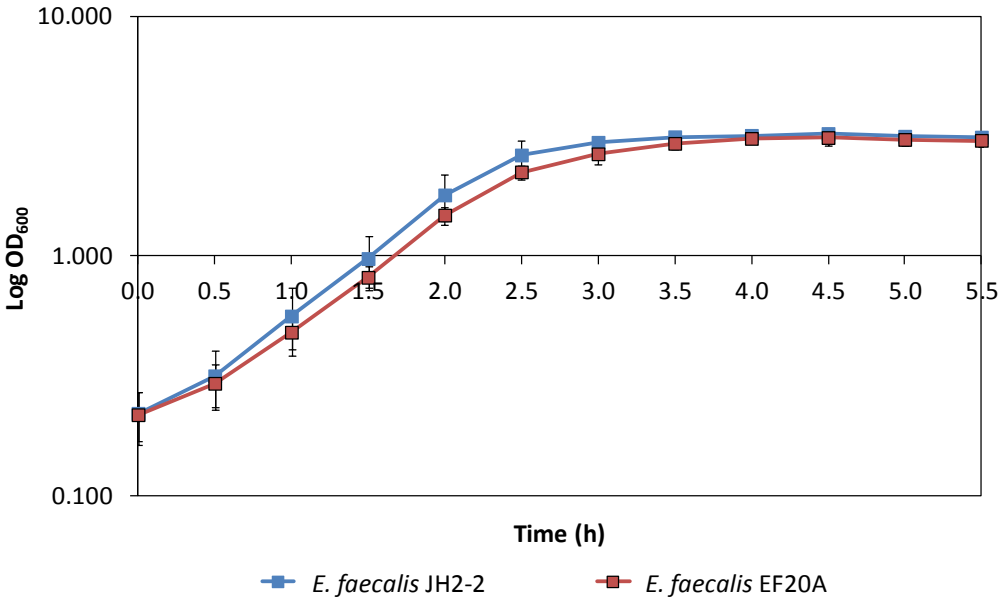

Figure 6.13 Comparison of the growth kinetics of *E. faecalis* JH2-2 and EF20A. Error bars indicate the standard deviation of three independent experiments.

6.4 Discussion

The conjugative transposon Tn*5397* was shown to transfer from *C. difficile* 630 to *E. faecalis* JH2-2, and from this host to *C. difficile* R20291 ribotype 027. This is the first report on the intergeneric transfer of Tn*5397* between these two bacteria although previous studies have indicated the transfer of this element from *C. difficile* strains to and from *B. subtilis* and between *C. difficile* strains (Mullany *et al*., 1990; Roberts *et al*., 1999). Studies by Launay *et al*. (2006) have shown that although intergeneric transfer of Tn*1549* between *C. symbiosum* and *E. faecalis* and *E. faecium* occurs both *in vitro* and *in vivo*, however higher number of transfers were obtained in *in vitro*. Although the transfer of Tn*5397* between *E. faecalis* and *C. difficile* occurs in the laboratory, which is different from the usual environment of the bacteria but the active movement of this element demonstrates that there is no obvious barrier for the exchange of conjugative elements. Therefore, the fact that we have not yet seen vancomycin resistant *C. difficile* may be due to either host factors or expression problems of the vancomycin proteins.

In addition, the transfer of Tn*5397* between *C. difficile* and *E. faecalis* does not appear to be restricted. The mean transfer frequency detected in this study concurs with the previous work by Agersø and co-workers (2006) who demonstrated the transfer of Tn*5397* between *E. faecium* strains, with the transfer frequency of 7 x 10^{-8} transconjugants per donor. In previously mentioned study by Launay *et al*. (2006), the intergeneric transfer of Tn*1549* between *C. symbiosum* and *E. faecalis*

and *E. faecium* was demonstrated to occur between 10^{-8} and 10^{-9} transconjugants per recipient. Launay and co-workers also suggested that the efficiency of transfer between *Clostridium* sp. and *Enterococcus* sp. appears to be both donor and recipient dependent, where the most efficient donor and recipient strains of *C. symbiosum* and *E. faecalis* used in their study have been identified.

Tn*5397* has been shown to integrate the genome of *E. faecalis* at a single site, based on the Southern blot analysis. This site is identified within an open reading frame that was predicted to encode a phosphotransferase (PTS) IIA component (locus_tag: EF_0461). The PTS IIA component is a major carbohydrate transport system in bacteria, involves in uptake and metabolism of sugars (Postma *et al*., 1993). The integration of Tn*5397* within this region probably due to the presence of TGATTT hexamer, which was also observed in both target sites of *C. difficile* 630 and *E. faecalis* JH2-2 suggested that this could be a preferred region for TndX binding to catalyse the insertion of this element.

Although Tn*5397* has been shown to integrate into a single specific site in *E. faecalis*, there is a possibility that different *E. faecalis* strains will have multiple insertion site as reported in *B. subtilis*. Studies by Wang *et al*. (2006) have shown that Tn*5397* has a preferred target site in *C. difficile*, $attB_{Cd}$. In *C. difficile* 630, Tn*5397* integrated into one preferred site (Wang *et al*., 2006), whereas in *C. difficile* R20291 ribotype 027, this element inserts into two target sites. These target sites

are used by Tn*5397* and can be occupied at the same time (Hussain *et al*., unpublished data). The integrated Tn*5397* in *E. faecalis* has also been shown to be flanked by the GA dinucleotides. Excision of Tn*5397* involves a 2 bp staggered cuts at 3‘ ends of the directly repeated GA dinucleotides at each end of the transposon. These sticky ends form the joint of a circular intermediate which is essential for conjugal transfer and transposition of this element (Wang *et al*., 2006). In this study, the circular intermediate of Tn*5397* was observed in all *E. faecalis* transconjugants as demonstrated by PCR amplification results hence provides an evident that this element is transferable from *E. faecalis* host.

Preliminary study on the effect on growth of acquiring Tn*5397* was carried out by comparative growth curves of *E. faecalis* JH2-2 and *E. faecalis* EF20A. Results suggest that the acquisition of Tn*5397* by *E. faecalis* and its integration within the orf encoding a IIA component, may show a small fitness burden. In order to determine the effect empirically a competitive assay should be used as we used in Chapter 3. Previous studies have evaluated the fitness cost associated with antibiotic resistance genes carried by transposons. Enne *et al*. (2005) have shown that acquisition of Tn*1* and Tn*7* which carry ampicillin and trimethoprim resistance genes, respectively had no cost on the fitness of *E. coli*. In another study by Foucault *et al*. (2010), it was demonstrated that Tn*1549* conferring vancomycin resistance genes carriage had no cost for the *E. faecalis* and *E. faecium* under noninduced state. However, a reduced fitness was observed when the expression of the resistance genes was induced. Fitness cost has also been shown to be

associated with the integration site of the transposons. Studies by Elena *et al*. (1998) illustrate a fitness cost of Tn*10* insertional mutants which was related to the insertion locus rather than to expression of tetracycline resistance. It has also been shown that the integration of Tn*1549* in the coding sequence of Enterococci is not costly, compared to the integration in the non-coding sequence (Foucault *et al*., 2010). It maybe that Tn*5397* has evolved to have a very low burden upon its host. This would make sense as it would therefore be more stable within the genome.

6.5 Conclusion

The reciprocal genetic exchange between *C. difficile* and *E. faecalis* was demonstrated. A single copy of Tn*5397* has integrated the *E. faecalis* genome within an open reading frame encoding a phosphotransferase (PTS) IIA component. Acquisition of Tn*5397* has caused a small fitness burden to *E. faecalis* EF20A.

Chapter 7.0

Final Conclusions and Future Work

7 Final Conclusions and Future Work

The work presented in this study was carried out in order to investigate the detailed molecular mechanisms of regulation that have evolved in the conjugative transposons Tn*916* and Tn*5397*. In the first results chapter (Chapter 3), a defined mutation was constructed in the start codon of *orf12*, the gene immediately upstream of *tet*(M) in Tn*916*. This mutant showed a delayed growth when challenged with tetracycline, presumably because the formation of the terminator structures upstream of *tet*(M) were always formed because the translation of *orf12* cannot occur due to the absence of a start codon. Therefore limited Tet(M) production will mean not as many ribosomes will be protected and the growth in tetracycline will be slower. This provides evidence that *orf12*, is involved in the transcriptional regulation of this element. As *orf12* consists of five rare amino acid residues among the aminoacyl-tRNA pool (cysteine, methionine and histidine) and the paucity of these amino acids could limit the translation rate of this region, therefore future work on this subject should aim to determine the significant level of each amino acid and its effect in the translation rate of *orf12*.

Furthermore, the relative fitness was compared between a differentially marked BS34A (contains wild type Tn*916*) strain and BS79A (contains Tn*916*Δ*orf12*). Without antibiotics, BS79A was 4% more fit than the BS92A (BS34AΔ*amyE*) strain. Following treatment with tetracycline a large decrease in fitness was seen at 5 h post-challenge (38% less fit than BS92A). Again this fitness cost can be attributed to the mutation in the start codon of *orf12* in BS79A for the same reasons as described above.

Next, the expression of the reporter gene (*gusA*) was measured in constructs containing the promoter upstream of *orf12*, with and without *orf12*. It was discovered that the expression of the reporter gene located downstream of the wild type promoter of Tn*916* was growth phase-dependent. The highest expression was seen in the lag phase culture, most likely due to a high amount of tRNA in the cell (as they had been in stationary phase overnight). Then the expression decreased as the log phase progressed. This can be attributed to the tRNAs being used up by the fast growing cells. This is the first time this pattern of basal level of expression has been seen with this system. Next, the expression levels were measured before and after exposure to tetracycline. It was found that the expression level of BS80A [P*tet*(M) Tn*916* (wild type)] increased after 1 h of exposure to tetracycline. This is in agreement with the hypothesis being tested. Lower levels of expression were seen in BS82A ([P*tet*(M) Tn*916* (start codon)], again as predicted, however a small increase was seen following exposure to tetracycline. It is thought this is due to the wild type copy of Tn*916* in the chromosome

protecting the ribosomes leading to increased basal levels of expression. In both the Tn*5397* wild type (BS84A) and the *orf26* start codon mutant (BS86A) constructs, no response was seen following the addition of tetracycline. This is discussed later.

Further experiments with biocides demonstrated that the regulation of Tn*916* does not necessarily depend on the presence of tetracycline. It has been hypothesised that the amount of charged tRNA molecules is the necessary trigger for the regulatory mechanism of Tn*916* (Roberts and Mullany, 2009). The expression of the reporter gene is upregulated upon exposure to the biocides; ethanol, hydrogen peroxide, chlorhexidine digluconate and sodium hypochlorite, all of which damage the cell in multiple ways. This data support the above hypothesis and suggest that any damage caused to the biological systems of bacteria, which affect translation could result in the accumulation of charged tRNA molecules in the cells. Upon sensing this stress condition, the element responsed by upregulating its transcriptional activity. This new knowledge is incorporated with the previous hypothesis and reviewed in Figure 7.1. As the translation of *orf12* is associated with the amount of charged tRNA, therefore future work on this subject should aim to determine the amount of the accumulated charged tRNA that leads to the faster translation of *orf12*.

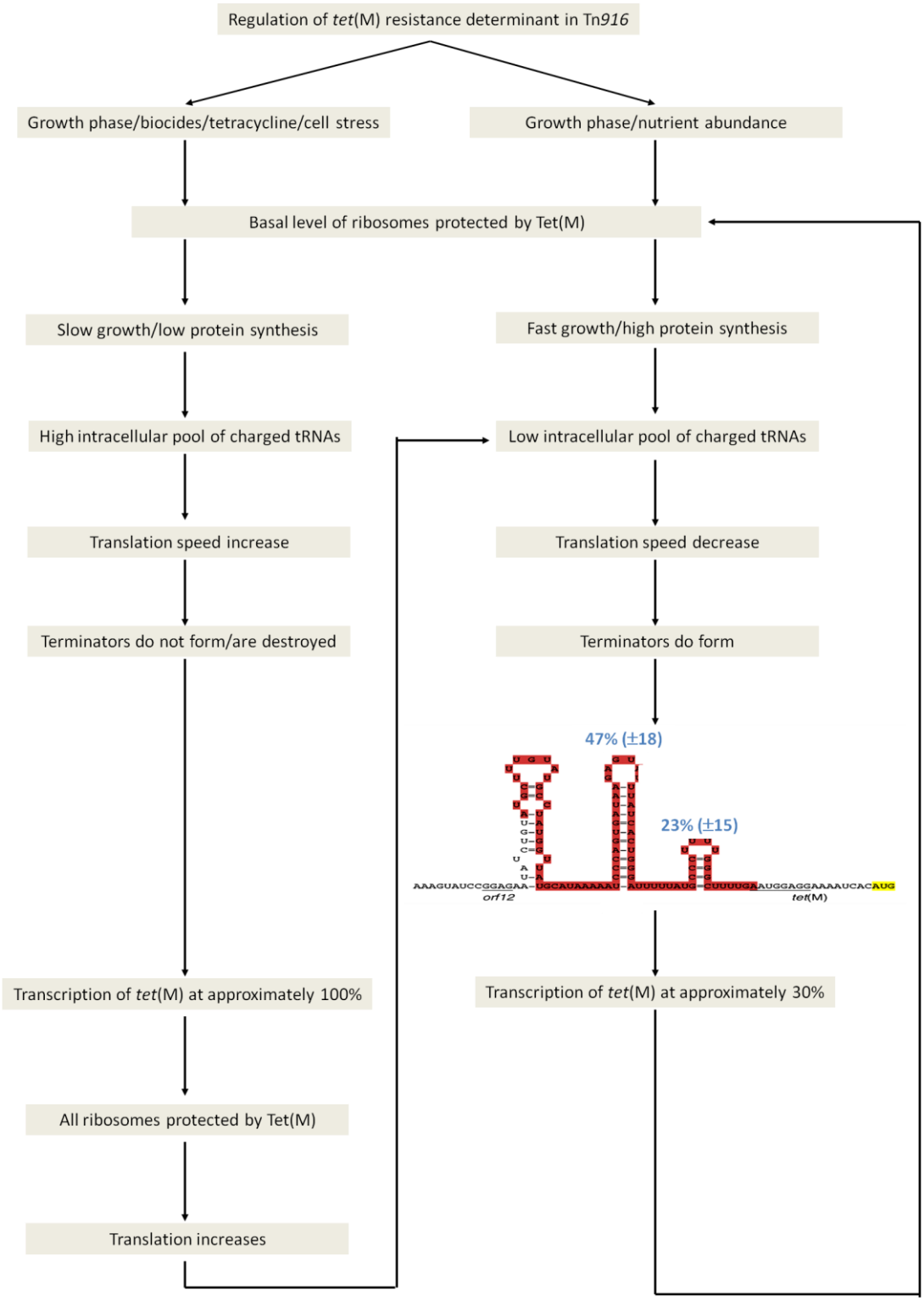

Figure 7.1 Regulation of *tet*(M) in Tn*916* (current view). Regulation of *tet*(M) resistance gene in Tn*916* involved the short open reading frame, *orf12* and is associated with several external factors that determine whether the expression of Tet(M) is upregulated or

downregulated. Malfunctioned caused to the biological systems of bacteria due to the presence of tetracycline or biocides, as well as when the cell is under stress condition leads to the slower growth and decrease in protein synthesis. As this happened the amount of charged tRNA in the system increases enabling a more rapid translation of *orf12* by the Tet(M)-protected ribosomes. The ribosomes are predicted to catch up the transcribing RNA polymerase and prevent the formation, or destroy the terminator structures. At this stage, the transcription of *tet*(M) is predicted to be approximately 100%. High level of protein translation leads to low level of charged tRNA in the system. Limited amount of charged tRNA eventually decreases the translation rate, and cause terminator structures to form. In contrast, when the amounts of nutrients in the cells are abundant, the bacteria grow faster and lead to high protein synthesis. This will lead to the shortage of tRNA molecules in the cells concurrently decreases the translation rate. As this happened, the ribosomes lags behind the extending RNA polymerase allowing the terminators to form. At this stage, the transcription of *tet*(M) is predicted to be approximately 30% [large and small terminators reduce transcription by up to 47% (± 18%) and 23% (± 15%), respectively. When all of the ribosomes are protected by Tet(M), the expression level will return to the basal level, which is growth-dependent.

The ability of mobile genetic elements to evacuate the dying host under stress condition has been highlighted in a number of studies including the SXT integrative conjugative element (Beaber *et al*., 2004) and the temperate phages (Penades *et al*., 2005). SXT, which is derived from *Vibrio cholerae* O139, encodes genes that confer resistance to chloramphenicol, sulphamethoxazole, trimethoprim and streptomycin (Waldor *et al*., 1996). This element responds to a variety of stress conditions i.e. environmental factors and antibiotics by upregulating the the expression of genes necessary for SXT transfer (Beaber *et al*., 2004). The temperate phages respond to stress condition by entering the lytic pathway that causes the host cell to lyse. Under this condition, the phage-encoded repressor protein that

controls the lytic pathway is repressed, thus inducing the prophage and lead to the production of new virions and lysis of the host cell (Madigan *et al*., 2000).

In Chapter 5, the efficiency of the terminators located in the regulatory region of Tn*916* was investigated using reporter constructs and using an algorithm designed to predict terminator efficiency in *E. coli*. In both analysis it was seen that the large terminator is more efficient (47% experimentally vs. 58% predicted by the algorithm) than the small terminator (23% experimentally vs. 28% predicted by the algorithm). This is the first time the efficiency has been reported for these terminators and again, supports the hypothesis. Prediction of the termination efficiency for the large Tn*5397* terminator could not be done as it does not fulfill one of the required parameters. This is due to the presence of an A residue between the stretch of T's and the base of the stem loop. This may in fact explain why no response was seen to tetracycline in the above experiments with tetracycline. The small terminator in Tn*5397* is identical to that in Tn*916*. Therefore, future work on this subject should focus on constructing the large terminator reporter plasmid of Tn*5397* so that the efficiency of this terminator can be determined experimentally. This could not be completed in the time available for this study.

Finally, the first reciprocal genetic transfer between *E. faecalis* and *C. difficile* was demonstrated in this study. Tn*5397* has been shown to integrate into the genome of *E. faecalis* at a preferred site, flanked by 5' GA dinucleotides as previously

suggested by Wang *et al*. (2006). The acquisition of this element has caused a small fitness burden to *E. faecalis* as determined by comparative growth curve. Competitive studies are required to determine the fitness effect relative to the recipient strain.

As conjugative transposons such as Tn*916* and Tn*5397* are responsible for the spread of antibiotic resistance genes, the continued research on the molecular basis of regulation of these conjugative transposons is essential, as it will provide an insight into the event, or events, that lead to the dissemination of the antibiotic resistance genes. If we fully understand the regulatory mechanism, then we may be able to come up with strategies, such as drug design, to control the spread.

References

Abbani, M., Iwahara, M. and Clubb, R. T. (2005) The structure of the excisionase (xis) protein from the conjugative transposon Tn*916* provides insights into the regulation of heterobivalent tyrosine recombinases. *Journal of Molecular Biology*, 347, 11-25.

Agersø, Y., Pedersen, A. G. and Aarestrup, F. M. (2006) Identification of Tn*5397*-like and Tn*916*-like transposons and diversity of the tetracycline resistance gene *tet*(M) in enterococci from humans, pigs and poultry. *Antimicrobial Agents and Chemotherapy*, 57, 832-839.

Alanis, A. J. (2005) Resistance to antibiotics: are we in the post-antibiotic era? *Archives of Medical Research*, 36, 697–705.

Ammor, M. S., Florez, A. B., van Hoek, A. H., de Los Reyes-Gavilan, C. G., Aarts, H. J., Margolles, A. and Mayo, B. (2008) Molecular characterization of intrinsic and acquired antibiotic resistance in lactic acid bacteria and bifidobacteria. *Journal of Molecular Microbiology and Biotechnology*, 14, 6-15.

Amyes, S. G. B. (2007) Enterococci and Streptococci. *International Journal of Antimicrobial Agents*, 29(3), 43-52.

Arsene, F., Tomoyasu, T. and Bukau, B. (2000) The heat shock response of *Escherichia coli*. *International Journal of Food Microbiology*, 55, 3-9.

Arthur, M., Reynolds, P. and Courvalin, P. (1996) Glycopeptide resistance in enterococci. *Trends in Microbiology*, 4, 401–407.

Ayoubi, P., Kilic, A. O. and Vijayakumar, M. N. (1991) Tn*5253*, the pneumococcal omega (cat tet) BM6001 element, is a composite structure of two conjugative transposons, Tn*5251* and Tn*5252*. *Journal of Bacteriology*, 173, 1617-1622.

Baines, S. D., O'Connor, R., Saxton, K., Freeman, J. and Wilcox, M. H. (2009) Activity of vancomycin against epidemic *Clostridium difficile* strains in a human gut model. *Journal of Antimicrobial Chemotherapy*, 663, 520-525.

Bannam, T. L., Crellin, P. K. and Rood, J. I. (1995) Molecular genetics of the chloramphenicol-resistance transposon Tn*4451* from *Clostridium perfringens*: the TnpX site-specific recombinases excises a circular transposon molecule. *Molecular Microbiology*, 16, 535-551.

Barbut, F., Mastrantonio, P., Delmee, M., Brazier, J., Kuijper, E. and Poxton, I. (2007) Prospective study of *Clostridium difficile* infections in Europe with phenotypic and genotypic characterisation of the isolates. *Clinical Microbiology and Infection* 13, 1048–1057.

Barile, S., Devirgiliis, C. and Perozzi, G. (2012) Molecular characterization of a novel mosaic *tet*(S/M) gene encoding tetracycline resistance in foodborne strains of *Streptococcus bovis*. *Microbiology*, 158, 2353–2362.

Beaber, J. W., Hochhut, B. and Waldor, M. K. (2003) SOS response promotes horizontal dissemination of antibiotic resistance genes. *Nature*, 427, 72-74.

Bedzyk, L. A., Shoemaker, N. B., Young, K. E. and Salyers, A. A. (1992) Insertion and excision of *Bacteroides* conjugative chromosomal elements. *Journal of Bacteriology*, 174, 166-172.

Belfort, M. and Perlman, P. S. (1995) Mechanims of intron mobility. *The Journal of Biological Chemistry*, 270(51), 30237-30240.

Belitsky, B. R., Janssen, P. J. and Sonenshein, A. L. (1995) Sites required for GltC-dependent regulation of *Bacillus subtilis* glutamate synthase expression. *Journal of Bacteriology*, 177(19), 5686-5695.

Bensoussan, R., Weiss, K. and Laverdiere, M. (1998) Vancomycin-resistant *Enterococcus*. *Scandinavian Journal of Gastroenterology*, 33(12), 1233-1238.

Bonten, M. J. M., Willems, R. and Weinstein, R. A. (2001) Vancomycin-resistant enterococci: why are they here, and where do they come from? *Infectious Diseases*, 1, 314-325.

Borukhov, S. and Nudler, E. (2008) RNA polymerase: the vehicle of transcription. *Trends in Microbiology*, 16(3), 126-134.

Breathnach, A. S. (2009) Nosocomial infections. *Medicine*, 37(10), 557-561.

Brochet, M., Da Cunha, V., Couvé, E., Rusniok, C., Trieu-Cuot, P. and Glaser, P. (2009) Atypical association of DDE transposition with conjugation specifies a new family of mobile elements. *Molecular Microbiology,* 71(4), 948–959.

Brouwer, M. S. M., Mullany, P. and Roberts, A. P. (2010) Characterization of the conjugative transposon Tn*6000* from *Enterococcus casseliflavus* 664.1H1 (formerly *Enterococcus faecium* 664.1H1). *FEMS Microbiology Letters*, 309, 71-76.

Brouwer, M. S. M., Warburton, P. J., Roberts, A. P., Mullany, P. and Allan, E. (2011) Genetic organisation, mobility and predicted functions of genes on integrated, mobile genetic elements in sequenced strains of *Clostridium difficile*. *PLOS One*, 6(8), 1-13.

Browning, D. S. and Busby, J. W. (2004) The regulation of bacterial transcription initiation. *Nature Reviews Microbiology*, 2, 1-9.

Burdett, V. (1986) Streptococcal tetracycline resistance mediated at the level of protein synthesis. *Journal of Bacteriology*, 165, 564-569.

Burdett, V. (1990) Nucleotide sequence of the *tet*(M) gene of Tn*916*. *Nucleic Acids Research*, 18, 6137.

Busby, S. J. W. and Savery, N. J. (2007) Encyclopedia of Life Sciences. In: *Transcription activation at bacterial promoters*. John Wiley & Sons, Ltd, pp. 1-9.

Buu-Hoi, A. and Horodniceanu, T. (1980) Conjugative transfer of multiple antibiotic resistance markers of *Streptococcus pneumoniae*. *Journal of Bacteriol*ogy, 143, 313-320.

Caparon, M. G. and Scott, J. R. (1989) Excision and insertion of the conjugative transposon Tn*916* involves a novel recombination mechanism. *Cell*, 59, 1027-1034.

Cartman, S. T., Heap, J. T., Kuehne, S. A., Cockayne, A. and Minton, N. P. (2010) The emergence of 'hypervirulance' in *Clostridium difficile*. *International Journal of Medical Microbiology*, 300, 387-395.

Celli, J. and Trieu-Cuot, P. (1998) Circularisation of Tn*916* is required for expression of the transposon-encoded transfer functions: characterisation of long tetracycline-inducible transcripts reading through the attachment site. *Molecular Microbiology,* 28, 103-117.

Chandler, J. R., and Dunny, G. M. (2004) Enterococcal peptide sex pheromones: synthesis and control of biological activity. *Peptides*, 25, 1377–1388.

Cheng, S-W. C., Lynch, E. C., Leason, K. R., Court, D. L., Shapiro, B. A. and Friedman, D. I. (1991) Functional importance of sequence in the stem-loop of a transcription terminator. *Science*, 254(5035), 1205-1207.

Christie, P. J., Korman, R. Z., Zahler, S. A., Adsit, J. C. and Dunny, G. M. (1987) Two conjugation systems associated with *Streptococcus faecalis* plasmid pCF10: identification of a conjugative transposon that transfers between *S. faecalis* and *B. subtilis*. *Journal of Bacteriology*, 169(6), 2529-2536.

Ciric, L., Jasni, A., de Vries, L. E., Agersø, Y., Mullany, P. and Roberts, A. P. (2011) The Tn*916*/Tn*1545* family of conjugative transposons. In: Roberts, A. P. and Mullany, P. *Bacterial Integrative Mobile Elements*. London: Landes Bioscience. pp. 1-17.

Ciric, L., Mullany, P. and Roberts, A. P. (2011) Antibiotic and antiseptic resistance genes are linked on a novel mobile genetic element: Tn*6087*. *Journal of Antimicrobial Chemotherapy*, In press.

Clewell, D. B., Flannagan, S. E. and Jaworski, D. D. (1995) Unconstrained bacterial promiscuity: the Tn*916*-Tn*1545* family of conjugative transposons. *Trends in Microbiology*, 3(6), 229-236.

Clewell, D. B. and Gawron-Burke, C. (1986) Conjugative transposons and the dissemination of antibiotic resistance. *Annual Review of Microbiology*, 40, 635-659.

Clewell, D. B and Weaver, K. E. (1989) Sex pheromones and plasmid transfer in *Enterococcus faecalis*. *Plasmid*, 21, 175-184.

Cochetti, I., Tili, E., Mingoia, M. and Varaldo, P. E. and Montanari, M. P. (2008) *erm*(B)-carrying elements in tetracycline-resistant pneumococci and correspondence between Tn*1545* and Tn*6003*. *Antimicrobial Agents and Chemotherapy*, 52(4), 1285-1290.

Connell, S. R., Tracz, D. M., Nierhaus, K. H. and Taylor, D. E. (2003) Ribosomal protection proteins and their mechanism of tetracycline resistance. *Antimicrobial Agents and Chemotherapy*, 47, 3675-3681.

Cookson, A. L., Noel, S., Hussein, H., Perry, R., Sang, C., Moon, C. D., Leahy, S. C., Altermann, E., Kelly, W. J. and Attwood, G. T. (2011) Transposition of Tn*916* in the four replicons of the *Butyrivibrio proteoclasticus* B316^{T} genome. *Research Letter*, 316, 144-151.

Cornely, O. A., Crook, D. W., Esposito, R., Poirier, A., Somero, M. S., Weiss, K., Sears, P. and Gorbach, S. (2012) Fidaxomicin versus vancomycin for infection with *Clostridium difficile* in Europe, Canada, and the USA: a double-blind, non-inferiority, randomised controlled trial. *The Lancet Infectious Diseases*, 12(4), 281-289.

Courvalin, P. and Carlier, C. (1986) Transposable multiple antibiotic resistance in *Streptococcus pneumoniae*. *Molecular and General Genetics*, 205, 291-297.

Crick, F. H. C., Barnett, L., Brenner, S. and Watts-Tobin, R. J. (1961) General nature of the genetic code for proteins. *Nature*, 192, 1227-1232.

d' Aubenton Carafa, F., Brody, E. and Thermes, C. (1990) Prediction of rho-independent *Escherichia coli* transcription terminators. A statistical analysis of their RNA stem-loop structures. *Journal of Molecular Biology*, 216, 835-858.

Dale, J. W. and Park., S. F. (2010) *Molecular genetics of bacteria*. 5th ed. John Wiley & Sons, Ltd.

Dann, C. E., Wakeman, C. A., Sieling, C. L., Baker, S. C., Imov, I. and Winkler, W. C. (2007) Structure and mechanism of a metal-sensing regulatory RNA. *Cell*, 7(130), 878-892.

Del Grosso, M., Camilli, R., Iannelli, F., Pozzi, G. and Pantosti, A. (2006) The *mef*(E)-carrying genetic element (mega) of *Streptococcus pneumoniae*: insertion sites and association with other genetic elements. *Antimicrobial Agents and Chemotherapy*, 50(10), 3361-3366.

Del Grosso, M., Camilli, R., Libisch, B., Füzi, M. and Pantosti, A. (2009) New composite genetic element of the Tn*916* family with dual macrolide resistance genes in a *Streptococcus pneumoniae* isolate belonging to clonal Complex 271. *Antimicrobial Agents and Chemotherapy*, 53, 1293-1294.

Del Grosso, M., d' Abusco, A. S., Iannelli, F., Pozzi, G. and Pantosti, A. (2004) Tn*2009*, a Tn*916*-like element containing *mef*(E) in *Streptococcus pneumoniae*. *Antimicrobial Agents and Chemotherapy*, 48(6), 2037-2042.

Dombroski, A. J., Walter, W. A., Record Jr, M. T., Siegele, D. A. and Gross, C. A. (1992) Polypeptides containing highly conserved regions of transcription initiation factor sigma 70 exhibit specificity of binding to promoter DNA. *Cell*, 70(3), 503-512.

Domingues, S., Harms, K., Fricke, W. F., Johnsen, P. J., da Silva, G. J. and Nielsen, K. J. (2012) Natural transformation facilitates transfer of transposons, integrons and gene cassettes between bacterial species. *PLOS Pathogens*, 8(8): e1002837.

Donskey, C. J., Ray, A. J., Hoyen, C. K., Fuldauer, P. D., Aron, D. C., Bonomo, R. A. (2003) Cocolonization and infection with multiple nosocomial pathogens in patients colonized with vancomycin-resistant enterococci. *Infection Control and Hospital Epidemiology*, 24, 242-245.

Doucet-Populaire, F., Trieu-Cout, P., Dosbaa, I., Andremont, A. and Courvalin, P. (1991) Inducible transfer of conjugative transposon Tn*1545* from *Enterococcus faecalis* to *Listeria monocytogenes* in the digestive tracts of gnotobiotic mice. *Antimicrobial Agents and Chemotherapy*, 35, 185-187.

Du, H. and Babitzke, P. (1998) *trp* RNA-binding attenuation protein-mediated long distance RNA refolding regulates translation of *trpE* in *Bacillus subtilis*. *The Journal of Biological Chemistry*, 273(7), 20494-20503.

Eckstein, B. C., Adam, D. A., Eckstein, E. C., Rao, A., Sethi, A. K., Yadavalli, G. K. and Donskey, C. J. (2006) Reduction of *Clostridium difficile* and vancomycin-resistant *Enterococcus* contamination of environmental surfaces after an intervention to improve cleaning methods. *BMC Infectious Diseases*, 7(61), 1-6.

Elena, S. F., Ekunwe, L., Hajela, N., Oden, S. A. and Lenski, R. E. (1998) Distribution of fitness effects caused by random insertion mutations in *Escherichia coli*. *Genetica*, 102/103, 349-358.

Elkins, C., Thomas, C. E., Seifert, H. S. and Sparling, P. F. (1991) Species-specific uptake of DNA by gonococci is mediated by a 10-base-pair sequence. *Journal of Bacteriology*, 173(12), 3911-3913.

Emerson, J. E., Reynolds, C. B., Fagan, R. P., Shaw, H. A., Goulding, D. and Fairweather, N. F. (2009) A novel genetic switch controls phase variable expression of CwpV, a *Clostridium difficile* cell wall protein. *Molecular Microbiology*, doi: 10.1111/j.1365-2958.2009.06812.x.

Emori, T. G. and Gaynes, R. P. (1993) An overview of nosocomial infections, including the role of the microbiology laboratory. *Clinical Microbiology Reviews*, 6(4), 428-442.

Enne, V. I., Delsol, A. A., Davis, G. R., Hayward, S. L., Roe, J. M. and Bennet, P. M. (2005) Assessment of the fitness impacts on *Escherichia coli* of acquisition of antibiotic resistance genes encoded by different types of genetic element. *Journal of Antimicrobial Chemotherapy*, 56(3), 544-551.

Ermolaeva, M. D., Khalak, H. G., White, O., Smith, H. O. and Salzberg, S. L. (2000) Prediction of transcription terminators in bacterial genomes. *Journal of Molecular Biology*, 301(1), 27-33.

Estrem, S. T., Gaal, T., Ross, W. and Gourse, R. L. (1998) Identification of an UP element consensus sequences for bacterial promoters. *Proceedings of the National Academy of Sciences*, 95, 9761-9766.

Farnham, P. J. and Platt, T. (1980) A model for transcription termination suggested by studies on the *trp* attenuator in vitro using base analogs. *Cell*, 20, 739-748.

Fineran, P. C., Petty, N. K. and Salmond, G. P. C. (2009) Transduction: host DNA transfer by bacteriophages. In: M. Schaechter, ed. *Encyclopedia of microbiology*. Oxford: Elsevier, pp. 666-679.

Flannagan, S. E., Zitzow, L. A., Su, Y. A. and Clewell, D. B. (1994) Nucleotide sequence of the 18 kb conjugative transposon Tn*916* from *Enterococcus faecalis. Plasmid*, 32**,** 350-354.

Foucault, M-L., Depardieu, F., Courvalin, P. and Grillot-Courvalin, C. (2010) Inducible expression eliminates the fitness cost of vancomycin resistance in enterococci. *Antimicrobial Agents and Chemotherapy,* 107(39), 16964–16969.

Franke, A. E. and Clewell, D. (1981) Evidence for a chromosome-borne resistance transposon (Tn*916*) in *Streptococcus faecalis* that is capable of conjugative transfer in the absence of a conjugative plasmid. *Journal of Bacteriol*ogy, 145, 494-502.

Frost, L. S., Leplae, R., Summers, A. O. and Toussaint, A. (2005) Mobile genetic elements: the agents of open source evolution. *Nature Reviews Microbiology*, 3, 722-732.

Golliger, J. A., Yang, X., Guo, H. and Roberts, J. W. (1989) Early transcribed sequences affect termination efficiency of *Escherichia coli* RNA polymerase. *Journal of Molecular Biology*, 205, 331-341.

Gollnick, P. and Babitzke, P. (2002) Transcription attenuation. *Biochimica et Biophysica Acta*, 1577, 240-250.

Gralla, J. and Crothers, D. M. (1973) Free energy of imperfect nucleic acid helices: II. Small hairpin loops. *Journal of Molecular Biology*, 73, 497-506.

Greenblatt, J. F. (2008) Transcription termination: pulling out all the stops. *Cell*, 132, 917-918.

Griffith, F. (1928) The significance of pneumococcal types. *Journal of Hygiene*, 27, 113-159.

Groebe, D. and Uhlenbeck, O. (1988) Characterization of RNA hairpin loop stability. *Nucleic Acids Research*, 16, 11725-11735.

Grohmann, E., Muth, G. and Espinosa, M. (2003) Conjugative plasmid transfer in Gram-positive bacteria. *Microbiology and Molecular Biology Reviews*, 67(2), 277-301.

Gruber, T. and Gross, C. (2003) Multiple sigma subunits and the partitioning of bacterial transcription space. *Annual Review of Microbiology*, 57, 441-466.

Gryczan, T. J., Grandi, G., Hahn, J., Grandi, R. and Dubnau, D. (1980) Conformational alteration of mRNA structure and the posttranscriptional regulation of erythromycin-induced drug resistance. *Nucleic Acids Research*, 8(24), 6081-6097.

Guérin, M., Robichon, N., Geiselmann, J. and Rahmouni, A. R**.** (1998) A simple polypyrimidine repeat acts as an artificial Rho-dependent terminator in vivo and in vitro. *Nucleic Acids Research*, 26*,* 4895-4900.

Gutiérrez-Preciado, A., Henkin, T. M., Grundy, F. J., Yanofsky, C. and Merino, E. (2009) Biochemical features and functional implications of the RNA-based T-box regulatory mechanism. *Microbiology and Molecular Biology Reviews*, 73(1), 36-61.

Hachler, H., Berger-Bachi, B. and Kayser, F. H. (1987) Genetic characterization of a *Clostridium difficile* erythromycin-clindamycin resistance determinant that is transferable to *Staphylococcus aureus*. *Antimicrobial Agents and Chemotherapy*, 31, 1039-1045.

Hadley, C. (2004) Overcoming resistance. *EMBO Reports*, 5(6), 550-552.

Hannan, S., Ready, D., Jasni, A. S., Rogers, M., Pratten, J. and Roberts, A. P. (2010) Transfer of antibiotic resistance by transformation with eDNA within oral biofilms. *FEMS Immunology and Medical Microbiology*, 59, 345-349.

Hardy, K. G. (1985) *Bacillus* cloning methods. In: D. M. Glover, ed. *DNA cloning: a practical approach*. Washington DC: IRL Press, vol 2, pp. 1-17.

Harley, C. B. and Reynolds, R. P. (1987) Analysis of *E. coli* promoter sequences. *Nucleic Acids Research*, 15(5), 2343-2361.

Hawley, D. K. and McClure, W. R. (1983) Compilation and analysis of *Escherichia coli* promoter DNA sequences. *Nucleic Acids Research*, 11, 2237-2255.

Hecker, M., and Volker, U. (2001) General stress response of *Bacillus subtilis* and other bacteria. *Advances in Microbial Physiology*, 44, 35-91.

Heinemann, J. A., Ankenbauer, R. G. and Amábile-Cuevas, C. F. (2000) Do antibiotics maintain antibiotic resistance? *Drug Discovery Today*, 5(5), 195-204.

Helmer, G., Casadaban, M., Bevan, M., Kayes, L. and Chilton, M-D. (1984) A new chimeric gene as a marker for plant transformation: the expression of *Escherichia coli* β-galactosidase in sunflower and tobacco cells*. Nature Biotechnology, 2, 520-527.*

Hendrix, R. W. (2002). Bacteriophage λ and its relatives. In: U. N. Streips, and R. E. Yasbin, ed. *Modern microbial genetics*. Wiley-Liss, Inc. Ch.5.

Henkin, T. M. and Yanofsky, C. (2002) Regulation by transcription attenuation in bacteria: how RNA provides instructions for transcription termination/antitermination decisions. *BioEssays*, 24, 700-707.

Hess, G. F. and Graham, R. S. (1990) Efficiency of transcriptional terminators in *Bacillus subtilis*. *Gene*, 95(1), 137-141.

Hippel, P. H. and Yager, T. D. (1991) Transcript elongation and termination are competitive kinetic processes. *Proceedings of the National Academy of Sciences*, 88, 2307-2311.

Hirt, H., Schlievert, P. M. and Dunny, G. M. (2002) In vivo induction of virulence and antibiotic resistance transfer in *Enterococcus faecalis* mediated by the sex pheromone-sensing system of pCF10. *Infection and Immunity*, 70(2), 716–723.

Hochhut, B., Jahreis, K., Lengeler, J. W. and Schmid, K. (1997) CTn*scr94*, a conjugative transposon found in Enterobacteria. *Journal of Bacteriology*, 179(7), 2097-2102.

Horn, N. S., Swindell, H., Dodd, H. and Gasson, M. (1991) Nisin biosynthesis genes are encoded by a novel conjugative transposon. *Molecular and General Genetics*, 228, 129-135.

Horodniceanu, T., Bougueleret, L. and Bieth, G. (1981) Conjugative transfer of multiple-antibiotic resistance markers in beta-hemolytic group A, B, F and G Streptococci in the absence of extrachromosomal deoxyribonucleic acid. *Plasmid*, 5, 127-137.

Hsueh, P. R., Liu, C. Y. and Luh, K. T. (2002) Current status of antimicrobial resistance in Taiwan. *Emerging Infectious Diseases*, 8, 132-137.

Huang, H., Weintraub, A., Fang, H. and Nord, C. E. (2009) Antimicrobial resistance in *Clostridium difficile*. *International Journal of Antimicrobial Agents*, 34, 516-522.

Hussain, H., Roberts, A. P. and Mullany, P. (2005) Generation of an erythromycin-sensitive derivative of *Clostridium difficile* strain 630 (630Δ*erm*) and demonstration that the conjugative transposon Tn*916*ΔE enters the genome of this strain at multiple sites. *Journal of Medical Microbiology*, 54, 137-141.

Jacob, A. E. and Hobbs, S. J. (1974) Conjugal transfer of plasmid-borne multiple antibiotic resistance in *Streptococcus faecalis* var. zymogenes. *Journal of Bacteriology*, 117(2), 360-372.

Jamieson, C. (2008) Healthcare-associated infection-hospital acquired infection. *Hospital Pharmacist*, 15, 7-12.

Jaworski, D. D. and Clewell, D. B. (1995) A functional origin of transfer (*oriT*) on the conjugative transposon Tn*916*. *Journal of Bacteriology*, 177, 6644-6651.

Jaworski, D. D., Flannagan S. E. and Clewell, D. B. (1996) Analyses of traA, int-Tn and xis-Tn mutations in the conjugative transposon Tn*916* in *Enterococcus faecalis*. *Plasmid*, 36, 201-208.

Jefferson, R. A., Kavanagh, T. A. and Bevan, M. W. (1987) GUS fusion: β-glucuronidase as a sensitive and versatile gene fusion marker in higher plants. *The EMBO Journal*, 6(13), 3901-3907.

Jeng, S. T., Lay, S. H., and Lai, H. M. (1997) Transcription termination by bacteriophage T3 and 5P6 RNA polymerases at Rho-independent terminators. *Canadian Journal of Microbiology*, 43, 1147-1156.

Jeon, B., Muraoka, W., Sahin, O. and Zhang, Q. (2008) Role of Cj1211 in natural transformation and transfer of antibiotic resistance determinants in *Campylobacter jejuni*. *Antimicrobial Agents and Chemotherapy*, 52(8), 2699-2708.

Kim, J-S., Carver, D. K. and Kathariou, S. (2006) Natural transformation-mediated transfer of erythromycin resistance in *Campylobacter coli* strains from turkeys and swine. *Applied and Environmental Microbiology*, 72(2), 1316–1321.

Kirst, H. A., Thompson, D. G. and Nicas, T. I. (1998) Historical yearly usage of vancomycin. *Antimicrobial Agents and Chemotherapy*, 42(5), 1303-1304.

Kortmann, J. and Narberhaus, F. (2012) Bacterial RNA thermometers: molecular zippers and switches. *Nature Reviews Microbiology*, 10, 255-265.

Krebs, J. E., Goldstein, E. S. and Kilpatrick, S. T. (2010) *Lewin's Essential GENES*. 2nd ed. Jones and Bartlett Publishers.

Landy, A. (1989) Dynamic, structural and regulatory aspects of lambda site-specific recombination. *Annual Review of Biochemistry*, 58, 913-949.

Launay, A., Ballard, S. A., Johnson, P. D. R., Grayson, M. L. and Lambert, T. (2006) Transfer of vancomycin resistance transposon Tn*1549* from *Clostridium symbiosum* to *Enterococcus* spp. in the gut of gnotobiotic mice. *Antimicrobial Agents and Chemotherapy*, 50(3), 1054-1062.

Lawley, T. D., Klimke, W. A., Gubbins, M. J. and Frost, L. S. (2003) F factor conjugation is a true type IV secretion system. *FEMS Microbiology Letters*, 224, 1-15.

Le Bouguènec, C., de Cespedes, G. and Horaud, T. (1988) Molecular analysis of a composite chromosomal conjugative element (Tn*3701*) of *Streptococcus pyogenes*. *Journal of Bacteriology*, 170, 3930-3936.

Leffler, D. A. and Lamont, J. T. (2009) Treatment of *Clostridium difficile*-associated disease. *Gastroenterology*, 136, 1899-1912.

Lenski, R. E., Rose, M. R., Simpson, S. C. and Tadler, S. C. (1991) Long-term experimental evolution in *Escherichia coli*. I. Adaptation and divergence during 2,000 generations. *The American Naturalist*, 138(6), 1315-1341.

Liang, S., Bipatnath, M., Xu, Y., Chen, S., Dennis, P., Ehrenberg, M. and Bremer, H. (1999) Activities of constitutive promoters in *Escherichia coli*. *Journal of Molecular Biology*, 292(1), 19-37.

Liu, X. and Matsumura, P. (1995) An alternative sigma factor controls transcription of flagellar class-III operons in *Escherichia coli*: gene sequence, overproduction, purification and characterization. *Gene*, 164(1), 81-84.

Lovett, P. S. (1990) Translation attenuation regulation of chloramphenicol resistance in bacteria-a review. *Gene*, 179, 157-162.

Lu, F. and Churchward, G. (1995) Tn*916* target DNA sequences bind the C-terminal domain of integrase protein with different affinities that correlate with transposon insertion frequency. *Journal of Bacteriology*, 177, 1938-1946.

Lynn, S. P., Kasper, L. M. and Gardner, J. F. (1988) Contributions of RNA secondary structure and length of the thymidine tract to transcription termination at the *thr* operon attenuator. *Journal of Biochemistry*, 263(1), 472-479.

Lyubetskaya, E. V., Leont'ev, L. A., Gelfand, M. S. and Lyubetsky, V. A. (2003) Search for alternative RNA secondary structures regulating expression of bacterial genes. *Molecular Biology*, 37, 707-716.

Madigan, M. T., Martinko, J. M. and Parker, J. (2000) *Brock Biology of Microorganisms*. 9th ed. Prentice Hall International Inc.

Majumdar, S. S. and Padiglione, A. A. (2012) Nosocomial infections in the intensive care unit. *Anaesthesia and Intensive Care Medicine*, 13(5), 204-208.

Mandal, M. and Breaker, R. R. (2004) Gene regulation by riboswitches. *Nature Reviews Molecular Cell Biology*, 5, 451-463.

Mandel, M. and Higa, A. (1970) Calcium-dependent bacteriophage DNA infection. *Journal of Molecular Biology*, 53, 159-162.

Manganelli, R., Ricci, S. and Pozzi, G. (1996) Conjugative transposon Tn*916*: evidence for excision with formation of 5'-protruding termini. *Journal of Bacteriology*, 178, 5813-5816.

Manganelli, R., Ricci, S. and Pozzi, G. (1997) The joint of Tn*916* circular intermediates is a homoduplex in *Enterococcus faecalis*. *Plasmid*, 38, 48-57.

Marra, D. and Scott, J. R. (1999) Regulation of excision of the conjugative transposon Tn*916*. *Molecular Microbiology*, 31(2), 609-621.

Martin, F. H. and Tinoco Jr., I. (1980) DNA-RNA hybrid duplexes containing oligo (dA:rU) sequences are exceptionally unstable and may facilitate termination of transcription. *Nucleic Acids Research*, 8(10), 2295-2299.

McDonnell, G. and Russel, A. D. (1999) Antiseptics and disinfectants: activity, action and resistance. *Clinical Microbiology Reviews*, 12(1), 147-179.

McDougal, L. K., Tenover, F. C., Lee, L. N., Rasheed, J. K., Patterson, J. E., Jorgensen, J. H. and LeBlanc, D. J. (1998) Detection of Tn*917*-like sequences within a Tn*916*-like conjugative transposon (Tn*3872*) in erythromycin-resistant isolates of *Streptococcus pneumoniae*. *Antimicrobial Agents and Chemotherapy*, 42(9), 2312-2318.

Melville, S. B., Labbe, R. and Sonensheini, A. L. (2005) Expression from the *Clostridium perfringens cpe* promoter in *C. perfringens* and *Bacillus subtilis*. *Infection and Immunity*, 62(12), 5550-5558.

Merino, E. and Yanofsky, C. (2005) Transcription attenuation: a highly conserved regulatory strategy used by bacteria. *Trends in Genetics*, 21, 260-264.

Merlin, C. D., Springael, D. and Toussaint, A. (1999) Tn*4371*: a modular structure encoding a phage-like integrase, a Pseudomonas-like catabolic pathway, and RP4/Ti-like transfer functions. *Plasmid*, 41, 40-54.

Michel, F. and Ferat, J-L. (1995) Structure and activities of group II introns. *Annual Review of Biochemistry*, 64, 435-461.

Miller, J. (1972) Experiments in Molecular Genetics, pp. 352-355. Cold Spring Harbor Laboratory, New York.

Min, Y-H, Kwon, A-R, Yoon, E-J, Shim, M-J and Choi, E-C. (2008) Translational attenuation and mRNA stabilization as mechanism of *erm*(B) induction by erythromycin. *Antimicrobial Agents and Chemotherapy*, 53(5), 1782-1789.

Moffat, J. G., Tate, W. P. and Lovett, P. S. The leader peptides of attenuation-regulated chloramphenicol resistance genes inhibit translational termination. *Journal of Bacteriology*, 176(22), 7115-7117.

Morse, M. L., Lederberg, E. M. and Lederberg, J. (1956) Transduction in *Escherichia coli* K-12. *Genetics*, 41, 142-156.

Mukhopadhyay, J., Kapanidis, A. N., Mekler, V., Kortkhonjia, E., Ebright, Y. W., Ebright, R. H. (2001) Translocation of σ^{70} with RNA polymerase during transcription: fluorescence resonance energy transfer assay for movement relative to DNA. *Cell*, 106, 453-463.

Mullany, P., Pallen, M., Wilks, M., Stephen, J. R. and Tabaqchali, S. (1996) A group II intron in a conjugative transposon from the Gram-positive bacterium, *Clostridium difficile*. *Gene*, 174, 145-150.

Mullany, P., Wilks, M., Lamb, I., Clayton, C., Wren, B. and Tabaqchali, S. (1990) Genetic analysis of a tetracycline resistance element from *Clostridium difficile* and its conjugal transfer to and from *Bacillus subtilis*. *Journal of General Microbiology*, 136, 1343-1349.

Mullany, P., Williams, R., Langridge, G. C., Turner, D. J., Whalan, R., Clayton, C., Lawley, T., Hussain, H., McCurrie, K., Morden, N., Allan, E. and Roberts, A. P. (2012) Behaviour and target site selection of the conjugative transposon Tn*916* in two different strains of toxigenic *Clostridium difficile*. *Applied Environmental Microbiology*, doi:10.1128/AEM.06193-11.

Mundy, L. M., Sahm, D. F. and Gilmore, M. (2000) Relationships between enterococcal virulence and antimicrobial resistance. *Clinical Microbiology Reviews*, 13(4), 513-522.

Murphy, D. B. and Pembroke, J. T. (1995) Transfer of the IncJ plasmid R391 to recombination deficient *Escherichia coli* K12: evidence that R391 behaves as a conjugal transposon. *FEMS Microbiology Letters*, 134, 153-158.

Narberhaus, F., Waldminghaus, T. and Chowdhury, S. (2005) RNA thermometers. *FEMS Microbiology Reviews*, 30, 3-16.

Naville, M. and Gautheret, D. (2009) Transcription attenuation in bacteria: theme and variations. *Briefings in Functional Genomics and Proteomics*, 8(6), 482-492.

Nelson, K. E., Richardson, D. L. and Dougherty, B. A. (1997) Tn*916* transposition in *Haemophilus influenza* Rd: preferential insertion into noncoding DNA. *Microbial and Comparative Genomics*, 2, 313–21.

Nesin, M., Svec, P., Lupski, J. R., Godson, G. N., Kreiswirth, B., Kornblum, J. and Projan, S. J. (1990) Cloning and nucleotide sequence of a chromosomally encoded tetracycline resistance determinant, *tetA*(M), from a pathogenic, methicillin-resistant strain of *Staphylococcus aureus*. *Antimicrobial Agents and Chemotherapy*, 34, 2273–2276.

Nikolich, M. P., Shoemaker, N. B., Wang, G. R. and Salyers, A. A. (1994) Characterization of a new type of *Bacteroides* conjugative transposons, Tcr Emr 7853. *Journal of Bacteriology*, 176, 6606-6612.

Novais, C., Freitas, A. R., Silveira, E., Baquero, F., Peixe, L., Roberts, A. P. and Coque, T. M. (2012) A *tet*(S/M) hybrid from CTn*6000* and CTn*916* recombination. *Microbiology Comment*, 157-158.

Novel, M. and Novel, G. (1973) Regulation of beta-glucuronidase synthesis in *Escherichia coli* K-12: pleiotropic constitutive mutations affecting uxu and uidA expression. *Journal of Bacteriology*, 127(1), 418-432.

Ozeki, H. and Ikeda, H. (1968) Transduction mechanisms. *Annual Reviews of Genetics*, 2, 245-278.

Paget, M. S. B. and Helmann, J. D. (2003) The σ^{70} family of sigma factors. *Genome Biology*, 4(1), 1-6.

Palmer, K. L., Kos, V. N. and Gilmore, M. S. (2010) Horizontal gene transfer and the genomics of enterococcal antibiotic resistance. *Current Opinion in Microbiology*, 13, 632-639.

Patterson, A. J., Rincon, M. T., Flint, H. J. and Scott, K. P. (2007) Mosaic tetracycline resistance genes are widespread in human and animal fecal samples. *Antimicrobial Agents and Chemotherapy*, 51, 1115-1118.

Penades, J. R., Ubeda, C., Maiques, E., Knecht, E., Lasa, I. and Novick, R. P. (2005) Antibiotic-induced SOS response promotes horizontal dissemination of pathogenicity island-encoded virulence factors in Staphylococci. *Molecular Microbiology*, 56, 836-844.

Pepin, J. (2008) Vancomycin for the treatment of *Clostridium difficile* infection: for whom is this expensive bullet really magic? *Clinical Infectious Diseases*, 46, 1493-1498.

Pituch, H. (2009) *Clostridium difficile* is no longer just a nosocomial infection or an infection adults. *International Journal of Antimicrobial Agents*, 33(S1), S42-S45.

Platt, T. and Richardson, J. P. (1992) *Escherichia coli* Rho factor: protein and enzyme of transcription termination. In *Transcriptional Regulation,* pp. 365–388. Ed. S. L. McKnight and K. R. Yamamoto. Cold Spring Harbor, New York, Cold Spring Harbor Laboratory.

Poduval, P. D., Kamath, R. P., Corpuz, M., Norkus, M. and Pitchumoni, C. S. (2000) *Clostridium difficile* and vancomycin-resistant enterococcus: the new nosocomial alliance. *The American Journal of Gastroenterology*, 95(12), 3513-5.

Poole, A. M. (2009) Horizontal gene transfer and the earliest stages of the evolution of life. *Research in Microbiology*, 160, 473-480.

Postma, P. W., Lengeler, J. W. and Jacobson, G. R. (1993) Phosphoenolpyruvate: carbohydrate phosphotransferase systems of bacteria. *Microbiological Reviews*, 57(3), 543–594.

Rao, L., Ross, W., Appleman, J. A., Gaal, T., Leirmo, S., Schlax, P. J., Record Jr, M. T. and Gourse, R. L. (1994) Factor independent activation of *rrnB* P1. An “extended” promoter with an upstream element that dramatically increases promoter strength. *Journal of Molecular Biology*, 235, 1421-1435.

Rauch, P. J. and De Vos, W. M. (1992) Characterization of the novel nisin-sucrose conjugative transposon Tn*5276* and its insertion in *Lactococcus lactis*. *Journal of Bacteriology*, 174, 1280-1287.

Regulski, E. E., Moy, R. H., Weinberg, Z., Barrick, J. E., Yao, Z., Ruzzo, W. L. and Breaker, R. R. (2008) A widespread riboswitch candidate that controls bacterial genes involved in molybdenum cofactor and tungsten cofactor metabolism. *Molecular Microbiology*, 68, 918-932.

Rice, L. B. (2006) Antimicrobial resistance in Gram-positive bacteria. *The American Journal of Medicine*, 119(6), 11-19.

Rice, L. B. and Carias, L. L. (1998) Transfer of Tn*5385*, a composite, multiresistance chromosomal element from *Enterococcus faecalis*. *Journal of Bacteriology*, 180, 714-721.

Rice, L. B., Carias, L. L., Marshall, S. H., Hutton-Thomas, R. and Rudin, S. (2007) Characterization of Tn*5386*, a Tn*916*-related mobile element. *Plasmid*, 58(1), 61-67.

Rice, L. B., Carias, L. L., Marshall, S., Rudin, S. D. and Hutton-Thomas, R. (2005) Tn*5386*, a novel Tn*916*-like mobile element in *Enterococcus faecium* D344R that interacts with Tn*916* to yield a large genomic deletion. *Journal of Bacteriology*, 187(19), 6668-6677.

Roberts, A. P. (2001) *Investigation into the molecular genetics of the conjugative transposon Tn*5397. PhD thesis. University of London.

Roberts, A. P., Braun, V., von Eichel-Streiber, C. and Mullany, P. (2000) Demonstration that the group II intron from Clostridial conjugative transposon Tn*5397* undergoes splicing in vivo. *Journal of Bacteriology*, 183(4), 1296-1299.

Roberts, A. P., Cheah, G., Ready, D., Pratten, J., Wilson, M. and Mullany, P. (2001a) Transfer of Tn*916*-like elements in microcosm dental plaques. *Antimicrobial Agents and Chemotherapy*, 45, 2943-2946.

Roberts, A. P., Hennequin, C., Elmore, M., Collignon, A., Karjalainen, T., Minton, N. and Mullany, P. (2003) Development of an integrative vector for the expression of antisense RNA *Clostridium difficile*. *Journal of Microbiological Methods*, 55(3), 617-624.

Roberts, A. P., Johanesen, P. A., Lyras, D., Mullany, P. and Rood, J. I. (2001b) Comparison of Tn*5397* from *Clostridium difficile*, Tn*916* from *Enterococcus faecalis* and CW459*tet*(M) element from *Clostridium perfringens* shows that they have similar conjugation regions but different insertion and excision modules. *Microbiology*, 147, 1243-1251.

Roberts, A. P. and Mullany, M. (2009) A modular master on the move: the Tn*916* family of mobile genetic elements. *Trends in Microbiology*, 17(6), 251-258.

Roberts, A. P., Pratten, J., Wilson, M. and Mullany, P. (1999) Transfer of a conjugative transposon, Tn*5397* in a model oral biofilms. *FEMS Microbiology Letters*, 117, 63-66.

Rocco, J. M. and Churchward, G. (2006) The integrase of the conjugative transposon Tn*916* directs strand- and sequence-specific cleavage of the origin of conjugal transfer, *oriT*, by the endonuclease Orf20. *Journal of Bacteriology*, 188, 2207-2213.

Ross, W., Gosink, K. K., Salomon, J., Igarashi, K., Zou, C., Ishihama, A., Severinov, K. and Gourse, R. L. (1993) A third recognition element in bacterial promoters: DNA binding by the alpha subunit of RNA polymerase. *Science*, 262, 1407-1413.

Rubens, C. E. and Heggen, L. M. (1988) Tn*916*ΔE: a Tn*916* transposon derivative expressing erythromycin resistance. *Plasmid*, 20(2), 137-142.

Rudy, C. K., Scott, J. R. and Churchward, G. (1997) DNA binding by the Xis protein of the conjugative transposon Tn*916*. *Journal of Bacteriology*, 179(8), 2567-2572.

Rudy, C. K., Taylor, L., Hinerfeld, D., Scott, J. R. and Churchward, G. (1997) Excision of a conjugative transposon in vitro by the Int and Xis proteins of Tn*916*. *Nucleic Acids Research*, 25, 4061-4066.

Russell, A. D. and Chopra, I. (1996) *Understanding antibacterial action and resistance*. 2nd ed. Ellis Horwood, Chichester.

Saitoh, T. and Ishihama, A. (1977) Biosynthesis of RNA polymerase in *Escherichia coli*: VI. Distribution of RNA polymerase subunits between nucleoid and cytoplasm. *Journal of Molecular Biology*, 115(3), 403-416.

Salyers, A. A., Shoemaker, N. B., Stevens, A. M. and Li, L-Y. (1995) Conjugative transposons: an unusual and diverse set of integrated gene transfer elements. *Microbiological Reviews*, 59(4), 579-590.

Scott, J. R., Bringel, F., Marra, D., Van Alstine, G. and Rudy, C. K. (1994) Conjugative transposition of Tn*916*: preferred targets and evidence for conjugative transfer of a single strand and for a double-stranded circular intermediate. *Molecular Microbiology*, 11(6), 1099-1108.

Scott, J. R. and Churchward, G. (1995) Conjugative transposition. *Annual Review of Microbiology*, 49, 367-397.

Sebaihia, M., Wren, B. W., Mullany, P., Fairweather, N. F., Minton, N., Stabler, R., Thomson, N. R., Roberts, A. P., Cerdeño-Tárraga, A. M., Wang, H., Holden, M. T. G., Wright, A., Churcher, C., Quail, M. A., Baker, S., Bason, N., Brooks, K., Chillingworth, T., Cronin, A., Davis, P., Dowd, L., Fraser, A., Feltwell, T., Hance, Z., Holroyd, S., Jagels, K., Moule, S., Mungall, K., Price, C., Rabbinowitsch, E., Sharp, S., Simmonds, M., Stevens, K., Unwin, L., Whithead, S., Dupuy, B., Dougan, G., Barrell, B. and Parkhill, J. (2006) The multidrug-resistant human pathogen *Clostridium difficile* has a highly mobile, mosaic genome. *Nature Genetics*, 38(7), 779-786.

Senghas, E., Jones, J. M., Yamamoto, M., Gawron-Burke, C. and Clewell, D. B. (1988) Genetic organization of the bacterial conjugative transposon Tn*916*. *Journal of Bacteriology*, 170, 245-249.

Serfiotis-Mitsa, D., Roberts, G. A., Cooper, L. P., White, J. H., Nutley, N., Cooper, A., Blakely, G. W. and Dryden, D. T. (2008) The *orf18* gene product from conjugative transposon Tn*916* is an ArdA antirestriction protein that inhibits Type I DNA restriction-modification systems. *Journal of Molecular Biology*, 383, 970-981.

Shoemaker, N. B., Barber, R. D. and Salyers, A. A. (1989) Cloning and characterization of a *Bacteroides* conjugal tetracycline-erythromycin resistance element by using a shuttle cosmid vector. *Journal of Bacteriology,* 171, 1294-1302.

Showsh, S. A. and Andrews Jr., R. E. (1992) Tetracycline enhances Tn*916*-mediated conjugal transfer. *Plasmid*, 28(3), 213-224.

Slauch, J. M. and Silhavy, T. J. (1991) Cis-acting *ompF* mutations that result in OmpR-dependent constitutive expression. *Journal of Bacteriology*, 173, 4039–4048.

Smith, M. C. M. and Thorpe, H. M. (2002) Diversity in the serine recombinases. *Molecular Microbiology*, 44(2), 299-307.

Smyth, E. T., Mcllvenny, G., Enston, J. E., Emmerson, A. M., Humphreys, H., Fitzpatrick, F., Davies, E., Newcombe, R. G. and Spencer, R. C. (2008) Four country healthcare associated infection prevalence 2006: overview of the results. *Journal of Hospital Infection*, 69(3), 230-248.

Soge, O. O., Beck, N. K., White, T. M., No, D. B. and Roberts, M. C. (2008) A novel transposon, Tn*6009*, composed of a Tn*916* element linked with a *Staphylococcus aureus mer* operon. *Journal of Antimicrobial Chemotherapy*, 62, 674–680.

Song, B., Wang, G. R., Shoemaker, N. B. and Salyers, A. A. (2009) An unexpected effect of tetracycline concentration: growth phase-associated excision of the *Bacteroides* mobilizable transposon NBU1. *Journal of Bacteriology*, 191(3), 1078-1082.

Stanton, T. B., McDowall, J. S. and Rasmussen, M. A. (2004) Diverse tetracycline resistance genotypes of *Megasphaera elsdenii* strains selectively cultured from swine feces. *Applied and Environmental Microbiology*, 70, 3754-3757.

Stark, W. M., Boocock, M. R. and Sherrat, D. J. (1992) Catalysis by site-specific recombinases. *Trends in Genetics*, 8, 432-439.

Storrs, M. J., Poyart-Salmeron, C., Trieu-Cuot, P. and Courvalin, P. (1991) Conjugative transposition of Tn*916* requires the excisive and integrative activities of the transposon-encoded integrase. *Journal of Bacteriology*, 173(14), 4347-4352.

Strainic, M. G., Sullivan, J. J., Velevis, A. and de Haseth, P. L. (1998) Promoter recognition by *Escherichia coli* RNA polymerase: effects of the UP element on an open complex formation and promoter clearance. *Biochemistry*, 37, 18074-18080.

Stroynowski, I., Kuroda, M. and Yanofsky, C. (1983) Transcription termination in vitro at the tryptophan operon attenuator is controlled by secondary structures in the leader transcript. *Proceedings of the National Academy of Sciences*, 80(8), 2206-2210.

Studholme, D. J. and Buck, M. (2000) The biology of enhancer-dependent transcriptional regulation in bacteria: insights from genome sequences. *FEMS Microbiology Letters*, 186, 1-9.

Su, Y. A., He, P., Clewell, D. B. (1992) Characterization of Tn*916*: evidence for regulation by transcription attenuation. *Antimicrobial Agents and Chemotherapy*, 36(4), 769-778.

Sudarsan, N., Lee, E. R., Weinberg, Z., Moy, R. H., Kim, J. N., Link, K. H. and Breaker, R. R. (2008) Riboswitches in eubacteria sense the second messenger cyclic di-GMP. *Science*, 321, 411-413.

Sugimoto, N., Kierzek, R. and Turner, D. H. (1987) Sequence dependence for the energetics of dangling ends and terminal base pairs in ribonucleic acid. *Biochemistry*, 26, 4554-4558.

Sundram, F., Guyot, A., Carboo, I., Green, S., Lilaonitkul, M. and Scourfield, A. (2009) *Clostridium difficile* ribotypes 027 and 106: clinical outcomes and risk factors. *Journal of Hospital Infection*, 72, 111-118.

Tanaka, K., Kusano, S., Fujita, N., Ishihama, A. and Takahashi, H. (1995) Promoter determinants for *Escherichia coli* RNA polymerase holoenzyme containing σ^{38} (the *rpoS* gene product). *Nucleic Acids Research*, 23(5), 827–834.

Telesnitsky, A. P. and Chamberlin, M. J. (1989) Sequences linked to prokaryotic promoters can affect the efficiency of downstream termination sites. *Journal of Molecular Biology*, 205(2), 315-30.

Thaker, M., Spanogiannopoulos, P. and Wright, G. D. (2010). The tetracycline resistome. *Cellular and Molecular Life Sciences*, 67, 419–431.

Thomas, C. M. and Nielsen, K. M. (2005) Mechanisms of, and barriers to, horizontal gene transfer between bacteria. *Nature Reviews Microbiology*, 3, 711-721.

Tsien, R. Y. (1998) The green fluorescent. *Annual Review of Biochemistry*, 67, 509-544.

Tuerk, C., Gauss, P., Thermes, C., Groebe, D., Gayle, M., Guild, N., Stormo, G., d' Aubenton Carafa, Y., Uhlenbeck, O., Tinoco Jr., I., Brody, E. and Gold, L. (1988) CUUCGG hairpins: Extraordinarily stable RNA secondary structures associated with various biochemical processes. *Proceedings of the National Academy of Sciences*, 85, 1364-1368.

Turner, P. C., McLenna, A. G., Bates, A. D. and White, M. R. H. (2000) *Molecular Biology*. 2nd ed. BIOS Scientific Publishers Limited.

Vitreschak, A. G., Minorov, A. A., Lyubetsky, V. A. and Gelfand, M. S. (2008) Comparative genomic analysis of T-box regulatory systems in bacteria. *RNA*, 14, 717-735.

Waldor, M. K., Tschäpe, H. and Mekalanos, J. J. (1996) A new type of conjugative transposon encodes resistance to sulfamethoxazole, trimethoprim and streptomycin in *Vibrio cholerae* O139. *Journal of Bacteriology*, 178(14), 4157-4165.

Wang, H. and Mullany, P. (2000) The large resolvase TndX is required and sufficient for integration and excision of derivatives of the novel conjugative transposon Tn*5397*. *Journal of Bacteriology*, 182, 6577–6583.

Wang, H., Roberts, A. P., Lyras, D., Rood, J. I., Wilks, M. and Mullany, P. (2000) Characterization of the ends and target sites of the novel conjugative transposon Tn*5397* from *Clostridium difficile*: excision and circularization is mediated by the large resolvase, TndX. *Journal of Bacteriology*, 182(13), 3775-3783.

Wang, H., Smith, M. C. M. and Mullany, P. (2006) The conjugative transposon Tn*5397* has a strong preference for integration into its *Clostridium difficile* target site. *Journal of Bacteriology*, 188(13), 4871-4878.

Wanner, B. L., Kodaira, R., Neidhart, F. C. (1977) Physiological regulation of a decontrolled *lac* operon. *Journal of Bacteriology*, 130, 212–222.

Waters, C. M. and Dunny, G. M. (2001) Analysis of functional domains of the *Enterococcus faecalis* pheromone-induced surface protein aggregation substance. *Journal of Bacteriology*, 183, 5659–5667.

Wigneshweraraj, S., Bose, D., Burrows, P. C., Joly, N., Schumacher, J., Rappas, M., Pape, T., Zhang, X., Stockley, P., Severinov, K. and Buck, M. (2008) Modus operandi of the bacterial RNA polymerase containing the σ^{54} promoter-specificity factor. *Molecular Microbiology*, 68(3), 538-546.

Woegerbauer, M., Jenni, B., Thalhammer, F., Graninger, W. and Burgmann, H. (2002) Natural genetic transformation of clinical isolates of *Escherichia coli* in urine and water. *Applied and Environmental Microbiology*, 68(1): 440–443.

Woodford, N. and Livermore, D. M. (2009) Infections caused by Gram-positive bacteria: a review of the global challenge. *Journal of Infection*, 59(S1) S4-S16.

Wu, L. J. and Errington, J. (1994) *Bacillus subtilis* SpoIIIE protein required for DNA segregation during asymmetric cell division. *Science*, 264, 572-575.

Wust, J. and Hardegger, U. (1983) Transferable resistance to clindamycin, erythromycin and tetracycline in *Clostridium difficile*. *Antimicrobial Agents and Chemotherapy*, 23, 784-786.

Xie, J., Pierce, J. G., James, R. C., Okano, A. and Boger, D. L. (2011) A redesigned vancomycin engineered for dual D-ala-D-ala and D-ala-D-lac binding exhibits potent antimicrobial activity against vancomycin-resistant bacteria**.** *Journal of the American Chemical Society*, 133(35), 13946–13949.

Yanisch-Perron, C., Vieira, J. and Messing, J. (1985) Improved M13 phage cloning vectors and host strains: nucleotide sequences of the M13mp18 and pUC19 vectors. *Gene*, 33, 103–119.

Yanofsky, C. (1981) Attenuation in the control of expression of bacterial operons. *Nature*, 289, 751-758.

Zinder, N. D. and Lederberg, J. (1952) Genetic exchange in *Salmonella*. *Journal of Bacteriology*, 64, 679-699.

Zuker, M. (2003) Mfold web server for nucleic acid folding and hybridization prediction. *Nucleic Acids Research*, 31(13), 3406-3415.

Appendix

Appendix A: Raw data of plasmid stability test

Plasmid stability of pHCMCO5/P*tet* (M) Tn*916* constructs

0.5 h	WT		PO		ST	
	BHI	BHI/CM	BHI	BHI/CM	BHI	BHI/CM
x 10-5	65	73	80	68	72	72
x 10-6	7	8	9	6	9	14
x 10-6	2	1	1	1	2	2

1.0 h	WT		PO		ST	
	BHI	BHI/CM	BHI	BHI/CM	BHI	BHI/CM
x 10-5	60	62	87	85	75	77
x 10-6	9	5	10	6	9	15
x 10-6	0	1	2	1	1	0

1.5 h	WT		PO		ST	
	BHI	BHI/CM	BHI	BHI/CM	BHI	BHI/CM
x 10-5	92	92	97	111	113	111
x 10-6	7	6	12	16	11	12
x 10-6	1	1	0	2	0	3

2.0 h	WT		PO		ST	
	BHI	BHI/CM	BHI	BHI/CM	BHI	BHI/CM
x 10-5	130	133	160	146	180	181
x 10-6	14	21	26	18	25	23
x 10-6	3	2	2	1	3	4

2.5 h	WT		PO		ST	
	BHI	BHI/CM	BHI	BHI/CM	BHI	BHI/CM
x 10-5	271	89	285	177	TNTC	212
x 10-6	39	14	40	23	55	32
x 10-6	5	1	6	2	5	2

3.0 h	WT		PO		ST	
	BHI	BHI/CM	BHI	BHI/CM	BHI	BHI/CM
x 10-5	168	41	TNTC	73	69	31
x 10-6	29	10	73	10	69	31
x 10-6	2	1	8	1	6	3

3.5 h	WT		PO		ST	
	BHI	BHI/CM	BHI	BHI/CM	BHI	BHI/CM
x 10-5	TNTC	57	80	66	TNTC	227
x 10-6	129	27	80	10	104	45
x 10-6	7	3	9	3	15	4

4.0 h	WT		PO		ST	
	BHI	BHI/CM	BHI	BHI/CM	BHI	BHI/CM
x 10-5	TNTC	120	TNTC	144	TNTC	106
x 10-6	131	39	219	35	183	82
x 10-6	18	8	29	6	25	9

*****TNTC: Too numerous to count

Plasmid stability of pHCMCO5/P*tet* (M) Tn*5397* constructs

0.5 h	WT		PO		ST	
	BHI	BHI/CM	BHI	BHI/CM	BHI	BHI/CM
x 10-5	91	69	72	72	75	66
x 10-6	9	13	7	7	7	9
x 10-6	0	0	1	0	1	0

1.0 h	WT		PO		ST	
	BHI	BHI/CM	BHI	BHI/CM	BHI	BHI/CM
x 10-5	93	103	85	78	67	73
x 10-6	9	9	11	12	11	11
x 10-6	2	1	0	0	1	1

1.5 h	WT		PO		ST	
	BHI	BHI/CM	BHI	BHI/CM	BHI	BHI/CM
x 10-5	98	116	89	98	113	99
x 10-6	14	16	14	9	14	14
x 10-6	2	1	0	1	1	2

2.0 h	WT		PO		ST	
	BHI	BHI/CM	BHI	BHI/CM	BHI	BHI/CM
x 10-5	194	200	209	208	133	174
x 10-6	35	23	27	23	29	26
x 10-6	9	4	5	3	2	4

2.5 h	WT		PO		ST	
	BHI	BHI/CM	BHI	BHI/CM	BHI	BHI/CM
x 10-5	TNTC	187	TNTC	TNTC	147	98
x 10-6	66	57	65	52	40	29
x 10-6	7	7	5	7	6	5

3.0 h	WT		PO		ST	
	BHI	BHI/CM	BHI	BHI/CM	BHI	BHI/CM
x 10-5	TNTC	130	TNTC	136	233	201
x 10-6	118	77	113	74	75	40
x 10-6	14	8	13	10	7	5

3.5 h	WT		PO		ST	
	BHI	BHI/CM	BHI	BHI/CM	BHI	BHI/CM
x 10-5	TNTC	TNTC	TNTC	TNTC	TNTC	TNTC
x 10-6	208	164	191	218	108	94
x 10-6	27	23	25	16	16	12

4.0 h	WT		PO		ST	
	BHI	BHI/CM	BHI	BHI/CM	BHI	BHI/CM
x 10-5	TNTC	TNTC	TNTC	TNTC	TNTC	TNTC
x 10-6	180	147	216	209	160	136
x 10-6	45	32	44	35	29	31

*****TNTC: Too numerous to count

Appendix B: Composition of media and solutions

Media/solutions	Composition
Luria-Bertani (LB) agar	g l^{-1}: 10.0 tryptone, 10.0 sodium chloride, 5.0 yeast extract and 15.0 agar (pH 7.0)
Luria-Bertani (LB) broth	g l^{-1}: 10.0 tryptone, 10.0 sodium chloride and 5.0 yeast extract (pH 7.0)
Brain heart infusion (BHI) agar	g L^{-1}: 12.5 brain infusion solids, 5.0 beef heart infusion solids, 10.0 proteose peptone, 5.0 sodium chloride, 2.5 disodium phosphate, 2.0 glucose, and 10.0 agar (pH 7.4)
Brain heart infusion (BHI) broth	g l^{-1}: 12.5 brain infusion solids, 5.0 beef heart infusion solids, 10.0 proteose peptone, 5.0 sodium chloride, 2.5 disodium phosphate and 2.0 glucose (pH 7.4)
Starch agar	g l^{-1}: 12.5 brain infusion solids, 5.0 beef heart infusion solids, 10.0 peptone, 5.0 sodium chloride, 2.5 disodium phosphate and 2.0 glucose, 4.0 starch and 10.0 agar (pH 7.4)
SP4X	g l^{-1}: 56.0 dipotassium phosphate, 24.0 potassium phosphate, 8.0 ammonium sulphate, 4.0 trisodium citrate dihydrate, 0.8 magnesium sulphate heptahydrate, 4.0 casamino acids and 4.0 yeast extract (pH 7.2)
SPI	v/v: 25 SP4X, 2.5 glucose (20%), 2.86 thymine (35 mg ml^{-1}), 5.0 amino acids solution [histidine, threonine and methionine (1 mg ml^{-1})], and 64.6 distilled water

Media/solutions	Composition
SPII	ml 90 ml^{-1}: 22.5 SP4X, 2.25 glucose (20%), 2.6 thymine (35 mg ml^{-1}) and 62.65 distilled water
SOC	10 ml: 2% tryptone, 0.5% yeast extract, 10 mM sodium chloride, 2.5 mM potassium chloride, 10 mM magnesium chloride, 10 mM magnesium sulphate and 20 mM glucose
Z buffer	1 L: 60 mM disodium hydrogen phosphate, 40 mM sodium dihydrogen phosphate, 10 mM potassium chloride, 1 mM magnesium sulphate heptahydrate and 50 mM 2-mercaptoethanol
Hybridisation buffer	w/v: 2.92 sodium chloride and 5.0 milk powder
20 x SSC	1L: 0.3 M trisodium citrate (pH 7.0) and 3 M sodium chloride
Primary wash buffer	1 L: 6 M urea, 0.4% SDS and 0.5X SSC
Depurination solution	1 L: 250 mM hydrochloric acid
Denaturation solution	1 L: 1.5 M sodium chloride and 0.5 M sodium hydroxide
Neutralisation solution	1 L: 1.5 M sodium chloride and 0.5 M Tris-HCl, pH 7.5
Loading buffer	v/v: 0.25% bromophenol blue, 0.25% xylene cyanol FF and 40% sucrose in sterile distilled water

Appendix C: Publications

1. Jasni, A. S., Mullany, P., Hussain, H., Roberts, A. P. (2010). Demonstration of conjugative transposon (Tn5397)-mediated horizontal gene transfer between *Clostridium difficile* and *Enterococcus faecalis*. *Antimicrobial Agents and Chemotherapy* 54(11), 4924-4926.

2. Ciric, L., Jasni, A., de Vries, L. E., Agersø, Y, Mullany, P. and Roberts, A. P. (2011) 'The Tn*916*/Tn*1545* Family of Conjugative Transposons' in Roberts, A. P. and Mullany, P. (ed.) Landes Bioscience and Springer Science+Business Media.